Interrogating DOT1L Recruitment by MLL-Fusion Proteins MLL-AF9 and MLL-ENL Towards the Development of Novel Targeted Therapy

by

Sierrah Marie Grigsby

A dissertation submitted in partial fulfillment
of the requirements for the degree of
Doctor of Philosophy
(Molecular and Cellular Pathology)
in the University of Michigan
2019

Doctoral Committee:

        Associate Professor Zaneta Nikolovska-Coleska, Chair
        Professor Yali Dou
        Associate Professor Ivan Maillard
        Assistant Professor Andrew Muntean

Sierrah Marie Grigsby

smgrigs@med.umich.edu

ORCID iD: 0000-0002-5410-8792

DEDICATION

This work is dedicated to my Guardian Angels:

My dearest Mother

Bettye Lois Albert Grigsby

February 1, 1966 – February 7, 2016

My dearest maternal Grandmother

Cloteal Albert

August 31, 1936 – November 12, 2014

My dearest paternal Grandfather

Tommie Lee Grigsby

October 10, 1932 - August 8, 2014

ACKNOWLEDGEMENTS

My journey to my Ph.D. has been riddled with many peaks and valleys, but through it all, I have been supported by my faith, family, friends, and colleagues. First and foremost, I would like to give thanks and honor to my Lord and Savior Jesus Christ. Isaiah 40:31 states, "but those who hope in the LORD will renew their strength. They will soar on wings like eagles; they will run and not grow weary, they will walk and not be faint." My faith provided me with the strength needed to finish this project with grace and courage.

I want to honor my parents Archie Edwin Grigsby and Dr. Bettye Lois Albert Grigsby for their undying love and support throughout my educational career. Unfortunately, my mother is not physically here to support me further, but I will carry her legacy with me as I pursue my dreams. My half-siblings Legend, Leah, and Camille who inspire me to be the best role model that I can be. To my maternal grandparents J.W. and Cloteal Albert, to whom I am deeply indebted for their love and support me during my early years, and I am truly grateful. To my paternal grandparents Murd and Tommie Lee Grigsby and Jimmie Nell Headrick for their words of encouragement. I would also like to acknowledge my God-parents Rev. Marion Phillips III, Dr. Rhonda Osborne, Harold Hankins and Cornelia Hankins who have been instrumental in my upbringing as surrogate parents when I have needed them. To my aunts Dr. DeEadra Albert-Green and Sheila Headrick-Sisk and extended family for their prayers and support throughout my journey in graduate school. My Aunt, DeEadra, and mother, Bettye, have always been my role models and friends. They were the first in my immediate family to receive their Ph.D., and I am exceedingly blessed to have my aunt's continued support.

lab for their experimental contributions to Chapter 2 of my thesis. Their studies critically rounded out the second half of those studies, and words cannot express my gratitude.

I had the opportunity to work with so many brilliant minds throughout my graduate studies, and I would like to thank the past lab members Dr. Chenxi Shen and Dr. Garrett Gibbons for their pioneering work on my project that helped lay the foundation for my studies and other projects that I worked on in the lab. Both Chenxi and Garrett trained me on biochemical, biophysical, and cell-based assays that I further developed throughout my time as a graduate student. I would also like to thank Lei Miao for his support while I tried to synthesize compounds and purify peptides for my project. I want to thank my current labmates, Karson Kump, Bing Zhou, Yuting Yang, Nurul Ansari, and Marcelo Murai for their fruitful lab discussions and for tolerating me as the "Lab Princess." I want to give a special thanks to Ahmed Samir Ahmed Mady who has been with me throughout my entire graduate school career at U of M. To Ahmed, I am the little sister he never wanted, and he is my dearest friend and colleague. I will be so sad to miss his presence with me in the lab, but I am very excited for his future as a scientist and hope we will continue to be in touch as we both set out on our journeys.

In the Department of Pathology, I would like to thank Laura Labut for all of her help and support throughout my graduate studies. Laura is not only a great administrator for the department but also a valued friend. On that same note, I would like to thank Tasha Thurman in the Procurement office for always helping me figure out ordering issues and being a listening ear when I need to talk through things that trouble me.

I would also like to thank my many friends in the Pathology department. Those who graduated before me and those who will soon follow. You all are the absolute best! My graduate career would not be what it was without your love and support throughout all of these years.

For those who I was unable to mention, I and want also to thank you. As you see, my life has been impacted in so many ways by a variety of people, and if I named everyone it would be longer than my actual dissertation work, but please know that I am grateful for the smallest gesture to the largest. I am who I am today because of all of the people I have encountered over the years. Thank you all!

TABLE OF CONTENTS

LIST OF FIGURES

LIST OF TABLES

ABSTRACT

The Mixed Lineage Leukemia (MLL) is a Trithorax (Trx) transcriptional regulator often implicated in leukemic oncogenesis. MLL1 rearrangement leukemia is a very aggressive form of leukemia that results from a translocation of chromosome 11q23. The translocation gives rise to a chimeric protein that consists of the N-terminus MLL and 1 of more than 80 fusion partners. The most common fusion partners are ENL, AF9, and AF4. ENL and AF9 are a part of the YEATS family of proteins, containing an N-terminal histone acetylation reading YEATS domain and a C-terminal ANC1 homology domain (AHD). AF9 and ENL's AHD recruit either the Super Elongation Complex (SEC) or the histone 3 lysine 79 (H3K79) histone methyltransferase (HMT) disrupter of telomeric silencing 1-like (DOT1L) to activate gene transcription. Recruitment of DOT1L proved to be essential for the transforming activity of multiple MLL fusion proteins. Our lab mapped the 10 amino acid (865 – 874) binding site on DOT1L, which binds to the AHD domain of AF9/ENL. Applying alanine mutagenesis studies, a point mutation, I867A, was identified sufficient to disrupt the AF9-DOT1L interaction in vitro and demonstrated that DOT1L lacking the 10 amino acids (Δ10) was unable to support transformation by MLL-AF9. In this study, we used a genetic approach to explore the role of DOT1L recruitment in leukemogenesis and normal hematopoiesis to further validate the disruption of the AF9-DOT1L and ENL-DOT1L protein-protein interactions (PPI) as a potential therapeutic approach. We demonstrate that disrupting the AF9-DOT1L PPI inhibits leukemic cell growth, downregulates *HOXA9* and *MEIS1* gene expression, leading to cell differentiation and inducing apoptosis. These observed effects were similar to enzymatic inhibition. Nevertheless, PPI deficient adult

hematopoietic cells completely reconstituted the bone marrow of mice; whereas, cells lacking DOT1L or its catalytic activity were not. We successfully designed a DOT1L peptidomimetic with a K_D of 10 nM against AF9 and 25 nM to ENL that is cellularly active and selective for MLL-AF9 transduced murine cells over a non-DOT1L dependent, E2A-HLF, cells. These results emphasize the critical role of the AF9-DOT1L PPI in leukemic cell growth, but not for adult hematopoiesis making it an attractive therapeutic approach for MLL-rearrangement leukemia.

Due to the homology between the AHD domain of AF9 and ENL, we utilized the same genetic approach as with MLL-AF9 to determine if blocking DOT1L recruitment in MLL-ENL cells would yield the same effect on leukemogenesis. We showed that blocking DOT1L recruitment is not sufficient to fully inhibit leukemic cell growth. We postulate that this is due the retention of the YEATS domain in the MLL-ENL fusion that is lost in MLL-AF9. We characterized two interactions that could be contributing to leukemogenesis, Paf1-YEATS, and YEATS-H3. We demonstrate that Paf1 directly interacts with ENL YEATS with a binding affinity of 15 nM and confirm the YEATS-H3K27ac interaction with a binding affinity of 80 μM. We developed a fragment-based screening method using DSF to identify compounds that bind to the YEATS domain. The development of these tools will allow us to probe both the YEATS-Paf1 and YEATS-H3 interactions to determine which interactions are critical for MLL-ENL driven leukemia. Overall, these studies show the characterization of several PPIs involved in MLL-AF9/ENL leukemia and the development of tools to further elucidate their roles in leukemic and non-leukemic contexts towards novel therapy.

CHAPTER 1

Introduction

1.1   Epigenetics

Each cell is comprised of the same genetic material, DNA; however, cell and tissue-specific transcription and DNA damage repair are regulated by epigenetic signatures that drive cell fate based on which genes are accessible by transcriptional machinery.[1-3] Epigenetic signatures affect genes through heritable phenotypic changes that do not involve altering the DNA sequence through the addition of functional groups to specific locations on DNA that can regulate transcription.[4,5] These alterations or post-translational modifications (PTMs) consist of DNA methylation, small-noncoding RNAs and histone modifications(Figure 1-1).[6-8] The presence or absence of PTMs modulates the formation of euchromatin (open chromatin) or heterochromatin (closed chromatin).[9] The accessibility of chromatin directly impacts the ability of transcription factor localization and RNA polymerase II recruitment to specific genes in response to developmental and environmental cues which is essential for healthy development and homeostasis.[10-14] This dissertation work focuses on the epigenetic regulation of histones in leukemic and non-leukemic development.

Histone modifications are covalent PTMs to histone proteins like methylation, phosphorylation, acetylation, ubiquitylation, sumoylation, and others.[15,16] PTMs are deposited by writer enzymes, removed by eraser enzymes and recognized by reader proteins.[17] The combination of reader, writer, and eraser proteins control the epigenome and chromatin structure regulating gene transcription.[15]
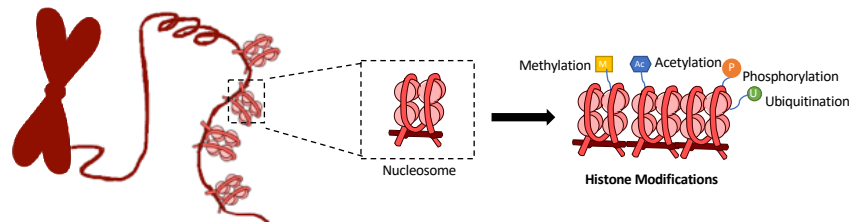
Writers:
- Histone Acetyltransferases (HATs)
  - GNATs
  - MYSTs
  - SRC
  - P300/ CBP
  - TAF$_{II}$250
- Histone methyltransferases (HMTs)
  - SET domain
    - MLL family
  - Non-SET domain
    - DOT1L
  - PRMTs

Readers:
- PHD domain
- Bromo domain
- WD40 domain
- ADD domain
- Tudor domain
- Chromo domain
- + more

Erasers:
- Histone Deacetylases (HDACS)
  - Class I
    - HDAC 1, 2, 3, 8
  - Class IIa
    - HDAC 5, 7, 9
  - Class IIb
    - HDAC 6, 10
  - Class III
    - Sirtuins 1-7
  - Class IV
    - HDAC 11
- Histone Demethylases
  - Jarid2
  - Jmjd1-3
  - UTX

Figure 1-1 Overview of epigenetic histone regulation and common histone regulating proteins.

1.1.1 Epigenetic writers, erasers, and readers

1.1.1.1 Epigenetic writers

Histone acetyltransferases (HATs) and Histone methyltransferases (HMTs) are histone modifying enzymes that regulate gene transcription.[18,19] Histone acetylation was proposed to affect DNA transcription in the 1960s.[20] In 1996, the first HAT, Gcn5 was identified.[21] Since

their initial discovery, 5 subfamilies of HATs emerged including GNATs (Gen5-acetyltranferases), MYSTs, SRC (steroid receptor coactivators), p300/CBP HATs and general transcription factor HATs that contain the $TAF_{II}250$ (Tetrahymena thermophila II) domain.[18,21-24] HATs acetylate lysine residues of histones by transferring an acetyl group from its cofactor acetyl-CoA.[25] To date, the presence of an acetyl-lysine is generally linked to gene activation and euchromatin.[26,27] HATs have also been shown to acetylate non-histone proteins like nuclear receptors and other transcription factors.[28-30]

HMTs are subdivided into SET domain-containing proteins, non-SET domain-containing proteins, and arginine-specific proteins that use s-adenosylmethionine (SAM) as a cofactor to catalyze the transfer of a methyl group to the lysine or arginine residue of histones.[31-33] SET domain containing HMTs like SuVar39, Enhancer of Zeste, and Trithorax can to methylate both histones 3 and 4 (H3 and H4).[33,34] Whereas, a non-SET domain containing HMT, Disruptor of telomeric silencing 1-like (DOT1L), is only able to methylate H3 due to the structural constraints of its SAM-binding site.[35] HMTs can either mono-, di-, or tri- methylate the amino group of lysine residues.[36] These HMTs regulate transcription methylation by either activating or repressing transcription depending on the context and level of methylation.[37] Modifications associated with gene activation include di- and tri H3K4 (H3K4me2 and H3K4me3), mono-, di-, and tri-H3K79 (H3K79me1 HeK79me2 and H3K79me3). Conversely, di- and tri-methylation of H3K9 and H3K27 (H3K9me2, H3K9me3, H3K27me2, and H3K27me3) are repressive marks.[38]

Protein arginine methyltransferases (PRMTs) are a subset of HMTs that specifically mono- or di- methylate arginine residues on histone tails. Arginine methylation marks are associated with gene activation (H4R3me2, H3R2me2, H3R17me2, H3R26me2) or repression (H3R2me2, H3R8me2, H3R8me2, H4R3me2).[39] Recently, newer modifications, like lysine

crotonylation (Cr) have added to the complexity of histone gene regulation.[40] The "epigenetic code" is a combination of histone PTMs like Me, P, Ac, Ub, and Cr that are involved in creating binding surfaces for protein complexes that are involved in chromatin and transcriptional regulation.

1.1.1.2 Epigenetic erasers

Epigenetic erasers are comprised of four classes of enzymes, histone deubiquitinases, histone phosphatases, histone deacetylases, and histone demethylases that can remove histone ubiquitination, phosphorylation, acetylation, and methylation PTMs respectively.[41-44] Histone deacetylases (HDACs) and histone demethylases. HDACs are enzymes capable of removing acetylation marks from histones and silence transcription. There are four classes of HDACs.[41] Class I comprised of HDACS 1, 2, 3, and 8. Class IIa comprised of HDACs 5, 7, and 9. Class IIb comprised of HDACs 6 and 10. Class III is comprised of all of the sirtuins (SirT1-7) while class IV contains only HDAC11.[45,46] Class I HDACs are known to be ubiquitously expressed and traditionally localize in the nucleolus.[47] It is thought that this class of HDACs predominantly deacetylate histone substrates repressing gene transcription.[48] Class I HDACs are highly conserved enzymes consisting or mainly the deacetylase domain with minimal amino acid extensions at the N- and C-terminus of the domain.[49] Knockout (KO) studies of the different Class I HDACs demonstrated that even though the enzymes are similar in structure, they are required for different functions in development. HDAC1 and 3 KO in mice is embryonic lethal with defects in proliferation and gastrulation respectively.[49-51] In contrast, HDAC2 and 8 KO mice produce viable offspring; however, they do not survive longer than 1 day postnatal.[50,52] HDAC2 KO mice develop cardiac malformation[50] while HDAC8 KO mice were observed to have craniofacial defects.[53] Class IIa HDACs have a large N-terminal extension that consists of a

myocyte enhancer factor 2 (MEF2) binding domain, chaperone protein 14-3-3 binding site before the deacetylase domain. Upon phosphorylation, class IIa HDACs bind to the chaperone 14-3-3 proteins, shuttling it from the nucleus into the cytoplasm. Once this class of HDAC is in the cytoplasm, it no longer binds MEF2, leaving it to associate to HAT p300 converting MEF2 from a gene repressor to a gene activator.[54,55] Unlike class I HDACs, class IIa HDACs have more tissue-specific expression patterns. HDAC4 is highly expressed in the brain and skeleton.[54,56] HDAC5 and 9 are highly expressed in the muscles, heart, and brain.[57,58] HDAC7 is expressed in thymocytes and endothelial cells.[59] Class IIb HDACs share homology in their deacetylase domains but have very different structures. HDAC6 and 10 are the main cytoplasmic demethylase and is the only HDACs with 2 demethylase domains.[41,60] HDAC6 deacetylates transmembrane proteins, chaperones, and cytoskeletal proteins.[61-64] Whereas, HDAC10 was recently shown to have immunoregulatory activity.[65] Class III HDACs, the Sirtuins, have a complexity of functions in various locations of the cell. They can deacetylate a variety of histone and non-histone substrates, and in addition to deacetylating substrates, SIRT5 can also desuccinylate and demalonylate proteins. Each sirtuin resides in different compartments in the cell. SIRT1 and SIRT2 are nuclear and cytoplasmic, SIRT3 is nuclear and mitochondrial, SIRT 4 and 5 are only mitochondrial, SITRT6 and 7 are found in the nucleus. Last, is the class IV HDAC11, which is the only HDAC in the class.[66] HDAC11 regulates the stability of DNA replication factor CDT1 and the expression on IL-10.[67] It is highly expressed in the brain, heart, muscle, kidney, and testis.[66,68] The interplay between lysine acetylation and deacetylation regulates not only histones and transcription but other HATs and HDACs, in various cellular processes like RNA processing, translation, metabolism, DNA repair, apoptosis and more.[69]

Like HDACs, histone demethylases modulate the various methylation marks to either repress active genes by demethylating activating marks or removing repressive marks to leave a gene poised for activation. Histone demethylases are clustered into two classes: amino oxidase homolog lysine demethylase 1 (KDM1) and JmjC domain-containing histone demethylases. KDM1 family of enzymes were first discovered because of their ability to demethylate the mono- and di-methylation states of lysine 4 on histone 3; however, due to the flavin adenine dinucleotide (FAD)-dependent amine oxidase reaction, tri-methylation cannot be demethylated by this enzyme.[70] This substrate limitation is overcome by the JmjC domain-containing demethylase that no longer require protonation of the lysine group and instead uses a hydroxylation reaction.[71-75] Together, both KDM1 and JmjC families of demethylases help maintain the balance of gene transcription of various cellular contexts. To date, all histone methylation marks have demethylase that can remove it excluding H3K79me. DOT1L is the only known histone methyltransferase to deposit H3K79me that was thought to only be removed during histone turnover.[76,77] Recent reports identified KDM2B as the first H3K79 demethylase.[78]

1.1.1.3 Epigenetic readers

Equally as important as writing and erasing histone modifications is for creating the messages through PTMs that regulate gene expression, gene locus specificity is needed to ensure the proper genes are activated and repressed. This specificity is achieved through epigenetic reader motifs that target histone modifying enzymes and complexes to the proper gene locus.[79] This specificity is mediated by protein-protein interaction (PPI) networks. These networks use readers to recognize the presence or absence of histone modifications and recruit other histone modifying enzymes or polymerase stabilizing complexes to regulate gene expression. In the case of histone acetylation, bromodomains and PHD finger are the two most common domains

associated with reading acetyl-lysine residues that bind to acetylated histones with a relatively weak binding affinity.[80-82] There substantial redundancy and overlap across the HATs in their gene activating capabilities. It is thought that acetylation marks work in tandem which allows for differential binding of readers to gene loci based on the number of histone reader domains present on the protein. The interplay of reader domain number and number of acetylation marks present at a gene locus helps to facilitate specific transcription.[83,84]

Interestingly, PHD domains ecognize not only acetylation marks but also unmodified H3K4 and histone methylation showing the diversity of functions among common readers.[85] Histone methylation is one of the most stable histone marks. Several methylation readers in conjunction with PHD, recognize both unmethylated H3K4 and modified histone residues including WD40 and ADD domains.[86] Other histone lysine readers like the Chromo, Tudor, MBT, PWWP and other domains read methylated histones.[87] Interestingly, outside of the canonical reader domains, Bromo-adjacent homology (BAH) domain on Sir3 is the only H3K79me reader reported to date.[88,89] Unlike histone acetylation readers, methylation readers bind more tightly to their designated marks.

1.1.1.4 Novel histone acylations and the novel acyl lysine reader YEATS domain

In recent years, due to the emerging role of histone acylation in cellular metabolism, there has been a push towards identifying novel histone acylation marks in addition to histone lysine acetylation.[40,90] Using new proteomic techniques, new acylations like crotonylation (Kcr), 2-hydroxyisobutyrylation (Khib), beta-hydroxybutyrylation (Kbhb), succinylation (Ksu), and many others were identified.[40,91-94] Most of the newly identified acyl modifications have the same pattern of histone acylation as lysine acetylation (Kac).[40] Interestingly, Kcr and Khib have additional acylation sites suggesting non-acetyl functions. The presence of these new acylation

groups has been implicated in spermatogenesis, inflammation, and starvation.[40,93,95] Histone acetyltransferase, p300, was identified as a HAT capable of transferring larger acyl groups from the respective acyl-coenzyme A (acyl-CoA) donor molecules and intermediate metabolites.[95-98] In addition to identifying histone acyl writers, HDAC3, Sirt1, Sirt2, and Sirt3 were identified as histone Kcr decrotonylases, and Sirt5 was reported to desuccinylate and deglutarylate substrates.[96,97,99,100]

In the midst of discovering these emerging acyl lysine marks, the YEATS domain, a new histone lysine acylation reader, was discovered that specifically recognizes histone lysine acylation marks preferring crotonylation over all other acylations with acetylation as the weakest.[101,102] The YEATS domain is structurally unique from other acyl lysine readers in that is adopts an aromatic sandwich pocket that envelops the long chained crotonyl group leaving an open-ended whole so that there is no steric hindrance with the protein making it ideal for loner groups.[103] This interaction is stabilized by an aromatic-π-aromatic stacking around the Kcr group.[104] In contrast, the bromodomain binding pocket has a shallower binding groove with an opening at the side, making it more suitable for shorter acylations.[103] Out of the bromodomain-containing proteins, only the second bromodomain of TAF1 and BRD9 can accommodate Kcr.[105] Recently, proteins containing double PHD finger (DPF) domains were characterized as another class of Kcr readers that has a different mechanism of Kcr recognition from the YEATS domain, incorporating complete encapsulation of the mark and hydrogen bonding.[106]

The YEATS family of proteins was first identified in yeast and is conserved through humans.[107] In humans, GAS41, YEATS2, ENL, and AF9, are only YEATS domain-containing proteins to date.[101-103,107-110] GAS41 is known to recruit the HAT, Tip60, to facilitate histone acetylation or enable H2A.Z deposition through SRCAP.[111] YEATS2, recruits HATs to

chromatin to facilitate acetylation.[107] AF9 and ENL are the most structurally similar human YEATS family members containing an N-terminal YEATS domain and C-terminal AHD domain that is important for mediating PPIs with other histone modifying proteins that are involved in transcription elongation, chromatin remodeling, and histone methylation.[107-109]

1.1.2 Histone crosstalk for regulation of gene activation

As aforementioned, PTM of various residues on histones can either positively or negatively impact transcription. Combinations of various histone PTMs and the recruitment of the associated protein complexes by the modifications lead to the physical modification of chromatin structure yielding a specific transcriptional outcome.[112,113] Histone crosstalk is a term to describe the complexity of histone modifications coregulation of adjacent marks dynamically to regulate transcription.[114] For example, H3K4me3 is enhanced by monoubiquitination of H2B; however, H3K4 methylation can be inhibited if the adjacent H3R2 is methylated first.[114] The many dynamic and critical roles of epigenetic regulators in development and homeostasis point to many areas where dysregulation of these signatures can lead to various human diseases such as cancer.

1.2 MLL family of proteins

Six proteins comprise the MLL family of histone methyltransferases, SETD1a, SETD1b, MLL1, MLL2, MLL3 and MLL4 (Figure 1-2A). MLLs function in multi-protein complexes that regulate their function to mono-, di- or tri- methylate H3K4.[115] MLL family of proteins cluster into 3 subfamilies similar to their Drosophila counterparts. SETD1a and SETD1b cluster into Set1-like proteins, MLL1 and MLL2 cluster into TRX-like proteins and MLL3 and MLL 4 are most similar to TRR-like proteins (Figure 1-2B). SETD1a and SETD1b are noted to regulate housekeeping functions by depositing H3K4me3 at the promoter regions of housekeeping

genes.[116,117] MLL1-4 regulate developmental genes.[118] MLL1 and MLL2 target *Hox* and other genes by depositing H3K4me2 or H3K4me3 at the promoter regions or Polycomb response elements (PRE).[119-121] In contrast, MLL3 and MLL4 function by monomethylating enhancers.[121,122] All six MLLs are part of protein complexes that are necessary for their function.[119] Each complex contains proteins ASH2, RBBP5, WDR5, and DPY30.[123-125] The addition of WDR82 and CXXC1 are critical for the function of SETD1a and SETD1b.[126,127] While, MLL1 and MLL2 both use the protein menin to help the complex interact with DNA. [127-129] MLL3 and MLL4 harboring complexes are distinguished by the presence of UTX, PXIP1, PGR1, and H3K27 demethylase, nuclear receptor cofactor 6 (NCOA6).[130-135]
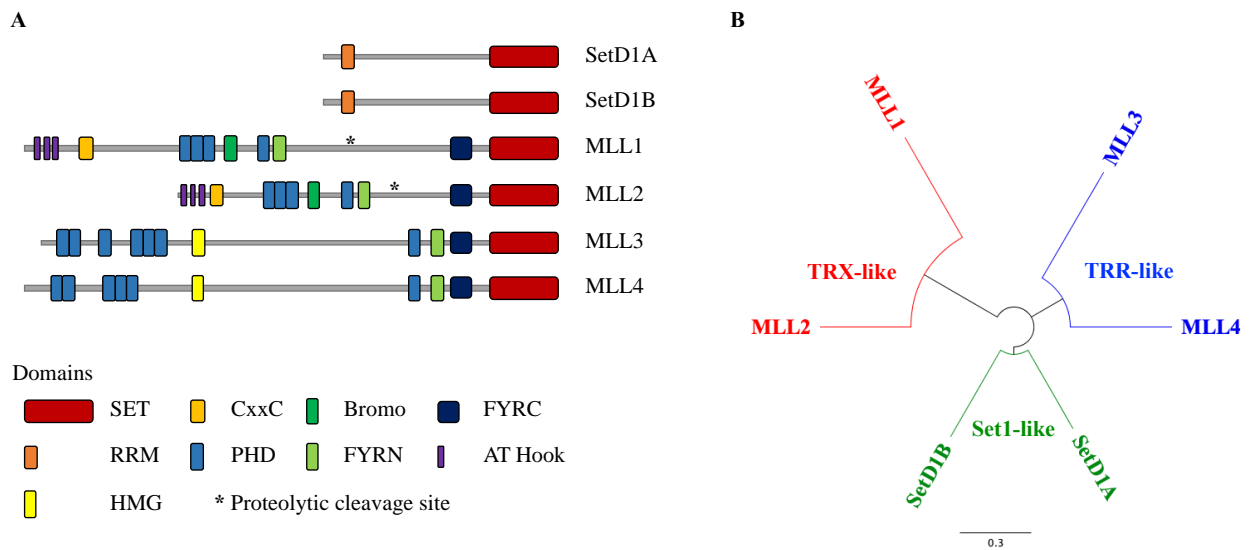
Figure 1-2 The MLL family of histone methyltransferase.

(A)Schematic of the important domains and cleavage points in each of the MLL family of H3K4 methyltransferases. (B) Phylogenetic tree showing the clustering of MLL family members by their Drosophila counterparts TRX-like (MLL1 and MLL2), TRR-like (MLL3 and MLL4), and Set1-like (SetD1A and SetD1B).

1.2.1 MLL1 and MLL2 in embryogenesis and development

MLL1 and MLL2 are closely related proteins that are required for embryogenesis; however, have distinct roles in development. *Mll*[-\-] mice are embryonic lethal at E10.5 with a loss of posterior *Hox* gene expression. *Mll*^{+/-} mice; however, can develop through adulthood, but they exhibit stunted growth, altered hematopoiesis, and an altered skeletal system.[136] These findings are similar to the structural abnormalities seen in *Drosophila trx* mutants.[137] A study showed that *Mll1* had a selective reduction of H3K4 in only about 5% of genes including not only *Hox* genes but also other regulators of development.[120] *Mll2*^{-/-} mice also die at E10.5; however, a conditional knockout at E8.5 yields a normal mouse with no noticeable defects other than in reproductive development.[138,139] This finding points to a distinctive difference in developmental regulation between the hematopoietic and skeletal development specific involvement of MLL1 and the reproductive targeted MLL2.

1.2.2 MLL1 and leukemogenesis

Mll1 gene is located on 11q23 chromosome that encodes a 3696 amino acid (aa) protein that is comprised of two subunits, an *N*-terminal subunit, and a *C*-terminal subunit.[140] MLL1 is proteolytically cleaved by threonine aspartase 1 (TASP 1), an endopeptidase that cleaves proteins into substrates by cleaving after an aspartate residue (Figure 1-2A).[141,142] After cleavage, *C*-terminus and *N*-terminus fragments associate with each other by the consensus interaction motifs. The N-terminus of MLL1 does not contain any histone modifying domains; however, the *C*-terminus contains a SET domain that carries out the H3K4 methylation. Both *N*- and *C*-terminal regions of DOT1L recruit various histone binding and modifying proteins to facilitate its overall function. Hallmarks of this protein are the CxxC domain that shares homology with other histone methyltransferases; four plant homeodomain (PHD) fingers, a transactivation

domain, and a SET domain. MLL1 chromatin binding is mediated by the *N*-terminus of MLL1 and its interactions with multiple endocrine neoplasia 1 (MEN1) and lens epithelium-derived growth factor (LEDGF).[128,129,143,144] These PPIs are important for the recruitment of MLL1 to chromatin.[145,146] The N-terminus of MLL1 also recruits polymerase-associated factor (PafC) via the CxxC motif that is located nears the MLL1 protein cleavage point. PafC then recruits super elongation complex (Sec) and positive transcription elongation factor (pTEFb). Along with histone methylation capabilities, *C*-terminal MLL1 can recruit MOF, a histone 4 lysine 16 (H4K16) acetyltransferase.[147] Other recruited proteins on the *C*-terminus of MLL1 are CREB-binding protein (CBP), WD repeat domain 5 (WDR5) and others.[115] Recruitment of the other proteins named above and association of both termini of MLL allow for its function to remodel chromatin and carry out its enzymatic activity.[115]

Chromosomal translocations of the *Mll1* gene result in fusion of the *N*-terminus of the protein to one of greater than 80 fusion partners.[148] Out of the many MLL-fusion proteins that have been identified there are six common partners (AF4, AF9, ENL, AF10, ELL, and AF6) that make up the majority of MLL-fusion leukemia.[148] MLL fusion partners AF9, ENL, AF4, and AF10, make up 93% and 49% of all MLL-driven acute lymphoblastic and acute myeloid leukemias, respectively.[149] The translocation event removes MLL1's ability to modify histones due to the loss of the *C*-terminal SET domain and recruit MOF to acetylate histones.[150,151] However, the fusion partner can recruit new protein complexes like the Super Elongation Complex (SEC) and DOT1L Complex (Dotcom).[152,153] The presence of the MLL-fusion proteins leads to the misregulation of MLL1 target genes like *HOXA9* and *Meis1* leading towards leukemogenesis by mistargeting gene-activating protein complexes.[154] MLL rearranged leukemia

is a type of aggressive blood cancer found in more than 70% of infant leukemias, more than 10% of therapy-resistant acute myeloid leukemia (AML) and 5% of *de novo* AML cases.[155]

1.3   Common MLL fusion proteins and complexes in leukemogenesis

1.3.1   Super Elongation Complex

MLL-ELL was one of the first identified MLL1 fusion partners.[156] ELL suppresses pausing of RNA Pol II, which links its presence with stabilizing active transcription.[157] Along these lines, other MLL1 fusion partners, AF4, AF9, and ENL, are all associated with the SEC complex.[158] AF4 acts as a scaffolding protein and interacts with multiple subunits of SEC. Directly AF4 binds to ELL and positive transcription elongation factor (p-TEFb) to phosphorylate the *C*-terminal domain of RNA Pol II that releases it from promoter-proximal pausing (Figure 1-3A).[159] Knockdown of any of the SEC subunits in cells harboring one of these MLL-fusions in the SEC complex, leads to a decrease in leukemogenesis.[160] Overall, this mechanism shows that an MLL-fusion protein harboring any of the SEC subunits can act as a scaffolding site for the recruitment of the remaining SEC proteins, stabilizing RNA Pol II leading towards the aberrant transcription of *HOX* genes and leukemic progression.[152]

1.3.2   DotCom Complex

Along with the SEC complex, the Dot1 complex (DotCom) is also recruited by native binders of DOT1L that are translocated to *MLL1*.[161] The proteins involved in DotCom are AF9, ENL, AF10, and AF17 (Figure 1-3B). MLL-AF9 and MLL-ENL fusions are able to directly recruit both the SEC and DotCom complexes to MLL1 target genes in a mutually exclusive manner either through AF4 of the SEC complex or DOT1L of DotCom (Figure 1-3C).[162] Whereas, MLL-AF10 and MLL-AF17 can directly recruit DotCom through DOT1L interactions or indirectly recruit SEC.[162,163] In addition to the recruitment of DOT1L directly by fusion

proteins, other groups have noted the ability of DOT1L to associate with p-TEFb, AF4 and other components of the SEC complex.[152] DOT1L has also been shown to interact with Wnt factors like TRRAP, SKP1, and Beta-catenin.[161,164] Inhibiting DOT1L's catalytic activity or removing *Dot1l* in mice with MLL-rearrangement leukemia inhibits leukemogenesis. Some groups have attributed this to Wnt signaling and Beta- catenin's role in leukemogenesis.[165] However, DOT1L driven leukemogenesis in MLL-AF9 and MLL-ENL leukemia is primarily attributed to DOT1L's recruitment to MLL-target gene loci.[166-168] The role of DOT1L and distinct mechanism in various fusion protein settings is still being elucidated; however, significant work has been done validating it as a therapeutic target for MLL-fusion leukemia.
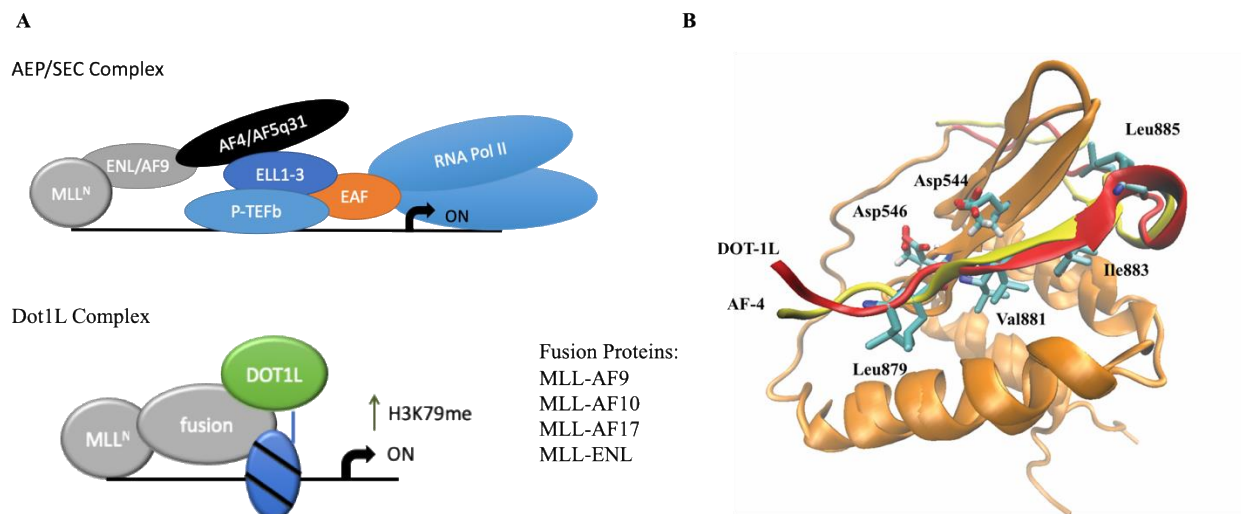
Figure 1-3 Common MLL-fusion protein complexes in MLL-rearrangement leuekmia.

(A) (Top) Schematic of the Super Elongation Complex (SEC) in complex with MLL-AF9 or MLL-ENL binding to AF4 recruiting the other subunits of SEC to MLL-target genes. (Bottom) Schematic of the different MLL-fusion proteins that recruit the DotCom complex to MLL-target genes depositing the H3K79 methylation mark and driving gene expression. (B) Solution NMR structure of the AF4-AF9 (yellow) and AF9-DOT1L (red) interaction overlaid to show the identical binding mode of AF4 and DOT1L to AF9 (PDB: 2LM0 and 2MV7).[167,169]

1.4   Disrupter of Telomeric Silencing 1-like (*Dot1l*)

The disruptor of telomeric silencing 1 (*Dot1*) gene was identified in a yeast genetic screen in which overexpression of the gene reduced silencing at telomeres and other repressed genes.[170] The function of Dot1 is conserved from yeast to humans; thus, the human homolog DOT1L has the same histone methyltransferase enzymatic activity. DOT1L is a non-SET domain-containing histone methyltransferase solely responsible for mono-, di-, and tri-methylation of H3K79. Knock out of *Dot1l* leads to a ubiquitous loss of H3K79 methylation suggesting there is no other enzyme to date responsible for this methylation mark. Also, there is no known demethylase of H3K79 methylation. DOT1L exclusively methylates on histones cores and is unable to methylate free histone tails.

1.4.1   Wildtype DOT1L regulatory functions

H3K79 methylation has numerous implications in development and normal biological processes. *Dot1l* null mice die between 9.5-13.5 days postcoitum.[171,172] Defects in yolk sac angiogenesis and cardiac dilation are suspected as the major cause for embryonic lethality. Embryonic stem cells derived from *Dot1l* mutant blastocysts display deficient heterochromatin establishment at centromeres and telomeres due to aneuploidy, telomere elongation, and proliferation defects.[173] Furthermore, defects in erythropoiesis were observed with deficient erythroid development, G0/G1 accumulation, and increased apoptosis, demonstrating an important role for Dot1l in prenatal hematopoiesis.[174]

Conserved from yeast to higher eukaryotic organisms, Dot1l is involved in double-strand break repair.[175] Loss of Dot1l results in defects in cell cycle regulation. In murine bonemarrow derived cell line, conditional loss of *Dot1l* leads to cell cycle arrest at G1/S phase and accumulation of G0/G1 cells with loss of S and G2/M phase cells.[175] In embryonic stem cells,

Dot1l loss blocks cell differentiation as a result of cell cycle arrest in G2/M phase and proliferation arrest. These studies indicate that Dot1l is required for the regulation of gene transcription in the early stages of embryonic stem cell differentiation.[175] Dot1l is also involved in mediating sodium (Na^+) uptake in epithelial cells in response to aldosterone via regulation of the epithelial Na^+ channel (*ENaC*) gene via H3K79 methylation of the gene promoter.[175] The mutually exclusive binding of either AF9 or AF17 mediates DOT1L's activity at the *ENaC* gene locus.[175] Additionally, DOT1L has a role in cardiac function by regulating the expression of the *Dystrophin (Dmd)* gene required for stabilization of the dystrophin-glycoprotein complex important for cardiomyocyte viability. Cardiac-specific loss of DOT1L results in cardiomyocyte cell death, heart chamber dilation, and systolic dysfunction phenotypes.[176] DOT1L methylation of H3K79 is also important for proper neuronal development through regulation of the TBR1 protein.[176]

Due to embryonic lethality and the need to understand the biological function of DOT1L in mammals, especially its role in MLL-fusion protein-mediated leukemogenesis, several conditional *Dot1l* deletion models were generated.[176] Conditional knockout of *Dot1l* in a postnatal setting demonstrated that systemic loss of *Dot1l* did not produce toxicity for 7-8 weeks. Mice with floxed *Dot1l at* 6-10-week-old were injected with tamoxifen to induce CreER mediated excision of *Dot1l* and showed complete loss of H3K79 methylation in bone marrow cells and other tissue. Mice lacking Dot1l became moribund and developed pancytopenia 8-12 weeks after tamoxifen injection. These findings demonstrated that Dot1l is required to maintain adult hematopoiesis.

1.4.2 DOT1L as a validated therapeutic target for MLL-rearrangement leukemia

Several preclinical reports note the importance of DOT1L in MLL-fusion leukemogenesis.[162,177] This is demonstrated by the upregulation of H3K79 methylation at a subset of MLL target genes such as *HoxA* genes and *Meis1* that are distinct from normal hematopoietic progenitor cells or other Acute Lymphoblastic Leukemias (ALLs) with germline MLL1. The aberrant H3K79 methylation profile in MLL-fusion ALLs also correlated with increased gene expression, especially for the *HoxA* gene cluster.[176]

These reports demonstrate that MLL-fusion proteins recruit DOT1L to MLL1-target genes where it carries out its enzymatic function of H3K79 methylation. Aberrant methylation leads to increased expression of genes such as *HoxA9* and *Meis1* which are critical transcription factors driving leukemogenic transformation.[130] Loss of DOT1L results in decreased H3K79 methylation and reduced expression of MLL1-target genes inhibiting leukemogenic transformation.[178,179] Several MLL-fusion proteins that have not been shown to interact with DOT1L directly also appear to depend on the histone methyltransferase for leukemogenic transformation although the mechanism is not understood.[180] Based on this model, DOT1L is an attractive therapeutic target for the treatment of leukemias bearing translocations of *MLL1*.

1.5 Therapeutic approaches for targeting DOT1L in leukemia

1.5.1 Targeting DOT1L catalytic domain

S-adenosylhomocysteine (SAH; Figure1-4), the demethylated reaction product of DOT1L enzymatic activity, was reported that can inhibit DOT1L enzymatic activity in nanomolar concentration. However, many enzymes utilize the SAM cofactor and are similarly inhibited by SAH, and significant efforts in academia and industry were aimed towards the development of selective DOT1L inhibitors. The first selective and cell active, SAM competitive

DOT1L inhibitor was EPZ004777 with K_i of ~0.3 nM and >1,000-fold selectivity for DOT1L over other HMTs.[57] The complex structure of EPZ004777 with DOT1L, revealed a significant conformational change in the SAM-binding pocket upon binding of the inhibitor, contributing to its selectivity to DOT1L. Upon EPZ004777 binding, an adjacent hydrophobic pocket is opening due to the DOT1L confirmation changes, where the tert-butyl phenyl group binds and contributes to its high binding potency and selectivity. Subsequent modifications led to the development of clinical candidate EPZ-5676, Pinometostat. (Figure 1-4)

In addition to Pinometostat, several covalent inhibitors of DOT1L were reported with subnanomolar potency.[181] (Song-1; Figure1-4) It is well known that adenosine derivatives have a very short half-life; thus there has been much attention devoted to the synthesis of inhibitors with improved metabolic stability. The first non-adenosine SAM analog inhibitor, Song-2, was reported where the ribose was replaced with a bioisostere, a cyclopentane. The non-adenosine compound is 2-3-fold weaker than its adenosine counterpart but has improved metabolic stability in a liver microsome assay.[182] (Song-2; Figure1-4) Recently, a new non-adenosine molecule was developed based on a fragment linkage approach fully abandoning the furan or cyclopentane core scaffold inherent to most SAM competitive molecules.[183] (Gaul-1; Figure 1-4) Gaul-1 is the most potent SAM-competitive DOT1L inhibitor to date.
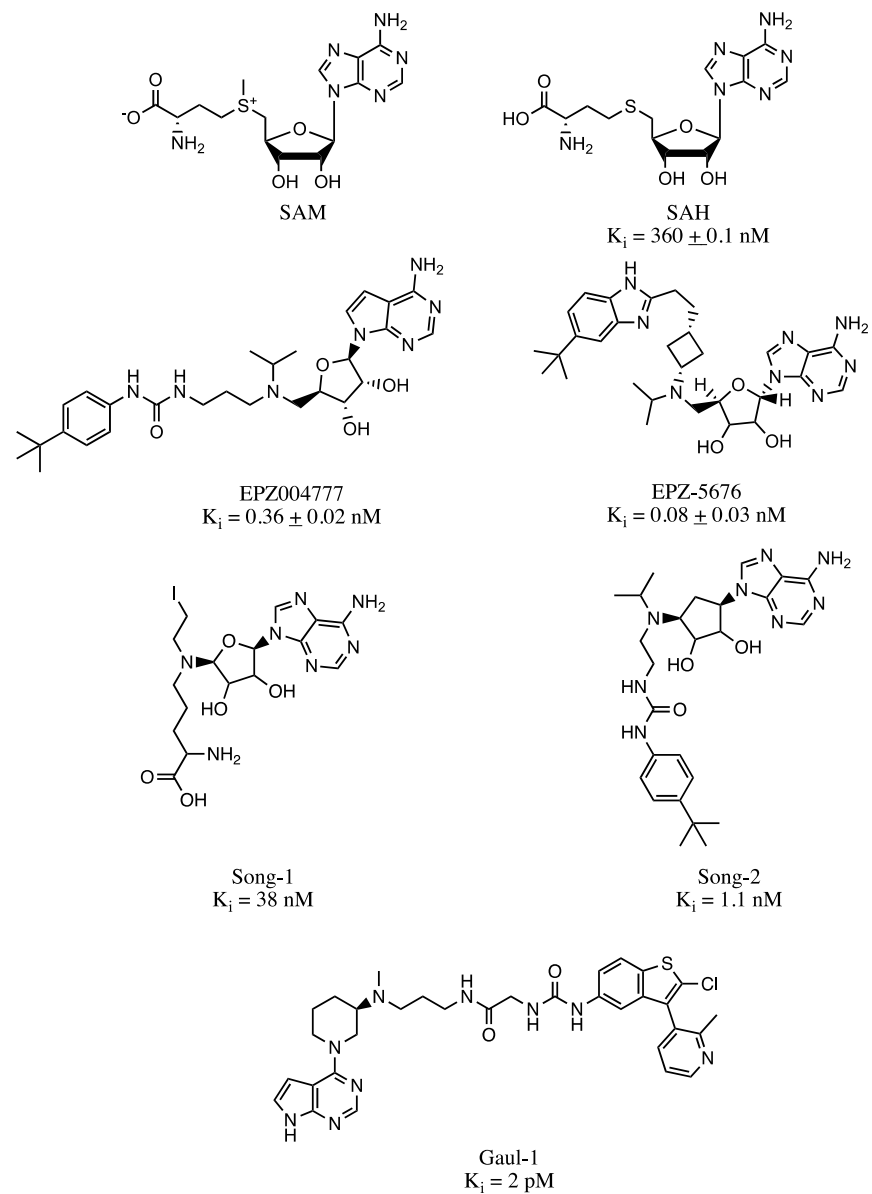
Figure 1-4 Potent inhibitors of DOT1L enzymatic activity.

1.5.2 *Dot1l* inactivation on non-leukemic hematopoiesis

Initially, it was demonstrated that DOT1L is required for embryonic development and DOT1L null mice die between 9.5-13.5 days postcoitum.[184,185] DOT1L deficient mice suffered from anemia and defective erythroid differentiation. Considering the potential for targeting DOT1L in leukemia, there is significant interest to investigate the role of DOT1L in normal hematopoiesis in developed mice. Therefore, conditional knockout models of DOT1L were developed and demonstrated that DOT1L is essential for maintenance of normal adult hematopoiesis. The inducible knockout of *Dot1l* led to depletion of hematopoietic stem cells and various lineage progenitors (granulocyte, monocyte, megakaryocyte, erythrocyte, etc.). This resulted in severe anemia and overall decrease in the bone marrow cellularity.[186,187] In contrast, a third study using DOT1L knockout in the hematopoietic compartment reported that mice display anemia with hypocellularity in the bone marrow, but DOT1L depletion did not cause a total loss of myeloid or lymphoid development.[177] Additional studies which target the enzymatic activity of DOT1L using the small molecule inhibitor EPZ004777 demonstrate a decrease in committed progenitor cells that was most apparent in common myeloid progenitors and megakaryocyte/erythroid common progenitors; however, the hematopoietic stem cell population was not affected.[188]

1.5.3 Targeting DOT1L's recruitment by MLL-fusion proteins

As mentioned previously, studies have shown that the PPIs between MLL-fusion proteins and DotCom/SEC are required for leukemogenesis.[152,160,168] Two of the most common fusions are MLL-AF9 and MLL-ENL. Both AF9 and ENL belong to YEATS domain protein family containing an *N*-terminus YEATS domain and a *C*-terminal hydrophobic, ANC1 homology domain (AHD), domain that binds to AF4 or DOT1L. NMR studies show that when

the *C*-terminus of AF9 is not bound to another protein, it is intrinsically disordered and becomes ordered upon ligand binding.[118] This has been demonstrated by observing the NMR structure of AF9-AF4 PPI and AF9-DOT1L PPI (Figure 1-3B).[167,169] For the first time, our group mapped the 10 amino acid interaction site between AF9/ENL and DOT1L (aa 865-874).[168] This region of DOT1L shares sequence homology to AF4 consistent with previous reports of a mutually exclusive binding of AF9 to SEC and DotCom.[189,190] Subsequent studies identified two additional sites; site 1 (aa 628-653), and site 3 (aa 878-900) that also interact with the AHD domain of AF9.[167] Site 1 binds the weakest to AF9 whereas site 3 binds with similar potency to site 2 (aa 865-874) and share a similar sequence.[167] Utilizing an alanine scanning approach, we were able to identify the residues isoleucine 867 and isoleucine 869 as critical hydrophobic anchors for DOT1L to bind to AHD.[168] Additionally, when the entire 10 aa AF9 binding sequence on DOT1L is removed (Δ10), MLL-AF9 transformed cells lost their self-renewal capabilities.[168] This was further confirmed in subsequent studies when all 3 AF9-binding sites were mutated.[167]

With the emerging evidence of the importance of DOT1L's function in hematopoiesis, we set out to validate targeting the PPI between DOT1L/AF4 and MLL-fusion proteins such as MLL-AF9 and MLL-ENL. This approach offers the potential benefit of inhibiting DOT1L recruitment to MLL-target genes while allowing for normal H3K79 methylation regulation in hematopoietic stem cells and other cellular lineages. Therefore, we predicted that cells containing the MLL-AF9 and MLL-ENL fusion proteins would be selectively sensitive to inhibitors blocking the AF9 or ENL interaction with DOT1L.

1.6   Summary

The epigenetic landscape is vital for normal development and maintenance of tissue- and cell-specific functions.[10] Misregulation of reader, writer, or eraser proteins can lead to various abnormal processes and cancer.[191,192] Due to the apparent shift in epigenetic programming from normal to cancer states, many epigenetic regulators are being identified as potential therapeutic targets for drug intervention.[193] In a variety of MLL-rearrangement leukemia subtypes, DOT1L's catalytic domain was identified and validated as a therapeutic target.[183,188] However, this approach does not take into account the functional importance of DOT1L in other tissues[175,176] and the potential on-target toxicities on non-leukemic hematopoiesis that may develop with the long-term, global enzymatic inhibition of DOT1L. Therefore, in order to leave DOT1L's enzymatic activity intact, we set out to validate targeting DOT1L's recruitment by MLL-AF9 and MLL-ENL as an alternative therapeutic approach. By blocking DOT1L's recruitment, it can carry out its normal functions in the absence of AF9 and ENL binding. To date, there is not enough evidence to determine if PPI inhibition will be more beneficial.

To address the therapeutic advantage of targeting the AF9/ENL and DOT1L PPI over enzymatic inhibition of DOT1L, this dissertation work studied the importance of the AF9 binding domain of DOT1L in leukemic cell growth by demonstrating that blocking the AF9 and DOT1L PPI inhibits cell proliferation, decreases H3K79me at MLL target genes *HOXA9* and *MEIS1*, leading to a decrease in their expression, induction of cell differentiation and apoptosis. Furthermore, we clarified the importance of DOT1L enzymatic activity and not the AF9-DOT1L PPI for non-leukemic hematopoiesis (Chapter 2). In addition to genetically blocking DOT1L recruitment, we developed cell active and selective peptidomimetics that mimic DOT1L's binding domain that interacts with the AF9/ENL AHD domain (Chapter 3). Based on previous

studies, we propose that the peptidomimetics can disrupt both AEP and SEC complexes in addition to blocking DotCom due to the conserved binding region on AF4 and DOT1L. These two studies highlight an alternative approach to targeting DOT1L that leaves its catalytic site intact to carry out its normal hematopoietic functions while specifically targeting the MLL-AF9 transformed cells. Lastly, in Chapter 4, we aimed to understand the role of the MLL-ENL fusion protein's YEATS domain on leukemogenesis. We confirmed that DOT1L alone is not solely responsible for leukemogenesis in MLL-ENL leukemia when the ENL YEATS domain is present. We also validated the direct interaction between Paf1 and ENL YEATS quantifying the binding affinity using a biophysical method and developed a fragment-based screening method to identify fragment molecules that bind the YEATS domain. These studies lay the foundation for developing chemical tools to interrogate the YEATS-PAF1 and YEATS-H3 interactions in leukemogenesis.

1.7   References

1.   Grzybek M, Golonko A, Walczak M, Lisowski P. Epigenetics of cell fate reprogramming and its implications for neurological disorders modelling. *Neurobiol Dis*. 2017;99:84-120.
2.   Moris N, Pina C, Arias AM. Transition states and cell fate decisions in epigenetic landscapes. *Nat Rev Genet*. 2016;17(11):693-703.
3.   Dabin J, Fortuny A, Polo SE. Epigenome Maintenance in Response to DNA Damage. *Mol Cell*. 2016;62(5):712-727.
4.   Holliday R. Epigenetics: a historical overview. *Epigenetics*. 2006;1(2):76-80.
5.   Goldberg AD, Allis CD, Bernstein E. Epigenetics: a landscape takes shape. *Cell*. 2007;128(4):635-638.
6.   Bird A. DNA methylation patterns and epigenetic memory. *Genes Dev*. 2002;16(1):6-21.
7.   Peschansky VJ, Wahlestedt C. Non-coding RNAs as direct and indirect modulators of epigenetic regulation. *Epigenetics*. 2014;9(1):3-12.
8.   Bannister AJ, Kouzarides T. Regulation of chromatin by histone modifications. *Cell Res*. 2011;21(3):381-395.
9.   Hsu TC. Differential rate in RNA synthesis between euchromatin and heterochromatin. *Exp Cell Res*. 1962;27:332-334.
10.   Li E. Chromatin modification and epigenetic reprogramming in mammalian development. *Nat Rev Genet*. 2002;3(9):662-673.
11.   Han P, Hang CT, Yang J, Chang CP. Chromatin remodeling in cardiovascular development and physiology. *Circ Res*. 2011;108(3):378-396.

12.   Kiefer JC. Epigenetics in development. *Dev Dyn*. 2007;236(4):1144-1156.

13.   Matilainen O, Quiros PM, Auwerx J. Mitochondria and Epigenetics - Crosstalk in Homeostasis and Stress. *Trends Cell Biol*. 2017;27(6):453-463.

14.   Abdelsamed HA, Zebley CC, Youngblood B. Epigenetic Maintenance of Acquired Gene Expression Programs during Memory CD8 T Cell Homeostasis. *Front Immunol*. 2018;9:6.

15.   Bowman GD, Poirier MG. Post-translational modifications of histones that influence nucleosome dynamics. *Chem Rev*. 2015;115(6):2274-2295.

16.   El Kennani S, Crespo M, Govin J, Pflieger D. Proteomic Analysis of Histone Variants and Their PTMs: Strategies and Pitfalls. *Proteomes*. 2018;6(3).

17.   Torres IO, Fujimori DG. Functional coupling between writers, erasers and readers of histone and DNA methylation. *Curr Opin Struct Biol*. 2015;35:68-75.

18.   Lee KK, Workman JL. Histone acetyltransferase complexes: one size doesn't fit all. *Nat Rev Mol Cell Biol*. 2007;8(4):284-295.

19.   Greer EL, Shi Y. Histone methylation: a dynamic mark in health, disease and inheritance. *Nat Rev Genet*. 2012;13(5):343-357.

20.   Allfrey VG, Faulkner R, Mirsky AE. Acetylation and Methylation of Histones and Their Possible Role in the Regulation of Rna Synthesis. *Proc Natl Acad Sci U S A*. 1964;51:786-794.

21.   Brownell JE, Zhou J, Ranalli T, et al. Tetrahymena histone acetyltransferase A: a homolog to yeast Gcn5p linking histone acetylation to gene activation. *Cell*. 1996;84(6):843-851.

22.   Parthun MR, Widom J, Gottschling DE. The major cytoplasmic histone acetyltransferase in yeast: links to chromatin replication and histone metabolism. *Cell*. 1996;87(1):85-94.

23.   Mizzen CA, Yang XJ, Kokubo T, et al. The TAF(II)250 subunit of TFIID has histone acetyltransferase activity. *Cell*. 1996;87(7):1261-1270.

24.   Bannister AJ, Kouzarides T. The CBP co-activator is a histone acetyltransferase. *Nature*. 1996;384(6610):641-643.

25.   Yuan H, Marmorstein R. Histone acetyltransferases: Rising ancient counterparts to protein kinases. *Biopolymers*. 2013;99(2):98-111.

26.   Guillemette B, Drogaris P, Lin HH, et al. H3 lysine 4 is acetylated at active gene promoters and is regulated by H3 lysine 4 methylation. *PLoS Genet*. 2011;7(3):e1001354.

27.   Kuo MH, Allis CD. Roles of histone acetyltransferases and deacetylases in gene regulation. *Bioessays*. 1998;20(8):615-626.

28.   Masumi A. Histone acetyltransferases as regulators of nonhistone proteins: the role of interferon regulatory factor acetylation on gene transcription. *J Biomed Biotechnol*. 2011;2011:640610.

29.   Singh BN, Zhang G, Hwa YL, Li J, Dowdy SC, Jiang SW. Nonhistone protein acetylation as cancer therapy targets. *Expert Rev Anticancer Ther*. 2010;10(6):935-954.

30.   Sterner DE, Berger SL. Acetylation of histones and transcription-related factors. *Microbiol Mol Biol Rev*. 2000;64(2):435-459.

31.   Del Rizzo PA, Trievel RC. Molecular basis for substrate recognition by lysine methyltransferases and demethylases. *Biochim Biophys Acta*. 2014;1839(12):1404-1415.

32.   Branscombe TL, Frankel A, Lee JH, et al. PRMT5 (Janus kinase-binding protein 1) catalyzes the formation of symmetric dimethylarginine residues in proteins. *J Biol Chem*. 2001;276(35):32971-32976.

33.   Trievel RC, Beach BM, Dirk LM, Houtz RL, Hurley JH. Structure and catalytic mechanism of a SET domain protein methyltransferase. *Cell*. 2002;111(1):91-103.

34. Dillon SC, Zhang X, Trievel RC, Cheng X. The SET-domain protein superfamily: protein lysine methyltransferases. *Genome Biol*. 2005;6(8):227.

35. Min J, Feng Q, Li Z, Zhang Y, Xu RM. Structure of the catalytic domain of human DOT1L, a non-SET domain nucleosomal histone methyltransferase. *Cell*. 2003;112(5):711-723.

36. Rice JC, Briggs SD, Ueberheide B, et al. Histone methyltransferases direct different degrees of methylation to define distinct chromatin domains. *Mol Cell*. 2003;12(6):1591-1598.

37. Nimura K, Ura K, Kaneda Y. Histone methyltransferases: regulation of transcription and contribution to human disease. *J Mol Med (Berl)*. 2010;88(12):1213-1220.

38. King JV, Liang WG, Scherpelz KP, Schilling AB, Meredith SC, Tang WJ. Molecular basis of substrate recognition and degradation by human presequence protease. *Structure*. 2014;22(7):996-1007.

39. Blanc RS, Richard S. Arginine Methylation: The Coming of Age. *Mol Cell*. 2017;65(1):8-24.

40. Tan M, Luo H, Lee S, et al. Identification of 67 histone marks and histone lysine crotonylation as a new type of histone modification. *Cell*. 2011;146(6):1016-1028.

41. Seto E, Yoshida M. Erasers of histone acetylation: the histone deacetylase enzymes. *Cold Spring Harb Perspect Biol*. 2014;6(4):a018713.

42. Keren I, Citovsky V. The histone deubiquitinase OTLD1 targets euchromatin to regulate plant growth. *Sci Signal*. 2016;9(459):ra125.

43. Banerjee T, Chakravarti D. A peek into the complex realm of histone phosphorylation. *Mol Cell Biol*. 2011;31(24):4858-4873.

44. Cloos PA, Christensen J, Agger K, Helin K. Erasing the methyl mark: histone demethylases at the center of cellular differentiation and disease. *Genes Dev*. 2008;22(9):1115-1140.

45. Gillette TG, Hill JA. Readers, writers, and erasers: chromatin as the whiteboard of heart disease. *Circ Res*. 2015;116(7):1245-1253.

46. Gregoretti IV, Lee YM, Goodson HV. Molecular evolution of the histone deacetylase family: functional implications of phylogenetic analysis. *J Mol Biol*. 2004;338(1):17-31.

47. Morris MJ, Monteggia LM. Unique functional roles for class I and class II histone deacetylases in central nervous system development and function. *Int J Dev Neurosci*. 2013;31(6):370-381.

48. Watson PJ, Fairall L, Schwabe JW. Nuclear hormone receptor co-repressors: structure and function. *Mol Cell Endocrinol*. 2012;348(2):440-449.

49. Lagger G, O'Carroll D, Rembold M, et al. Essential function of histone deacetylase 1 in proliferation control and CDK inhibitor repression. *EMBO J*. 2002;21(11):2672-2681.

50. Montgomery RL, Davis CA, Potthoff MJ, et al. Histone deacetylases 1 and 2 redundantly regulate cardiac morphogenesis, growth, and contractility. *Genes Dev*. 2007;21(14):1790-1802.

51. Montgomery RL, Potthoff MJ, Haberland M, et al. Maintenance of cardiac energy metabolism by histone deacetylase 3 in mice. *J Clin Invest*. 2008;118(11):3588-3597.

52. Trivedi CM, Luo Y, Yin Z, et al. Hdac2 regulates the cardiac hypertrophic response by modulating Gsk3 beta activity. *Nat Med*. 2007;13(3):324-331.

53. Haberland M, Montgomery RL, Olson EN. The many roles of histone deacetylases in development and physiology: implications for disease and therapy. *Nat Rev Genet*. 2009;10(1):32-42.

54. Lu J, McKinsey TA, Zhang CL, Olson EN. Regulation of skeletal myogenesis by association of the MEF2 transcription factor with class II histone deacetylases. *Mol Cell*. 2000;6(2):233-244.

55. Youn HD, Grozinger CM, Liu JO. Calcium regulates transcriptional repression of myocyte enhancer factor 2 by histone deacetylase 4. *J Biol Chem*. 2000;275(29):22563-22567.

56. Vega RB, Matsuda K, Oh J, et al. Histone deacetylase 4 controls chondrocyte hypertrophy during skeletogenesis. *Cell*. 2004;119(4):555-566.

57. Zhang CL, McKinsey TA, Chang S, Antos CL, Hill JA, Olson EN. Class II histone deacetylases act as signal-responsive repressors of cardiac hypertrophy. *Cell*. 2002;110(4):479-488.

58. Chang S, McKinsey TA, Zhang CL, Richardson JA, Hill JA, Olson EN. Histone deacetylases 5 and 9 govern responsiveness of the heart to a subset of stress signals and play redundant roles in heart development. *Mol Cell Biol*. 2004;24(19):8467-8476.

59. Chang S, Young BD, Li S, Qi X, Richardson JA, Olson EN. Histone deacetylase 7 maintains vascular integrity by repressing matrix metalloproteinase 10. *Cell*. 2006;126(2):321-334.

60. Zhang Y, Kwon S, Yamaguchi T, et al. Mice lacking histone deacetylase 6 have hyperacetylated tubulin but are viable and develop normally. *Mol Cell Biol*. 2008;28(5):1688-1701.

61. Tang X, Gao JS, Guan YJ, et al. Acetylation-dependent signal transduction for type I interferon receptor. *Cell*. 2007;131(1):93-105.

62. Zhang X, Yuan Z, Zhang Y, et al. HDAC6 modulates cell motility by altering the acetylation level of cortactin. *Mol Cell*. 2007;27(2):197-213.

63. Kovacs JJ, Murphy PJ, Gaillard S, et al. HDAC6 regulates Hsp90 acetylation and chaperone-dependent activation of glucocorticoid receptor. *Mol Cell*. 2005;18(5):601-607.

64. Matsuyama A, Shimazu T, Sumida Y, et al. In vivo destabilization of dynamic microtubules by HDAC6-mediated deacetylation. *EMBO J*. 2002;21(24):6820-6831.

65. Wang M, Cheng F, Chen J, et al. A Novel Role for Histone Deacetylase 10 (HDAC10) in the Regulation of PD-L1 Expression and Immune Tolerance Mediated By Antigen Presenting Cells (APCs). 2017;130(Suppl 1):3561-3561.

66. Gao L, Cueto MA, Asselbergs F, Atadja P. Cloning and functional characterization of HDAC11, a novel member of the human histone deacetylase family. *J Biol Chem*. 2002;277(28):25748-25755.

67. Glozak MA, Seto E. Acetylation/deacetylation modulates the stability of DNA replication licensing factor Cdt1. *J Biol Chem*. 2009;284(17):11446-11453.

68. Liu H, Hu Q, Kaufman A, D'Ercole AJ, Ye P. Developmental expression of histone deacetylase 11 in the murine brain. *J Neurosci Res*. 2008;86(3):537-543.

69. Choudhary C, Kumar C, Gnad F, et al. Lysine acetylation targets protein complexes and co-regulates major cellular functions. *Science*. 2009;325(5942):834-840.

70. Shi Y, Lan F, Matson C, et al. Histone demethylation mediated by the nuclear amine oxidase homolog LSD1. *Cell*. 2004;119(7):941-953.

71. Christensen J, Agger K, Cloos PA, et al. RBP2 belongs to a family of demethylases, specific for tri-and dimethylated lysine 4 on histone 3. *Cell*. 2007;128(6):1063-1076.

72. Fodor BD, Kubicek S, Yonezawa M, et al. Jmjd2b antagonizes H3K9 trimethylation at pericentric heterochromatin in mammalian cells. *Genes Dev*. 2006;20(12):1557-1562.

73.   Klose RJ, Kallin EM, Zhang Y. JmjC-domain-containing proteins and histone demethylation. *Nat Rev Genet*. 2006;7(9):715-727.
74.   Tsukada Y, Fang J, Erdjument-Bromage H, et al. Histone demethylation by a family of JmjC domain-containing proteins. *Nature*. 2006;439(7078):811-816.
75.   Whetstine JR, Nottke A, Lan F, et al. Reversal of histone lysine trimethylation by the JMJD2 family of histone demethylases. *Cell*. 2006;125(3):467-481.
76.   Ng HH, Feng Q, Wang H, et al. Lysine methylation within the globular domain of histone H3 by Dot1 is important for telomeric silencing and Sir protein association. *Genes Dev*. 2002;16(12):1518-1527.
77.   Klose RJ, Zhang Y. Regulation of histone methylation by demethylimination and demethylation. *Nat Rev Mol Cell Biol*. 2007;8(4):307-318.
78.   Kang JY, Kim JY, Kim KB, et al. KDM2B is a histone H3K79 demethylase and induces transcriptional repression via sirtuin-1-mediated chromatin silencing. *FASEB J*. 2018;32(10):5737-5750.
79.   Yun M, Wu J, Workman JL, Li B. Readers of histone modifications. *Cell Res*. 2011;21(4):564-578.
80.   Dhalluin C, Carlson JE, Zeng L, He C, Aggarwal AK, Zhou MM. Structure and ligand of a histone acetyltransferase bromodomain. *Nature*. 1999;399(6735):491-496.
81.   Ragvin A, Valvatne H, Erdal S, et al. Nucleosome binding by the bromodomain and PHD finger of the transcriptional cofactor p300. *J Mol Biol*. 2004;337(4):773-788.
82.   Lange M, Kaynak B, Forster UB, et al. Regulation of muscle development by DPF3, a novel histone acetylation and methylation reader of the BAF chromatin remodeling complex. *Genes Dev*. 2008;22(17):2370-2384.
83.   Valls E, Sanchez-Molina S, Martinez-Balbas MA. Role of histone modifications in marking and activating genes through mitosis. *J Biol Chem*. 2005;280(52):42592-42600.
84.   Fischer JJ, Toedling J, Krueger T, Schueler M, Huber W, Sperling S. Combinatorial effects of four histone modifications in transcription and differentiation. *Genomics*. 2008;91(1):41-51.
85.   Sanchez R, Zhou MM. The PHD finger: a versatile epigenome reader. *Trends Biochem Sci*. 2011;36(7):364-372.
86.   Lan F, Collins RE, De Cegli R, et al. Recognition of unmethylated histone H3 lysine 4 links BHC80 to LSD1-mediated gene repression. *Nature*. 2007;448(7154):718-722.
87.   Musselman CA, Khorasanizadeh S, Kutateladze TG. Towards understanding methyllysine readout. *Biochim Biophys Acta*. 2014;1839(8):686-693.
88.   Onishi M, Liou GG, Buchberger JR, Walz T, Moazed D. Role of the conserved Sir3-BAH domain in nucleosome binding and silent chromatin assembly. *Mol Cell*. 2007;28(6):1015-1028.
89.   Armache KJ, Garlick JD, Canzio D, Narlikar GJ, Kingston RE. Structural basis of silencing: Sir3 BAH domain in complex with a nucleosome at 3.0 A resolution. *Science*. 2011;334(6058):977-982.
90.   Sabari BR, Zhang D, Allis CD, Zhao Y. Metabolic regulation of gene expression through histone acylations. *Nat Rev Mol Cell Biol*. 2017;18(2):90-101.
91.   Huang H, Lin S, Garcia BA, Zhao Y. Quantitative proteomic analysis of histone modifications. *Chem Rev*. 2015;115(6):2376-2418.
92.   Chen Y, Sprung R, Tang Y, et al. Lysine propionylation and butyrylation are novel post-translational modifications in histones. *Mol Cell Proteomics*. 2007;6(5):812-819.

93.   Dai L, Peng C, Montellier E, et al. Lysine 2-hydroxyisobutyrylation is a widely distributed active histone mark. *Nat Chem Biol*. 2014;10(5):365-370.

94.   Xie Z, Dai J, Dai L, et al. Lysine succinylation and lysine malonylation in histones. *Mol Cell Proteomics*. 2012;11(5):100-107.

95.   Xie Z, Zhang D, Chung D, et al. Metabolic Regulation of Gene Expression by Histone Lysine beta-Hydroxybutyrylation. *Mol Cell*. 2016;62(2):194-206.

96.   Tan M, Peng C, Anderson KA, et al. Lysine glutarylation is a protein posttranslational modification regulated by SIRT5. *Cell Metab*. 2014;19(4):605-617.

97.   Dutta A, Abmayr SM, Workman JL. Diverse Activities of Histone Acylations Connect Metabolism to Chromatin Function. *Mol Cell*. 2016;63(4):547-552.

98.   Sabari BR, Tang Z, Huang H, et al. Intracellular crotonyl-CoA stimulates transcription through p300-catalyzed histone crotonylation. *Mol Cell*. 2015;58(2):203-215.

99.   Hirschey MD, Zhao Y. Metabolic Regulation by Lysine Malonylation, Succinylation, and Glutarylation. *Mol Cell Proteomics*. 2015;14(9):2308-2315.

100.   Park J, Chen Y, Tishkoff DX, et al. SIRT5-mediated lysine desuccinylation impacts diverse metabolic pathways. *Mol Cell*. 2013;50(6):919-930.

101.   Zhao D, Li Y, Xiong X, Chen Z, Li H. YEATS Domain-A Histone Acylation Reader in Health and Disease. *J Mol Biol*. 2017;429(13):1994-2002.

102.   Li Y, Zhao D, Chen Z, Li H. YEATS domain: Linking histone crotonylation to gene regulation. *Transcription*. 2017;8(1):9-14.

103.   Li Y, Sabari BR, Panchenko T, et al. Molecular Coupling of Histone Crotonylation and Active Transcription by AF9 YEATS Domain. *Mol Cell*. 2016;62(2):181-193.

104.   Vagner J, Qu H, Hruby VJ. Peptidomimetics, a synthetic tool of drug discovery. *Curr Opin Chem Biol*. 2008;12(3):292-296.

105.   Flynn EM, Huang OW, Poy F, et al. A Subset of Human Bromodomains Recognizes Butyryllysine and Crotonyllysine Histone Peptide Modifications. *Structure*. 2015;23(10):1801-1814.

106.   Xiong X, Panchenko T, Yang S, et al. Selective recognition of histone crotonylation by double PHD fingers of MOZ and DPF2. *Nat Chem Biol*. 2016;12(12):1111-1118.

107.   Schulze JM, Wang AY, Kobor MS. YEATS domain proteins: a diverse family with many links to chromatin modification and transcription. *Biochem Cell Biol*. 2009;87(1):65-75.

108.   Li Y, Wen H, Xi Y, et al. AF9 YEATS domain links histone acetylation to DOT1L-mediated H3K79 methylation. *Cell*. 2014;159(3):558-571.

109.   Erb MA, Scott TG, Li BE, et al. Transcription control by the ENL YEATS domain in acute leukaemia. *Nature*. 2017;543(7644):270-274.

110.   Zhao D, Guan H, Zhao S, et al. YEATS2 is a selective histone crotonylation reader. *Cell Res*. 2016;26(5):629-632.

111.   Hsu CC, Zhao D, Shi J, et al. Gas41 links histone acetylation to H2A.Z deposition and maintenance of embryonic stem cell identity. *Cell Discov*. 2018;4:28.

112.   Suganuma T, Workman JL. Signals and combinatorial functions of histone modifications. *Annu Rev Biochem*. 2011;80:473-499.

113.   Bell O, Tiwari VK, Thoma NH, Schubeler D. Determinants and dynamics of genome accessibility. *Nat Rev Genet*. 2011;12(8):554-564.

114.   Lee JS, Shukla A, Schneider J, et al. Histone crosstalk between H2B monoubiquitination and H3 methylation mediated by COMPASS. *Cell*. 2007;131(6):1084-1096.

115. Shilatifard A. The COMPASS family of histone H3K4 methylases: mechanisms of regulation in development and disease pathogenesis. *Annu Rev Biochem*. 2012;81:65-95.

116. Lin H, Min Z, Tao Q. The MLL/Setd1b methyltransferase is required for the Spemann's organizer gene activation in Xenopus. *Mech Dev*. 2016;142:1-9.

117. Lee JH, Skalnik DG. Wdr82 is a C-terminal domain-binding protein that recruits the Setd1A Histone H3-Lys4 methyltransferase complex to transcription start sites of transcribed human genes. *Mol Cell Biol*. 2008;28(2):609-618.

118. Muller S, Nayak A. Inhibition of MLL1 histone methyltransferase brings the developmental clock back to naive pluripotency. *Stem Cell Investig*. 2016;3:58.

119. Eissenberg JC, Shilatifard A. Histone H3 lysine 4 (H3K4) methylation in development and differentiation. *Dev Biol*. 2010;339(2):240-249.

120. Wang P, Lin C, Smith ER, et al. Global analysis of H3K4 methylation defines MLL family member targets and points to a role for MLL1-mediated H3K4 methylation in the regulation of transcriptional initiation by RNA polymerase II. *Mol Cell Biol*. 2009;29(22):6074-6085.

121. Rickels R, Hu D, Collings CK, et al. An Evolutionary Conserved Epigenetic Mark of Polycomb Response Elements Implemented by Trx/MLL/COMPASS. *Mol Cell*. 2016;63(2):318-328.

122. Zhao JX, Zhang HX, Li B, et al. Role of MLL3 in regulating cardiac stem cells following cardiac cachexia. *Eur Rev Med Pharmacol Sci*. 2017;21(21):4924-4929.

123. Yokoyama A, Wang Z, Wysocka J, et al. Leukemia proto-oncoprotein MLL forms a SET1-like histone methyltransferase complex with menin to regulate Hox gene expression. *Mol Cell Biol*. 2004;24(13):5639-5649.

124. Song JJ, Kingston RE. WDR5 interacts with mixed lineage leukemia (MLL) protein via the histone H3-binding pocket. *J Biol Chem*. 2008;283(50):35258-35264.

125. Vedadi M, Blazer L, Eram MS, Barsyte-Lovejoy D, Arrowsmith CH, Hajian T. Targeting human SET1/MLL family of proteins. *Protein Sci*. 2017;26(4):662-676.

126. Lee JH, Skalnik DG. CpG-binding protein (CXXC finger protein 1) is a component of the mammalian Set1 histone H3-Lys4 methyltransferase complex, the analogue of the yeast Set1/COMPASS complex. *J Biol Chem*. 2005;280(50):41725-41731.

127. Wu M, Wang PF, Lee JS, et al. Molecular regulation of H3K4 trimethylation by Wdr82, a component of human Set1/COMPASS. *Mol Cell Biol*. 2008;28(24):7337-7344.

128. Hughes CM, Rozenblatt-Rosen O, Milne TA, et al. Menin associates with a trithorax family histone methyltransferase complex and with the hoxc8 locus. *Mol Cell*. 2004;13(4):587-597.

129. Milne TA, Hughes CM, Lloyd R, et al. Menin and MLL cooperatively regulate expression of cyclin-dependent kinase inhibitors. *Proc Natl Acad Sci U S A*. 2005;102(3):749-754.

130. Cho YW, Hong S, Ge K. Affinity purification of MLL3/MLL4 histone H3K4 methyltransferase complex. *Methods Mol Biol*. 2012;809:465-472.

131. Sze CC, Shilatifard A. MLL3/MLL4/COMPASS Family on Epigenetic Regulation of Enhancer Function and Cancer. *Cold Spring Harb Perspect Med*. 2016;6(11).

132. Morgan MA, Shilatifard A. Drosophila SETs its sights on cancer: Trr/MLL3/4 COMPASS-like complexes in development and disease. *Mol Cell Biol*. 2013;33(9):1698-1701.

133. Lee S, Lee JW, Lee SK. UTX, a histone H3-lysine 27 demethylase, acts as a critical switch to activate the cardiac developmental program. *Dev Cell*. 2012;22(1):25-37.

134. Cho YW, Hong T, Hong S, et al. PTIP associates with MLL3- and MLL4-containing histone H3 lysine 4 methyltransferase complex. *J Biol Chem*. 2007;282(28):20395-20406.
135. Callen E, Faryabi RB, Luckey M, et al. The DNA damage- and transcription-associated protein paxip1 controls thymocyte development and emigration. *Immunity*. 2012;37(6):971-985.
136. Yu BD, Hess JL, Horning SE, Brown GA, Korsmeyer SJ. Altered Hox expression and segmental identity in Mll-mutant mice. *Nature*. 1995;378(6556):505-508.
137. Ingham PWaW, R. Trithorax: A new homoeotic mutation of Drosophila melanogaster causing transformations of abdominal and thoracic imaginal segments - I. Putative role during embryogenesis. *Molecular and General Genetics*. 1980;179(3):607-614.
138. Andreu-Vieyra CV, Chen R, Agno JE, et al. MLL2 is required in oocytes for bulk histone 3 lysine 4 trimethylation and transcriptional silencing. *PLoS Biol*. 2010;8(8).
139. Glaser S, Lubitz S, Loveland KL, et al. The histone 3 lysine 4 methyltransferase, Mll2, is only required briefly in development and spermatogenesis. *Epigenetics Chromatin*. 2009;2(1):5.
140. de Boer J, Walf-Vorderwülbecke V, Williams O. In focus: MLL-rearranged leukemia. *Leukemia*. 2013;27(6):1224-1228.
141. Yokoyama A, Kitabayashi I, Ayton PM, Cleary ML, Ohki M. Leukemia proto-oncoprotein MLL is proteolytically processed into 2 fragments with opposite transcriptional properties. *Blood*. 2002;100(10):3710-3718.
142. Hsieh JJ, Ernst P, Erdjument-Bromage H, Tempst P, Korsmeyer SJ. Proteolytic cleavage of MLL generates a complex of N- and C-terminal fragments that confers protein stability and subnuclear localization. *Mol Cell Biol*. 2003;23(1):186-194.
143. Yokokawa F, Wang G, Chan WL, et al. Discovery of tetrahydropyrazolopyrimidine carboxamide derivatives as potent and orally active antitubercular agents. *ACS Med Chem Lett*. 2013;4(5):451-455.
144. Yokoyama A, Cleary ML. Menin critically links MLL proteins with LEDGF on cancer-associated target genes. *Cancer Cell*. 2008;14(1):36-46.
145. Yokoyama A, Somervaille TC, Smith KS, Rozenblatt-Rosen O, Meyerson M, Cleary ML. The menin tumor suppressor protein is an essential oncogenic cofactor for MLL-associated leukemogenesis. *Cell*. 2005;123(2):207-218.
146. Caslini C, Yang Z, El-Osta M, Milne TA, Slany RK, Hess JL. Interaction of MLL amino terminal sequences with menin is required for transformation. *Cancer Res*. 2007;67(15):7275-7283.
147. Mishra BP, Zaffuto KM, Artinger EL, et al. The histone methyltransferase activity of MLL1 is dispensable for hematopoiesis and leukemogenesis. *Cell Rep*. 2014;7(4):1239-1247.
148. Meyer C, Kowarz E, Hofmann J, et al. New insights to the MLL recombinome of acute leukemias. *Leukemia*. 2009;23(8):1490-1499.
149. Winters AC, Bernt KM. MLL-Rearranged Leukemias-An Update on Science and Clinical Approaches. *Front Pediatr*. 2017;5:4.
150. Tkachuk DC, Kohler S, Cleary ML. Involvement of a homolog of Drosophila trithorax by 11q23 chromosomal translocations in acute leukemias. *Cell*. 1992;71(4):691-700.
151. Gu Y, Nakamura T, Alder H, et al. The t(4;11) chromosome translocation of human acute leukemias fuses the ALL-1 gene, related to Drosophila trithorax, to the AF-4 gene. *Cell*. 1992;71(4):701-708.
152. Smith E, Lin C, Shilatifard A. The super elongation complex (SEC) and MLL in development and disease. *Genes Dev*. 2011;25(7):661-672.

153.   Slany RK. When speed matters: leukemogenic transformation by MLL fusion proteins. *Cell Cycle*. 2010;9(13):2475-2476.

154.   Collins CT, Hess JL. Deregulation of the HOXA9/MEIS1 axis in acute leukemia. *Curr Opin Hematol*. 2016;23(4):354-361.

155.   Yip BH, So CWE. Mixed lineage leukemia protein in normal and leukemic stem cells. *Experimental Biology and Medicine*. 2013;238(3):315-323.

156.   Shilatifard A, Lane WS, Jackson KW, Conaway RC, Conaway JW. An RNA polymerase II elongation factor encoded by the human ELL gene. *Science*. 1996;271(5257):1873-1876.

157.   Shilatifard A. Identification and purification of the Holo-ELL complex. Evidence for the presence of ELL-associated proteins that suppress the transcriptional inhibitory activity of ELL. *J Biol Chem*. 1998;273(18):11212-11217.

158.   Luo Z, Lin C, Shilatifard A. The super elongation complex (SEC) family in transcriptional control. *Nat Rev Mol Cell Biol*. 2012;13(9):543-547.

159.   Scholz B, Kowarz E, Rossler T, Ahmad K, Steinhilber D, Marschalek R. AF4 and AF4N protein complexes: recruitment of P-TEFb kinase, their interactome and potential functions. *Am J Blood Res*. 2015;5(1):10-24.

160.   Lin C, Smith ER, Takahashi H, et al. AFF4, a component of the ELL/P-TEFb elongation complex and a shared subunit of MLL chimeras, can link transcription elongation to leukemia. *Mol Cell*. 2010;37(3):429-437.

161.   Mohan M, Herz HM, Takahashi YH, et al. Linking H3K79 trimethylation to Wnt signaling through a novel Dot1-containing complex (DotCom). *Genes Dev*. 2010;24(6):574-589.

162.   Bernt KM, Armstrong SA. A role for DOT1L in MLL-rearranged leukemias. *Epigenomics*. 2011;3(6):667-670.

163.   Wood K, Tellier M, Murphy S. DOT1L and H3K79 Methylation in Transcription and Genomic Stability. *Biomolecules*. 2018;8(1).

164.   Gibbons GS, Owens SR, Fearon ER, Nikolovska-Coleska Z. Regulation of Wnt signaling target gene expression by the histone methyltransferase DOT1L. *ACS Chem Biol*. 2015;10(1):109-114.

165.   Sierra J, Yoshida T, Joazeiro CA, Jones KA. The APC tumor suppressor counteracts beta-catenin activation and H3K4 methylation at Wnt target genes. *Genes Dev*. 2006;20(5):586-600.

166.   Steger DJ, Lefterova MI, Ying L, et al. DOT1L/KMT4 recruitment and H3K79 methylation are ubiquitously coupled with gene transcription in mammalian cells. *Molecular and cellular biology*. 2008;28(8):2825-2839.

167.   Kuntimaddi A, Achille NJ, Thorpe J, et al. Degree of recruitment of DOT1L to MLL-AF9 defines level of H3K79 Di- and tri-methylation on target genes and transformation potential. *Cell Rep*. 2015;11(5):808-820.

168.   Shen C, Jo SY, Liao C, Hess JL, Nikolovska-Coleska Z. Targeting recruitment of disruptor of telomeric silencing 1-like (DOT1L): characterizing the interactions between DOT1L and mixed lineage leukemia (MLL) fusion proteins. *The Journal of Biological Chemistry*. 2013;288(42):30585-30596.

169.   Leach BI, Kuntimaddi A, Schmidt CR, Cierpicki T, Johnson SA, Bushweller JH. Leukemia fusion target AF9 is an intrinsically disordered transcriptional regulator that recruits multiple partners via coupled folding and binding. *Structure*. 2013;21(1):176-183.

170.   Reisenauer MR, Wang SW, Xia Y, Zhang W. Dot1a contains three nuclear localization signals and regulates the epithelial Na+ channel (ENaC) at multiple levels. *Am J Physiol Renal Physiol*. 2010;299(1):F63-76.

171.   Zhang W, Hayashizaki Y, Kone BC. Structure and regulation of the mDot1 gene, a mouse histone H3 methyltransferase. *Biochem J*. 2004;377(Pt 3):641-651.

172.   Zhang W, Xia X, Jalal DI, et al. Aldosterone-sensitive repression of ENaCalpha transcription by a histone H3 lysine-79 methyltransferase. *Am J Physiol Cell Physiol*. 2006;290(3):C936-946.

173.   Zhang W, Xia X, Reisenauer MR, Hemenway CS, Kone BC. Dot1a-AF9 complex mediates histone H3 Lys-79 hypermethylation and repression of ENaCalpha in an aldosterone-sensitive manner. *Journal of Biological Chemistry*. 2006;281(26):18059-18068.

174.   Zhang W, Xia X, Reisenauer MR, et al. Aldosterone-induced Sgk1 relieves Dot1a-Af9-mediated transcriptional repression of epithelial Na+ channel alpha. *J Clin Invest*. 2007;117(3):773-783.

175.   Xiao Z, Chen L, Zhou Q, Zhang W. Dot1l deficiency leads to increased intercalated cells and upregulation of V-ATPase B1 in mice. *Exp Cell Res*. 2016;344(2):167-175.

176.   Krivtsov AV, Feng Z, Lemieux ME, et al. H3K79 methylation profiles define murine and human MLL-AF4 leukemias. *Cancer Cell*. 2008;14(5):355-368.

177.   Bernt KM, Zhu N, Sinha AU, et al. MLL-rearranged leukemia is dependent on aberrant H3K79 methylation by DOT1L. *Cancer Cell*. 2011;20(1):66-78.

178.   Chen L, Deshpande AJ, Banka D, et al. Abrogation of MLL–AF10 and CALM–AF10-mediated transformation through genetic inactivation or pharmacological inhibition of the H3K79 methyltransferase Dot1l. *Leukemia*. 2013;27(4):813-822.

179.   Nguyen AT, Taranova O, He J, Zhang Y. DOT1L, the H3K79 methyltransferase, is required for MLL-AF9–mediated leukemogenesis. *Blood*. 2011;117(25):6912-6922.

180.   Jo SY, Granowicz EM, Maillard I, Thomas D, Hess JL. Requirement for Dot1l in murine postnatal hematopoiesis and leukemogenesis by MLL translocation. *Blood*. 2011;117(18):4759-4768.

181.   Anglin JL, Deng L, Yao Y, et al. Synthesis and structure-activity relationship investigation of adenosine-containing inhibitors of histone methyltransferase DOT1L. *J Med Chem*. 2012;55(18):8066-8074.

182.   Deng L, Zhang L, Yao Y, et al. Synthesis, Activity and Metabolic Stability of Non-Ribose Containing Inhibitors of Histone Methyltransferase DOT1L. *Medchemcomm*. 2013;4(5):822-826.

183.   Mobitz H, Machauer R, Holzer P, et al. Discovery of Potent, Selective, and Structurally Novel Dot1L Inhibitors by a Fragment Linking Approach. *ACS Med Chem Lett*. 2017;8(3):338-343.

184.   Jones B, Su H, Bhat A, et al. The histone H3K79 methyltransferase Dot1L is essential for mammalian development and heterochromatin structure. *PLoS Genet*. 2008;4(9):e1000190.

185.   Feng Y, Yang Y, Ortega MM, et al. Early mammalian erythropoiesis requires the Dot1L methyltransferase. *Blood*. 2010;116(22):4483-4491.

186.   Jo SY, Granowicz EM, Maillard I, Thomas D, Hess JL. Requirement for Dot1l in murine postnatal hematopoiesis and leukemogenesis by MLL translocation. *Blood*. 2011;117(18):4759-4768.

187.   Nguyen AT, He J, Taranova O, Zhang Y. Essential role of DOT1L in maintaining normal adult hematopoiesis. *Cell Res*. 2011;21(9):1370-1373.

188. Daigle SR, Olhava EJ, Therkelsen CA, et al. Selective Killing of Mixed Lineage Leukemia Cells by a Potent Small-Molecule DOT1L Inhibitor. *Cancer Cell*. 2011;20(1):53-65.

189. Yokoyama A, Lin M, Naresh A, Kitabayashi I, Cleary ML. A Higher-Order Complex Containing AF4 and ENL Family Proteins with P-TEFb Facilitates Oncogenic and Physiologic MLL-Dependent Transcription. *Cancer Cell*. 2010;17(2):198-212.

190. Biswas D, Milne TA, Basrur V, et al. Function of leukemogenic mixed lineage leukemia 1 (MLL) fusion proteins through distinct partner protein complexes. *Proc Natl Acad Sci U S A*. 2011;108(38):15751-15756.

191. Lund AH, van Lohuizen M. Epigenetics and cancer. *Genes Dev*. 2004;18(19):2315-2335.

192. Moosavi A, Motevalizadeh Ardekani A. Role of Epigenetics in Biology and Human Diseases. *Iran Biomed J*. 2016;20(5):246-258.

193. Gelato KA, Shaikhibrahim Z, Ocker M, Haendler B. Targeting epigenetic regulators for cancer therapy: modulation of bromodomain proteins, methyltransferases, demethylases, and microRNAs. *Expert Opin Ther Targets*. 2016;20(7):783-799.

CHAPTER 2

Elucidating the Importance of DOT1L's AF9-Binding Domain in MLL-AF9 Leukemia and Normal Hematopoiesis

2.1   Abstract

MLL1 gene rearrangements underlie the pathogenesis of aggressive MLL-driven acute leukemias. AF9, one of the most common MLL-fusion partners, recruits the histone H3K79 methyltransferase DOT1L to MLL-target genes, constitutively activating transcription of pro-leukemic targets. DOT1L has emerged as a therapeutic target in patients with MLL-driven leukemia. However, global DOT1L enzymatic inhibition may lead to off-target toxicities in non-leukemic contexts that could decrease the therapeutic index of DOT1L inhibitors. To bypass this problem, we developed a novel approach targeting specific protein-protein interactions (PPI) that mediate DOT1L recruitment to MLL fusion partners, and we compared the effects of enzymatic and PPI inhibition on leukemic and non-leukemic hematopoiesis. MLL-AF9 cell lines were engineered to carry mutant *DOT1L* constructs with a defective AF9 interaction site or lacking enzymatic activity. Utilizing the defective AF9 interaction mutant cell lines, we observed complete disruption of DOT1L recruitment blocking DOT1L recruitment to critical target genes and inhibiting leukemic growth followed by downregulation of H3H79 methylation leading towards a decrease in *HOXA9* and *MEIS1* expression, cell differentiation, and apoptosis. To evaluate the overall impact of DOT1L loss in non-leukemic hematopoiesis, we first assessed the impact of acute *Dot1l* inactivation in adult mouse bone marrow. We observed a rapid reduction in myeloid progenitor cell numbers within 7 days, followed by loss of long-term hematopoietic

stem cells. Furthermore, WT and PPI-deficient DOT1L mutants but not an enzymatically inactive DOT1L mutant were able to rescue long-term hematopoiesis. These data show that the AF9-DOT1L interaction is dispensable in non-leukemic hematopoiesis. Our findings support targeting of the MLL-AF9—DOT1L interaction as a promising therapeutic strategy that is selectively toxic to MLL-driven leukemic cells.

2.2 Introduction

2.2.1 Mixed Lineage Leukemia

The *Mixed Lineage Leukemia 1* (*MLL1*) gene is located on chromosome 11q23 and encodes a histone 3 lysine 4 (H3K4) methyltransferase.[1,2] The *MLL1* locus contains a breakpoint region upstream of the SET domain that is involved in chromosomal translocations, generating oncogenic fusion proteins that combine its DNA binding *N*-terminus with one of over 80 different partners.[3] The most common fusion partners, AF9, ENL, AF4, and AF10, together account for >90% and 50% of all MLL-driven acute lymphoblastic and myeloid leukemia, respectively.[4] Leukemia driven by MLL-fusions account for approximately 10% of adult and 60% of infant leukemia, that is associated with a poor prognosis.[5-8] MLL-fusion interact with histone methyltransferase (HMT) <u>D</u>isrupter <u>of</u> <u>T</u>elomeric <u>s</u>ilencing <u>1</u>-<u>L</u>ike (DOT1L) directly or indirectly in macromolecular complexes that promote transcriptional elongation, including ENL-associated protein (EAP, containing AF4, AF5, AF9, AF10, ENL, DOT1L, and pTEFb); AEP (containing AF4, AF5, ENL, and pTEFb); super elongation complex (SEC, containing AF4, AF9, ENL, AFF4, ELL1, and pTEFb), and DotCom (DOT1-L complex, containing DOT1L, AF9, ENL, AF10, AF17, and several WNT pathway modifiers).[9-13] Despite certain variations in these reported multi-protein complexes, they collectively recruit the DOT1L to MLL-target genes, which is required for leukemogenesis. DOT1L is the only HMT known to catalyze the mono-, di- and trimethylation of histone H3 at lysine 79 (H3K79) that shows a high correlation with active gene transcription.[14] DOT1L recruitment by MLL-fusions leads to abnormal methylation of H3K79 at *MLL*-target genes and enhanced expression of a characteristic set of genes that drive leukemogenesis, including *HOXA9* and *MEIS1*.[15-17] Inhibiting the enzymatic activity of DOT1L by genetic ablation or small-molecule inhibition was sufficient to suppress

leukemogenesis in preclinical models of MLL-fusion leukemia validating DOT1L as a promising therapeutic target.[15,18-20]

2.2.2   DOT1L enzymatic inhibitor in clinical trials

Pinometastat (EPZ-5676), a potent DOT1L enzymatic inhibitor, and its analogs show selective inhibition of DOT1L's H3K79me activity in MLL-fusion cell lines and murine leukemia models, further validating DOT1L as a therapeutic target in MLL-fusion leukemia.[21-24] These promising results led to the initiation of phase 1 clinical trials. The first trial was a dose escalation trial to monitor for toxicity, optimal dose and efficacy in adult patients with relapsed/refractory leukemia. Out of 49 patients, only 6 had an objective response determined by morphologic CR, cytogenic CR, PR and resolution of leukemic cutis. Even though globally H3K79me2 was reduced, inhibition of H3K79 dimethylation at *HoxA9* and *Meis1* loci varied from 13-91%. Despite issues with efficacy and incomplete H3K79me2 across patients, some patients benefited from DOT1L enzymatic inhibition.[25] In addition to the initial trial in adults, a subsequent phase 1 trial in children reported ~40% of patients having a reduction in peripheral and bone marrow blasts, although transient. This trial also noted adverse events in >15% of the patients including anemia, thrombocytopenia and leukopenia with no objective responses.[26] Together, both trials showed suboptimal efficacy, although some patients derived benefit when H3K79me2 was reduced. These studies suggest that DOT1L is a valid therapeutic target, and that more complete global suppression of H3K79me may be desirable. Conversely, DOT1L's enzymatic activity regulates diverse cellular functions including DNA repair and cell cycle regulation, cardiac function, embryogenesis, and hematopoiesis.[12,27-32] Taking into the consideration that DOT1L is essential in development and that a significant percent of MLL-

rearrangement leukemia patients are infants, it is important to develop an alternative, safer therapeutic strategy.

2.2.3   Targeting the AF9-DOT1L protein-protein interaction

In an attempt to better understand DOTL1 PPIs and gain information for small molecule design and targeting, our laboratory, we reported biochemical, biophysical and functional characterization of the PPIs between DOT1L and MLL fusions AF9/ENL.[33] The binding site in DOT1L that interacts with the ANC Homology Domain (AHD) domain of AF9 and ENL was mapped to a 10-amino acid region (amino acids 865-874), highly conserved in DOT1L from a variety of species. Alanine scanning mutagenesis revealed isoleucine 867 and isoleucine 869 of DOT1L as essential for the interaction between AF9/ENL and DOT1L. Importantly, functional studies show that the mapped AF9/ENL interacting site is essential for immortalization by MLLAF9 and DOT1L lacking the AF9 interacting residues (Δ10) showed significant reduction in colony formation similar to the effects of DOT1L enzymatic inactivation.[33] Consistent with our findings, a recent study reported that DOT1L has three AF9 binding sites: 638-647 (site 1) and 879-888 (site 3) in addition to the site 2, 865-874, identified in our study (Figure 2-1A).[34] Interestingly, binding motifs at site 2 and site 3 have almost identical sequence and represent the high-affinity motif in DOT1L. This study further confirmed that DOT1L recruitment by binding to AF9 is necessary for the colony-forming ability of MLL-AF9 and hematopoietic transformation.[34] In addition, Kuntimaddi et al. observed that the degree of DOT1L recruitment to the MLL-AF9 fusion proteins differentially affects H3K79me2 and me3 levels at certain subsets of MLL-AF9 target genes. Recently we reported a class of peptidomimetics based on the 7mer DOT1L peptide, providing a proof-of-concept for development of nonpeptidic compounds

to inhibit DOT1L activity by targeting its recruitment and the interactions between DOT1L and MLL-oncofusion proteins, AF9 and ENL.[35]

2.2.4   Goals for the study

In this study, we further investigate the importance of DOT1L recruitment by MLL-AF9 in MLL fusion protein transformation as well as in non-leukemic hematopoiesis. Using a genetic approach, we compared the inhibitory effects of disrupting the AF9-DOT1L interaction and DOT1L enzymatic activity in leukemia cells harboring the MLL-AF9 oncoprotein as well as in non-leukemic adult bone marrow. We show that the interaction between AF9 and DOT1L is critical for MLL-AF9 driven leukemia and blocking of this PPI inhibits H3K79 methylation at MLL-target genes, leading to downregulated expression of MLL-target genes, cell cycle arrest, apoptosis, and differentiation, in a similar way as the enzymatic inhibition. Furthermore, DOT1L enzymatic inhibition leads to the rapid depletion of hematopoietic progenitor cells and followed by loss of hematopoietic stem cells (HSCs) and hematopoietic failure. Importantly, in contrast to DOT1L enzymatic inhibition, disrupting the AF9-DOT1L PPIs in non-leukemic cells allowed for sustained hematopoiesis. Overall, this study is providing evidence that targeting DOT1L recruitment by AF9 and leaving the enzymatic activity intact is providing therapeutic advantages, particularly in regards to decreased possible side effects on hematopoiesis.
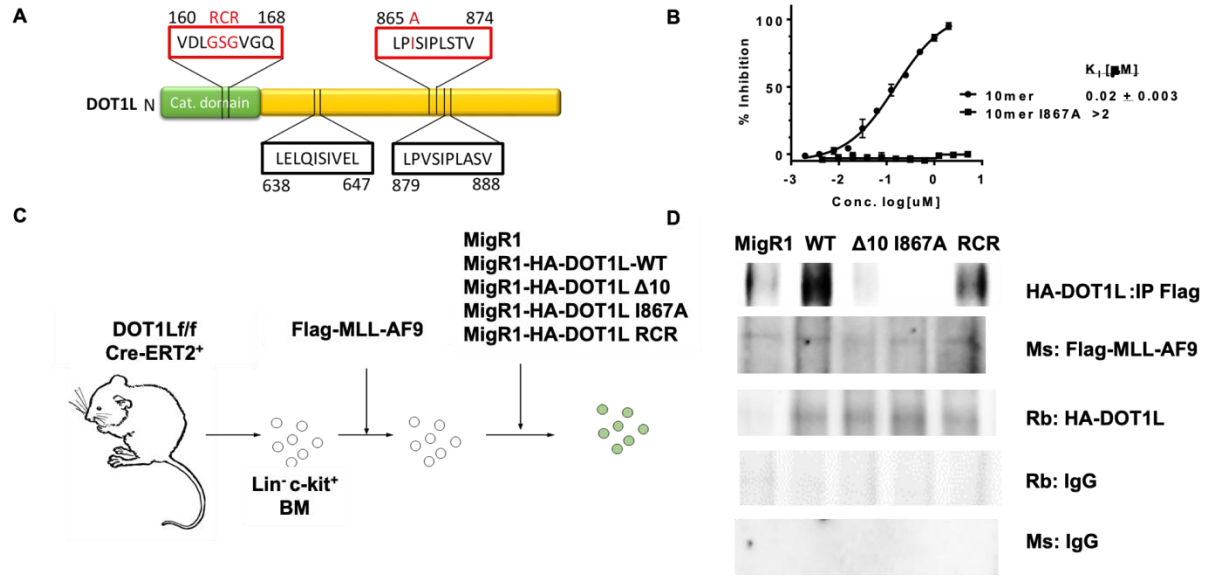
Figure 2-1 A single amino acid change blocks AF9-DOT1L protein-protein interaction.

(A) Protein diagram of DOT1L highlighting the catalytic domain mutation from residues 163-165 and AF9 binding domains at residues 638-647, 865-874 and 879-888. The red boxes indicate regions of the protein that were mutated for the following studies. (B) Fluorescence Polarization assay showing the that the 10mer peptide from residues 865-874 can compete for binding with AF9 with a fluorescein-labeled DOT1L peptide with a KI of 20nM; whereas, mutating Isoleucine 867 to alanine can no longer bind AF9 with a KI greater than 2 μM. (C) Schematic of the process of generating f/f DOT1L MLL-AF9 cell lines with different DOT1L constructs reintroduced. Cells were harvested from the bone marrow of f/f DOT1L CreERT2 mice. The bone marrow was lineage depleted and transduced will MLL-AF9. MLL-AF9 were selected by neomycin treatment then subjected to a secondary transduction with either MigR1 as an empty vector control of one of four DOT1L constructs including, DOT1l-WT, DOT1L-Δ10, DOT1L-I867A (Δ10 and I867A mutants block AF9-DOT1L interaction), and DOT1L-RCR (enzymatically inactive DOT1L protein). These cells were then GFP sorted and used for DOT1L excision studies. (D) co-Immunoprecipitation (co-IP) using Flag-MLL-AF9 to pulldown HA-DOT1L in the five established murine cell lines showing disruption of the MLL-AF9 and DOT1L protein-protein interaction in the Δ10 and I867A mutants cell lines as well as the MigR1 cell line where HA-DOT1L is not present with corresponding Rb (rabbit) and Ms (mouse) IgG controls.

2.3   Results

2.3.1   Characterization of MLL-AF9-transformed cells in the presence of different DOT1L constructs

Our previous work identified a direct interaction between the AHD of AF9 and ENL with the DOT1L 10 amino acid region, aa 865-874 (Figure 2-1A), deeming residues, L865, I867,

I869, and L871, as critical for their binding.[33] Using a fluorescence polarization (FP)-based assay, we confirmed that the DOT1L WT 10-mer peptide binds AF9 with a K_I of 20 nM, whereas, the mutant I867A 10-mer peptide does not show binding up to 10 μM (Figure 2-1B), demonstrating that the I867A point mutation is sufficient to disrupt the AF9-DOT1L interaction. An independent study confirmed the 10 amino-acid interaction site and identified two additional DOT1L motifs as AF9 binding sites: aa 638-647 and aa 879-888 (Figure 2-1A).[34]

Based on these studies and to further validate the consequences from blocking the AF9-DOT1L PPI in leukemic cells, we established several MLL-AF9-transformed cell lines. Bone marrow from floxed *Dot1l* mice,[30] were transduced with a leukemogenic MSCV-MLL-AF9 construct. Several *Dot1lf/f CreER(T2)*[+], MLL-AF9, cell lines were established carrying retroviral vectors expressing either HA-tagged wild type DOT1L (WT-DOT1L), DOT1L lacking 10 amino acid AF9 binding site, aa865-874 (Δ10-DOT1L), DOT1L mutated at I867 to alanine, which completely abrogates binding of DOT1L to AF9 (I867A-DOT1L), DOT1L with a GSG to RCR mutation in the SAM-binding domain lacking enzymatic activity (RCR-DOT1L), or MigR1 empty vector control (Figure 2-1C).[18,36,37] The expression of exogenous MLL-AF9 and that of all DOT1L constructs was validated by qRT-PCR, showing that all cell lines generated contained transcripts for both MLL-AF9 and DOT1L except the empty vector cell line expressing only MLL-AF9 (Figure 2-2A). This expression profile was confirmed by western blot detection of HA-tagged DOT1L and Flag-MLL-AF9 proteins as expected (Figure 2-2B).

To validate that our Δ10-DOT1L and I867A-DOT1L cell lines have blocked DOT1L recruitment in comparison to our negative control MigR1 cell line and our PPI intact cell lines WT-DOT1L and RCR-DOT1L, we used co-immunoprecipitation (co-IP). As expected, MLL-AF9 was unable to immunoprecipitate the Δ10 DOT1L and I867A DOT1L proteins, whereas

41

WT DOT1L and RCR DOT1L proteins with intact AF9-DOT1L interaction site had preserved interactions (Figure 2-1D). To further verify the interactions between AF9 and DOT1L in cells, a Duolink Proximity Ligation Assay (PLA) was used. Oligonucleotide PLA probes coupled to secondary antibodies that recognize the primary antibodies used to detect the HA (DOT1L constructs) and Flag (MLL-AF9) tagged proteins producing a red signal that can be detected using fluorescent microscopy. As expected, we detected the interaction between MLL-AF9 with WT DOT1L and RCR DOT1L since both of these DOT1L constructs retain the capability to interact with AF9. In contrast, the PLA signal was not observed in the Δ10-DOT1L and I867A-DOT1L mutant cell lines where DOT1L recruitment was inhibited (Figure 2-2C). Overall, these results demonstrate that established MLL-AF9 transformed cell lines with different exogenous DOT1L constructs can be used to study and compare the biological effects inhibiting DOT1L recruitment and enzymatic inhibition in the context of leukemogenesis and non-leukemic hematopoiesis.
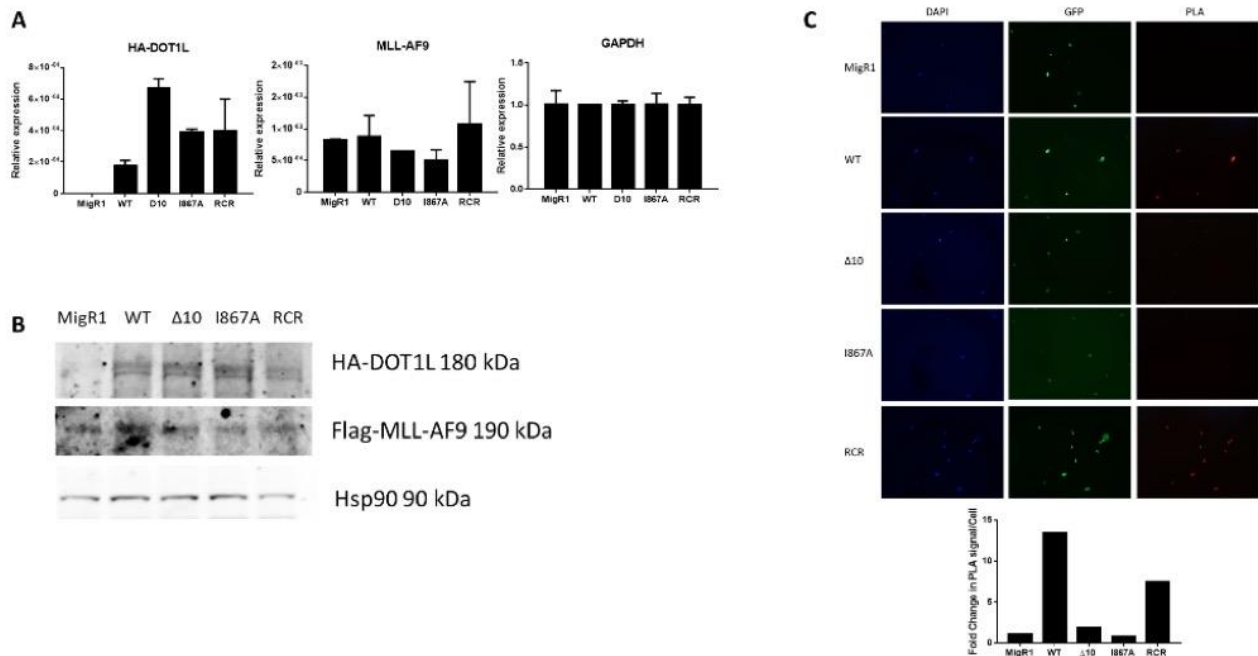
Figure 2-2 Validation of the expression and interaction of DOT1L constructs and MLL-AF9 in established murine cell lines.

(A) Expression levels of HA-DOT1L constructs and MLL-AF9 in the established cell lines. Cells containing mutant constructs have a higher level of transcript present than WT; however, the expression of wild type is sufficient for rescuing the phenotype of endogenous DOT1L deletion. However, no significant difference in MLL-AF9 expression and corresponding GAPDH control (B) Western Blot of lysate from MLL-AF9 cell lines with different DOT1L constructs showing that the HA-DOT1L and Flag-MLL-AF9 constructs are expressed and recognized by the HA and Flag antibodies that were using in subsequent experiments in the MLL-AF9 cell lines (C) Proximity Ligation Assay (PLA) of the Flag tagged MLL-AF9 murine cell lines with MigR1-HA-DOT1L constructs and average quantification of PLA signal per cell. The cells were fixed with EtOH and incubated with HA and Flag antibodies to capture the AF9-DOT1L interaction. The first column shows the DAPI staining showing the presence of cells followed by the GFP that is showing the cells that is expressing the DOT1L constructs and the last column show the PLA signal that is observed when the two antibodies are in close proximity indicating a protein-protein interaction. (Olympus IX83 Inverted Microscope; Original magnification x200)

2.3.2 Targeted disruption of protein-protein interactions between MLL-AF9 and DOT1L suppress leukemia cell growth and promotes their differentiation and apoptosis

To examine the importance of DOT1L recruitment by MLL-AF9 in leukemic cell proliferation, the above characterized *Dot1lf/f CreER-T2$^+$ MLL-AF9* cell lines were cultured in the presence of 4-OHT or the EtOH vehicle. These studies allowed us to evaluate and compare the effect of blocking the AF9-DOT1L PPI with the hallmark phenotypic response from DOT1L enzymatic inhibition. *Dot1l* excision was maintained as shown by genotyping the cell lines at the termination of the experiment (Figure 2-3A).
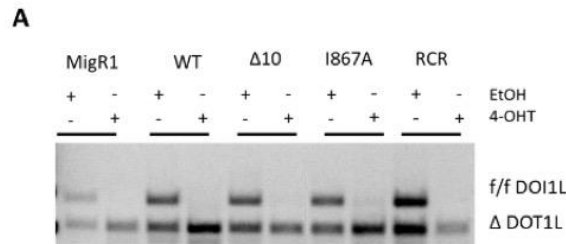
Figure 2-3 *Dot1L* excision is maintained throughout the course of the experiment.

(A) Genotyping of f/f DOT1L CreERT2 MLL-AF9 cell lines with DOT1L constructs showed excision of endogenous DOT1L for the duration of the experiment. The figure shows a

representative genotyping at Day 3. Genotyping primers GAAGTTCCTATTCCGAAGTT and GAACCACAGGATGCTTCAG: f/f Dot1l allele (927bp) and ΔDOT1L allele (244bp).[38]
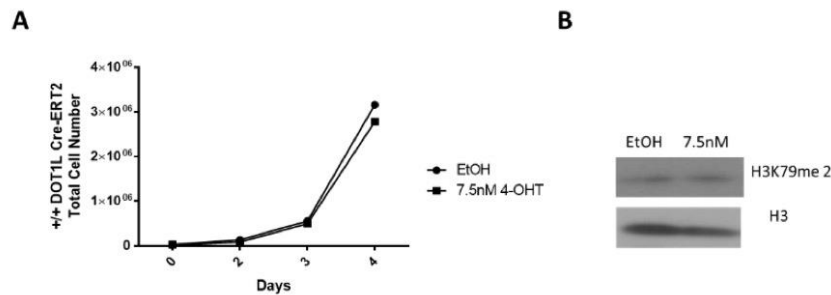
Figure 2-4: Assessing 7.5nM 4-OHT is toxicity and Cre induction in the DOT1L constructs and MLL-AF9 in established murine cell lines.

(A) WT DOT1L CreERT2 MLL-AF9 cells were treated with 7.5nM tamoxifen (4-OHT) showing no effect on cell proliferation (B) Western blot showing no effect on H3K79me2 after 4 days of 4-OHT treatment.

To confirm that growth defects were not due to 4-OHT toxicity, but due to *Dot1l* excision, *Dot1l*$^{+/+}$*CreER-T2*$^{+}$ murine cells were treated with 4-OHT, demonstrating no effect on cell proliferation or H3K79me2 methylation status of the cells (Figure 2-4A-B). As expected, upon treatment with 4-OHT, the MigR1 and enzymatically deficient RCR-DOT1L cell lines did not sustain cellular proliferation.[15,16,33,34] Control leukemia cells expressing WT-DOT1L showed a rescue of proliferation, confirming that the observed phenotype was due to loss of Dot1l and its HMT activity. Strikingly, the Δ10-DOT1L and I867A-DOT1L cell lines exhibited high sensitivity to blocking of the AF9 and DOT1L PPI showing a significant decrease in cell proliferation to the same extent as MigR1 and RCR-DOT1L cells (Figure 2-5A). These findings provide strong evidence that disrupting the interactions between MLL-AF9 and DOT1L by the previously identified minimum targeting domain (Δ10; 865-874 aa), and by a single point mutation (I867A) effectively inhibits MLL-AF9 cells proliferation.

To dissect the underlying mechanisms for the induced anti-leukemic effect and confirm the disruption of DOT1L recruitment to the MLL target gene loci, *HOXA9* and *MEIS1,* a

chromatin immunoprecipitation coupled with qPCR (ChIP-qPCR) was performed (Figure 2-5B). As expected, WT-DOT1L and RCR-DOT1L with an intact AF9-binding domain, were immunoprecipitated at the promoter region of both loci. Moreover, in Δ10-DOT1L and I867A-DOT1L leukemia cells, DOT1L localization to these loci was significantly reduced (Figure 2-5C). To confirm that loss of DOT1L recruitment was solely due to blocked recruitment by MLL-AF9, we also performed ChIP for Flag-MLL-AF9, showing its equal localization across the cell lines (Figure 2-5D). These results were also recapitulated at Intron 8 of *MEIS1* (Figure 2-6A).
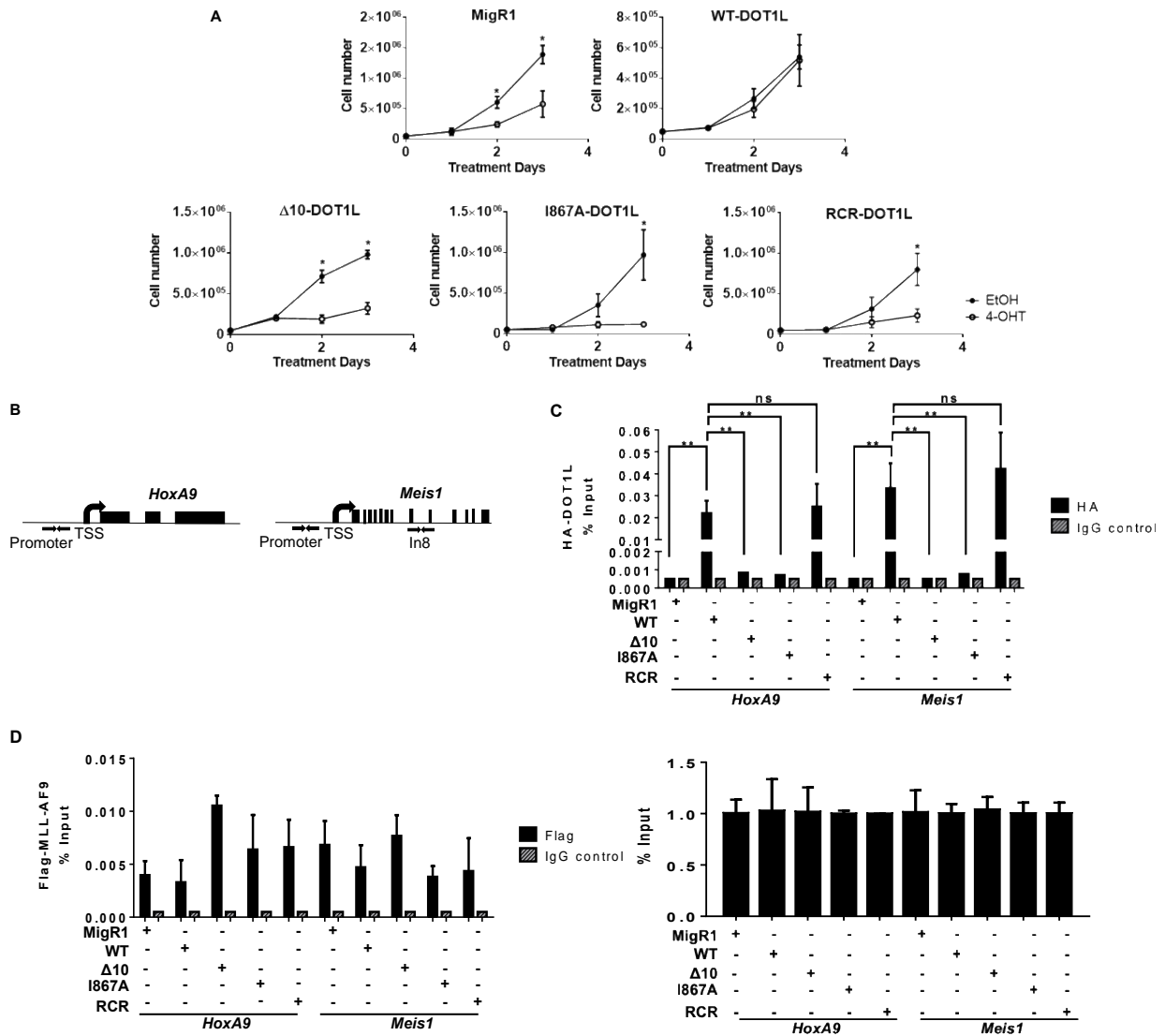
Figure 2-5 MLL-AF9 mediated proliferation is dependent on the interaction and recruitment of DOT1L.

(A) Cells were treated at day 0 and day 2 with 7.5nM tamoxifen (4-OHT) and monitored for cell proliferation. Mutating the AF9-DOT1L interaction site (Δ10 and I867A) significantly reduces cellular proliferation at a similar level to complete deletion (MigR1) or enzymatic inhibition (RCR) of DOT1L in MLL-AF9 cells. (n≥4) (B) Schematic representation of *HoxA9* and *Meis1* gene loci with arrows indicating the location of chromatin Immunoprecipitation qPCR (ChIP-qPCR) primers for the promoter region. (C) Using an anti-HA antibody, DOT1L constructs were immunoprecipitated, showing disruption of the MLL-AF9 and DOT1L interaction at the *HoxA9* and *Meis1* promoter. Only WT and RCR constructs with the intact PPI interaction site were detected. There was minimal to no enrichment over background for I867A and Δ10. (D) An anti-Flag ChIP-qPCR for MLL-AF9 showed no significant difference in localization to both HoxA9 and Meis1 promoters in each cell line with corresponding % input control (representative data from 2 independent experiments). Significance key calculated using a t-test on Prizm 6 software (ns P> 0.05, * P≤ 0.05, ** P≤ 0.01, *** P≤ 0.001, **** P≤ 0.0001).
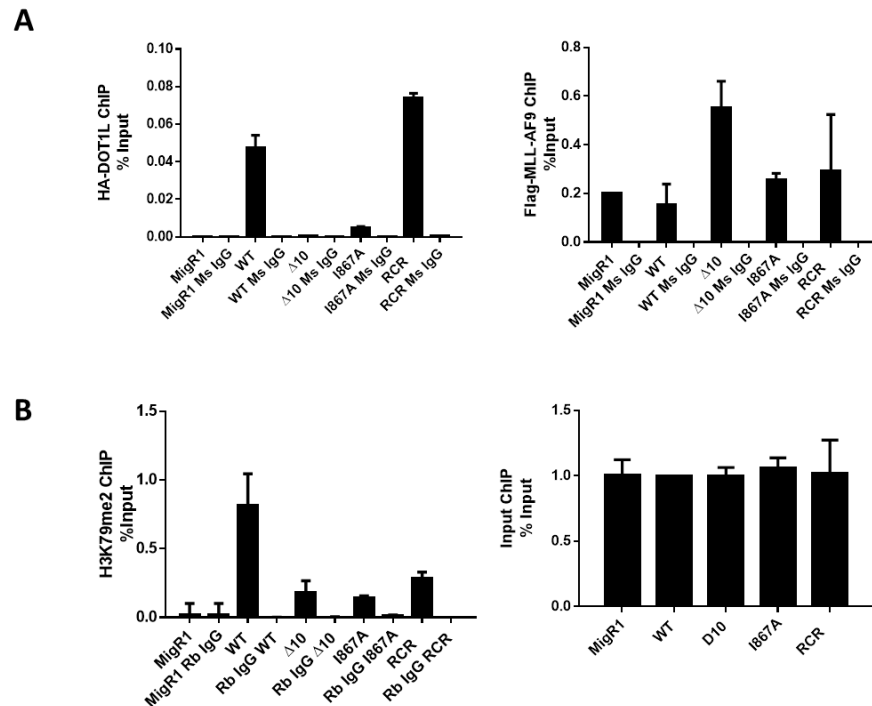
Figure 2-6 ChIP at Intron 8 of Meis1.

(A) ChIP-qPCR using an HA antibody, DOT1L constructs were pulled down showing discretion of the MLL-AF9 and DOT1L interaction at Intron 8 of *Meis1*. Only WT and RCR constructs with the intact PPI interaction site were detected. There was minimal to no enrichment over background for I867A and Δ10. A Flag ChIP-qPCR for MLL-AF9 showed no significant difference in localization to both HoxA9 and Meis1 promoters in each cell line. (B) With an

antibody for H3K79me2, we confirmed the decrease in methylation at the Meis1 gene locus t intron 8 in the MigR1, Δ 10, I867A and RCR cells in comparison to WT with corresponding % input control. (representative data from 2 independent experiments)

Previously, we observed that cells containing WT-DOT1L and Δ10-DOT1L with intact HMT domain were able to retain H3K79me2 after the first round of plating in colony-formation assay, while RCR-DOT1L failed to restore H3K79me2.[33] However, after the second round of plating there were not enough Δ10-DOT1L cells remaining to measure H3K79me, so no endpoint H3K79me was taken. In this study, we overcame that limitation and observed an overall slower change in global H3K79me2 in the PPIs mutant cells in comparison to cells expressing RCR-DOT1L. On day 2, Δ10-DOT1L and I867A-DOT1L showed modest changes in H3K79me2, while RCR mutation leads to a global loss of H3K79me2. By day 3, all engineered cell lines showed no detectable H3K79me2 (Figure 2-7A-B). Thus, different kinetic rate of histone methylation changes was observed on the global H3K79me2 level comparing constructs with impaired AF9 binding site, Δ10-DOT1L and I867A-DOT1L which showed modest decrease in this epigenetic mark, versus RCR-DOT1L cells with complete loss of H3K79me2 at day 2. To further assess the effects disrupting the DOT1L and AF9 interactions in MLL-AF9 leukemia cells expressing wild type or mutant DOT1L on H3K79me when proliferation is slowed, we performed ChIP-qPCR for H3K79me2. As expected, significant decreased H3K79me2 was identified on target genes, specifically at the *Hoxa9* and *Meis1* promoter region, as well as intron 8 of *Meis1* in all cell lines (Figure 2-6B and 2-7B). These findings collectively provide evidence that H3K79me2 mark on the target genes, *Hoxa9* and *Meis1*, is significantly decreased as a result of blocking DOT1L's recruitment leading to inhibition of cellular proliferation.

We further characterized the cause of proliferative defects in these cells and evaluated well-established mechanisms of cell death when DOT1L's function is genetically or pharmacologically inhibited.[19,39,40] Knowing that DOT1L primarily drives *HOXA9* and *MEIS1* expression for the initiation and maintenance of MLL-AF9 leukemia, we expected that with H3K79me2 decreased, we would see a profound decrease in MLL-target gene expression.[41-44] Indeed, we saw a significant decrease in *HOXA9* and *MEIS1* expression in Δ10-DOT1L and I867A-DOT1L leukemia cells, comparable to the changes induced by MigR1 and RCR-DOT1L. Importantly, these results correlated well with decreased H3K79me2 and blocked recruitment of DOT1L at both target loci (Figure 2-7C-D) In addition to downregulation of MLL-target genes, several studies showed that upon DOT1L enzymatic inhibition, cells harboring the MLL-AF9 fusion protein are driven to cell differentiation and apoptosis.[39] Thus, we explored if our cell lines would recapitulate this phenotype. Δ10-DOT1L and I867A-DOT1L cells revealed that inhibiting DOT1L recruitment led to cell cycle arrest and apoptosis in a similar manner as enzymatic inactivation (Figure 2-7E). In addition, Wright-Giemsa staining confirmed alterations in cell morphology from leukemic myeloblasts to differentiated cells when blocking DOT1L recruitment. This was further validated with concurrent increased expression of the monocyte differentiation marker, CD14, and decreased c-Kit (CD117), a hematopoietic stem/progenitor marker (Figure 2-7F). Altogether, these data provide functional confirmation of the importance and critical role of DOT1L recruitment for MLL-AF9-driven leukemogenesis, validating the PPI as a potential therapeutic target.
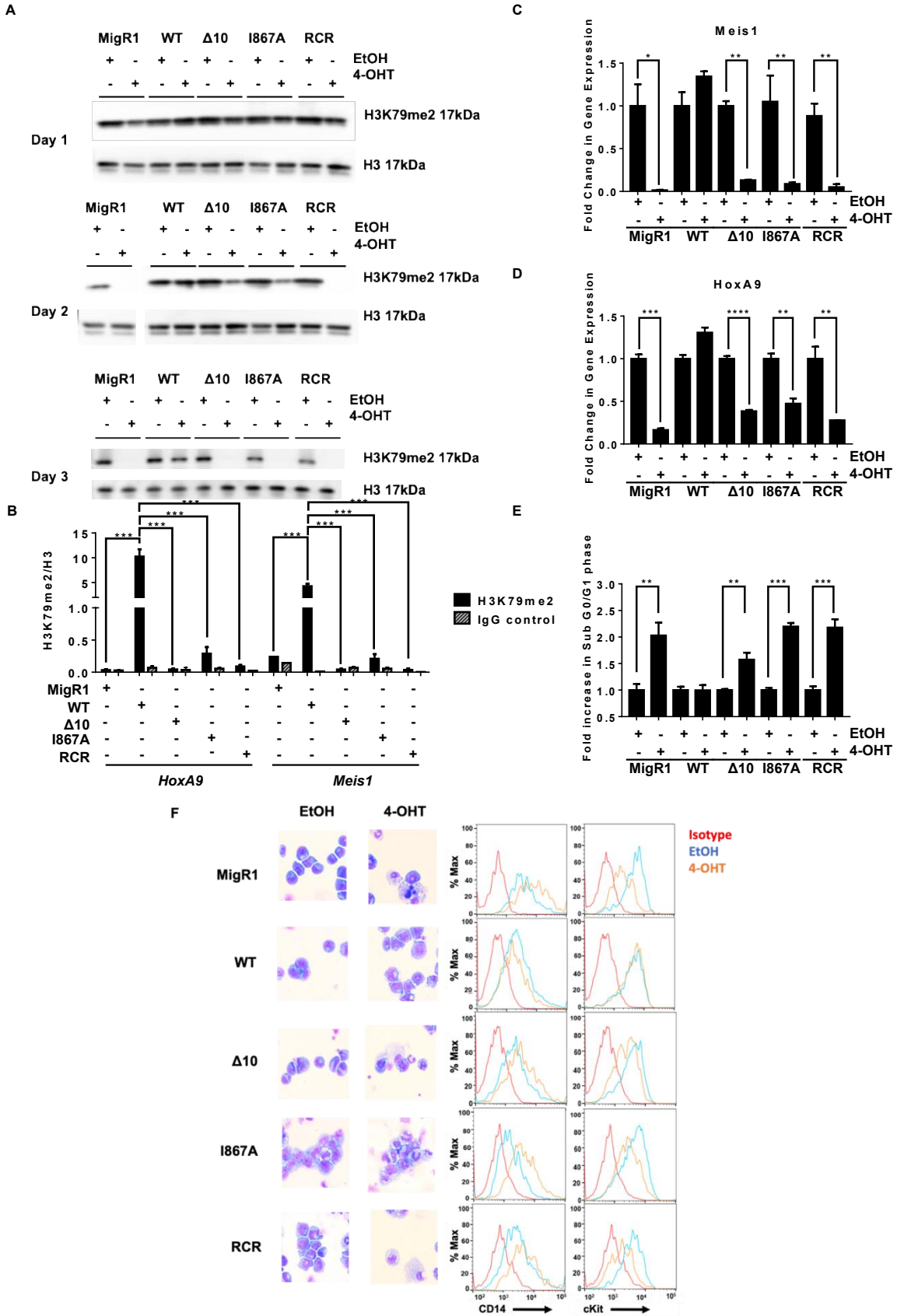
Figure 2-7 Disrupting the MLL-AF9 and DOT1L interaction has the same consequence on leukemogenesis as enzymatic inactivation of DOT1L.

(A) H3K79me2 for Days 1-3 of the proliferation assay showing a slower decrease in protein-protein inhibition cell lines than enzymatically inactivated or empty vector controls. (n≥2) (B) ChIP-qPCR for H3K79me2 for *HoxA9* and *Meis1* promoters plotted relative to H3 for each cell line, confirmed the decrease in H3K79me2 in the MigR1, Δ 10, I867A and RCR cells in comparison to WT. (representative data from 2 independent experiments) (C) The abundance of MLL target genes *Meis1* and (D) *HoxA9* mRNA is significantly reduced in 4-OHT-treated cells in comparison to EtOH-treated controls in the MigR1, Δ10, I867A, and RCR-transduced cells. Expression of these genes was not decreased in the WT control cell line when comparing treated and non-treated cells. (E) Apoptosis was measured by quantifying the percentage of cells in the sub G_0/G_1 phase of cell cycle. showing an induction of apoptosis in the MigR1, Δ10, I867A, and RCR cells upon 4-OHT treatment. (F) Wright-Giemsa stain of cells after 4-OHT treatment (Olympus IX83 Inverted Microscope; Original magnification x400) and corresponding flow cytometry for cell differentiation marker CD14 and progenitor marker c-Kit, showing cell differentiation in MigR1, Δ10, I867A, and RCR cells while WT cells retain their blast-like morphology and cell surface markers. (n≥2) Significance key calculated using a t-test in Prism 6 software (ns P> 0.05, * P≤ 0.05, ** P≤ 0.01, *** P≤ 0.001, **** P≤ 0.0001).

2.3.3 The role of DOT1L, its enzymatic activity and AF9-binding site in normal hematopoiesis

Constitutive and conditional *Dot1l* knockout models show that *Dot1l* is essential for embryonic development, as well as prenatal and postnatal hematopoiesis.[30-32] In past studies, the effects of *Dot1l* inactivation became apparent as early as 2 weeks post excision in vivo, showing a rapid loss of all three lineage populations as well as decreased hematopoietic stem and progenitor populations.[30,45,46] However, persistent unexcised progenitors could have influenced the magnitude of the functional effects. Here, we aimed to identify the early events following highly efficient *Dot1l* loss in adult murine hematopoiesis. To achieve a high degree of gene inactivation and avoid compensation by undeleted progenitors, we introduced a type I interferon-inducible *Mx1-Cre* allele to the *Dot1lf/f* background. The *Mx1-Cre* transgene encodes a Cre recombinase that yields robust excision of floxed genes upon poly(I:C) injection *in vivo*.[47,48] Mice were administered poly(I:C) with 3 subsequent injections and sacrificed 7 days after the

initial injection to inactivate *Dot1l* in the hematopoietic system. Bone marrow (BM) cellularity showed no significant differences between *Dot1l-WT* and *Dot1l-null* mice up to 1 week after *Dot1l* deletion, whereas at day 10 post-excision we started to observe a significant decrease in total BM cellularity (Figure 2-8A). We observed complete *Dot1l* excision upon poly(I:C) injection in *Mx1-Cre+* mice (Figure 2-9A), together with decreased H3K79 methylation at days 7 and 10 (Figure 2-8B), confirming that *Dot1l* was efficiently inactivated in these mice.

We next carefully examined the impact of *Dot1l* excision on hematopoietic stem cell and progenitor populations. For long-term hematopoietic stem cells (LT-HSCs) identified by the CD150+CD48– Lineage–Sca-1+c-Kit+ (LSK) phenotype and for the LSK cells, there was no significant initial alteration in total cell numbers in the *Dot1l*-excised mice at day 7 (Figure 2-9B).[49] Downstream myeloid progenitor subsets were also evaluated by fractionating the Lineage-c-Kit+ (LK) compartment with additional markers (CD41, CD105, CD150 and CD16/32).[50] We observed a significant decrease in the number of Pre-Megakaryocyte-erythroid (Pre-MegE:CD41-CD16/32-CD150+LK) and Granulocyte-Macrophage Progenitor (GMP:CD41-CD16/32+LK) in *Dot1l*-deficient mice (Figure 2-8C-D), with a significant decrease in CFU-GM colony-forming activity from *Dot1l*-deficient bone marrow (Figure 2-8E). These findings indicate that *Dot1l* loss affects hematopoietic progenitor function even ahead of its effects on HSCs.
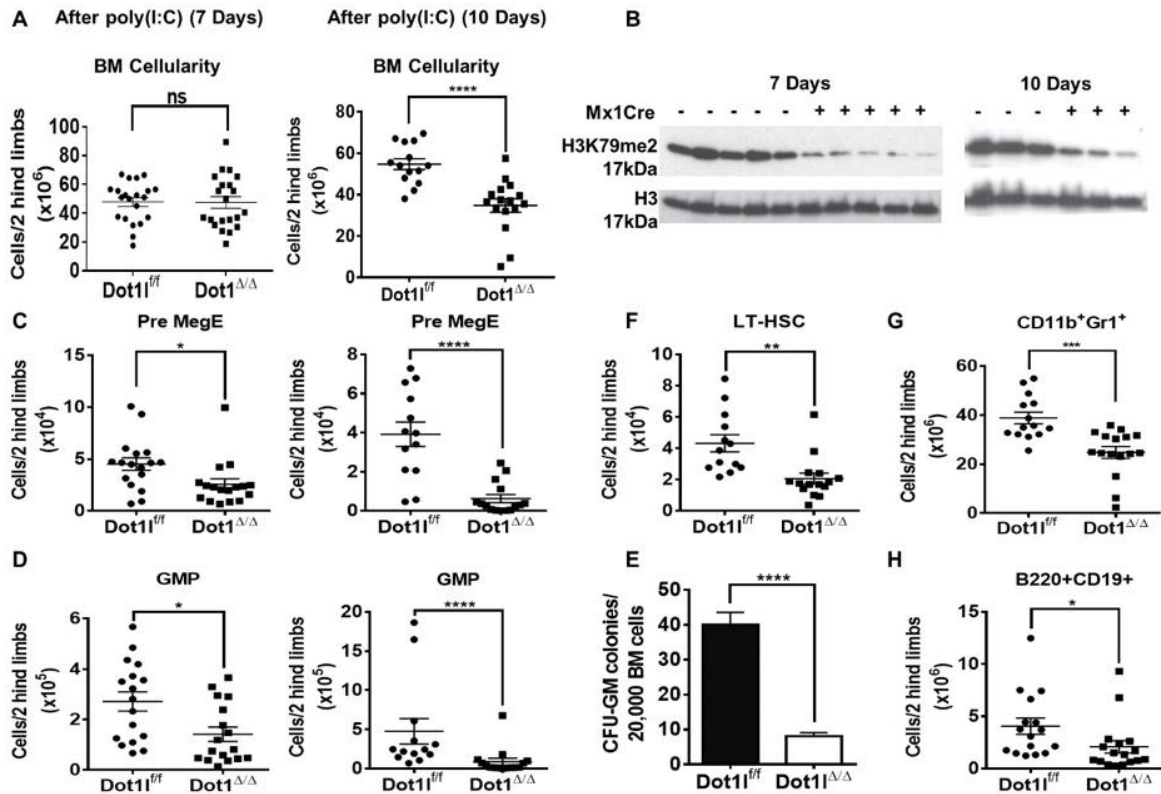
Figure 2-8 *DOT1L* inactivation in the adult bone marrow leads to rapid depletion of myeloid progenitors, followed by decrease in the numbers of hematopoietic stem cells

(A) (left) Bone marrow cellularity in Dot1lf/f Mx-Cre- and Dot1lf/f Mx-Cre+ mice 7 days post poly(I:C) induction (n=21/group, pooled from 5 independent experiments; mean +/- SEM). (right) Bone marrow cellularity decreases in Dot1lf/f Mx-Cre+ mice 10 days post poly(I:C) induction. (n=14-16/group, pooled from 3 independent experiments; mean +/- SEM). (B) Western blot shows decreased H3K79me2 in total BM at (left) day 7 and (right) day 10; (C) Flow cytometric analysis quantification shows Pre MegE (CD150+CD105-CD16/32-CD41-LK) are significantly decreased as early as (left) day 7 and continue to be depleted by (right) day 10. (D) Quantification of flow cytometric analysis showing granulocyte-macrophage progenitors (GMP) (CD16/32+CD150-CD41-LK) are significantly decreased as early as (left) day 7 and continue to decrease through (right) day 10. (E) Myeloid colony formation by wild-type vs Dot1l-null BM in CFU-GM assays (n=8/group with triplicate plates; mean +/- SEM; pooled from 2 experiments) showing a lack of colony formation potential in Dot1l Δ/Δ mice in comparison to Dot1l WT. (F-H) Profound decrease in LT-HSC, CD11b+Gr1+ BM myeloid cells, and B220+ CD19+B cells at day 10 post poly(I:C).
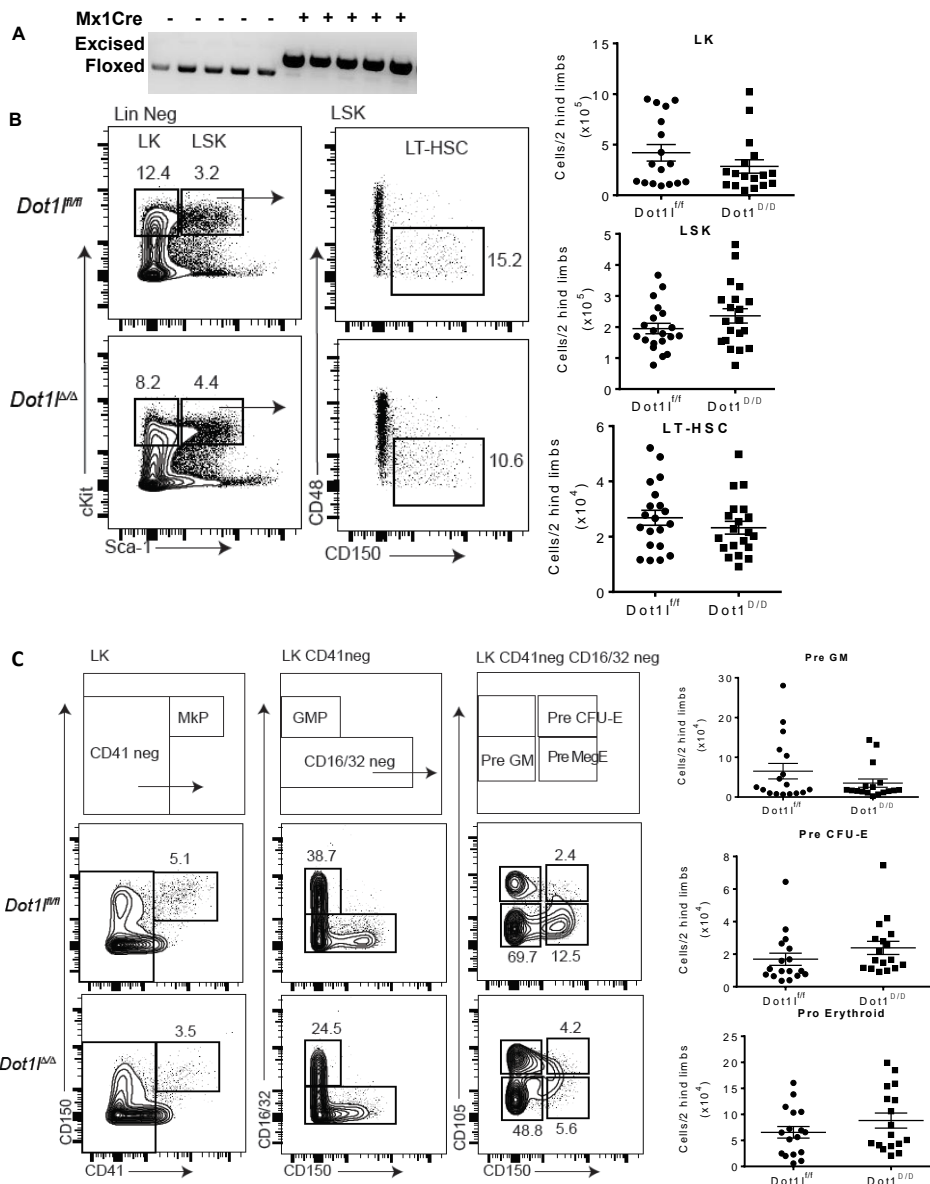
Figure 2-9 Day 7 of DOT1L inactivation shows early impacts some progenitor cell populations.

(A) Excision PCR showing high excision efficiency in Dot1l$^{f/f}$ Mx-Cre+ mice (n=5/group, representative of 5 independent experiments). (B) Flow cytometric analysis of LSK and LT-HSCs (CD150$^+$CD48$^-$LSK), showing no alterations in Dot1l-null HSCs 7 days post deletion (n=20/group; pooled from 5 independent experiments; mean +/- SEM). Quantification of LK, LSK and LT-HSC. (C) Flow cytometric analysis of progenitor cell compartments. MkP (CD41$^+$CD150$^+$LK), GMP (CD16/32$^+$CD150$^-$CD41$^-$LK), Pre CFU-E (CD150$^+$CD105$^+$CD16/32$^-$CD41$^-$LK), Pre MegE (CD150$^+$CD105$^-$CD16/32$^-$CD41$^-$LK), Pre GM (CD150$^-$CD105$^-$CD16/32$^-$

53

CD41⁻LK) Quantification shows a decrease in Pre-GM cells in mice lacking Dot1l and no changes in Pre CFU-E and Pro-Erythroid cells. (n=17/group; pooled from 5 independent experiments; mean +/- SEM).
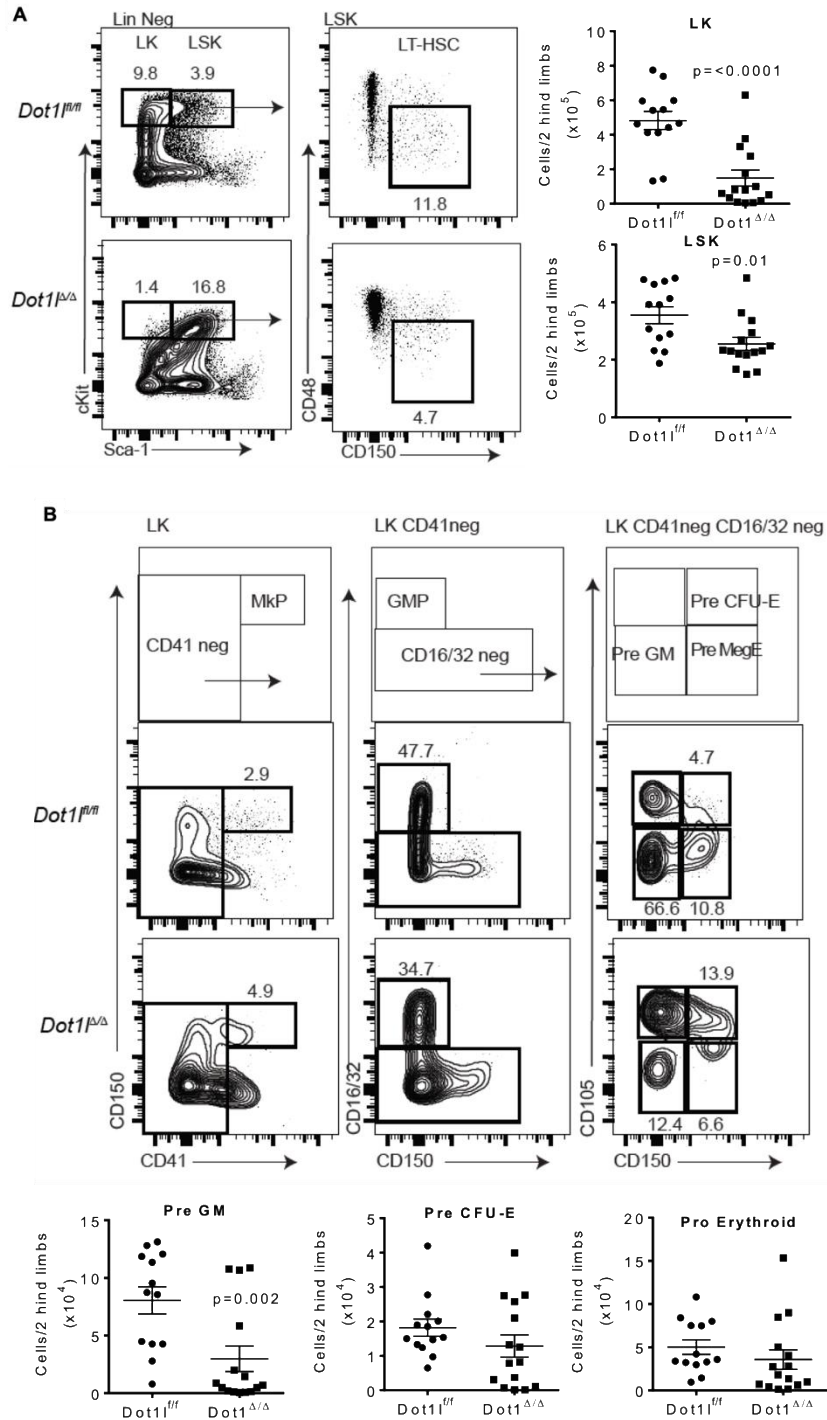
Figure 2-10 HSCs and progenitors are depleted 10 days after Dot1l inactivation.

(A) Flow cytometric analysis of LK, LSK and LT-HSCs (CD150⁺CD48⁻LSK), showing a decrease in Dot1l-null HSCs 10 days post deletion. (n=13-15/group; pooled from 3 experiments;

mean +/- SEM). Quantification of LK and LSK. (B) Flow cytometric analysis of progenitor cell compartments. MkP (CD41$^+$CD150$^+$LK), GMP (CD16/32$^+$CD150$^-$CD41$^-$LK), Pre CFU-E (CD150$^+$CD105$^+$CD16/32$^-$CD41$^-$LK), Pre MegE (CD150$^+$CD105$^-$CD16/32$^-$CD41$^-$LK), Pre GM (CD150$^-$CD105$^-$CD16/32$^-$CD41$^-$LK). Loss of Dot1l decreases Pre-GM, Pre CFU-E and Pro Erythroid progenitors. (n=13-15/group; pooled from 3 experiments; mean +/- SEM).

Since there was no initial alteration in HSCs, but clear depletion of progenitor cells as early as 7 days post *Dot1l* excision, we evaluated hematopoiesis at a later time point. At day 10, *Dot1l*-null mice had significant depletion in LK progenitors, LSK progenitors, LT-HSCs, and Pre-GM cells. (Figure 2-8H and 2-10A-B). Pro-Erythroid and Pre-CFU-E cells were also trending downward in numbers (Figure 2-10B). Furthermore, CD11b+Gr1+ myeloid and B220+CD19+ B cells significantly decreased (Figure 2-8G-H). These data are consistent with a profound effect of *Dot1l* loss on a broad range of primitive HSCs and progenitor cells.

We next evaluated whether inhibiting the AF9-DOT1L PPI or enzymatic inhibition would differ in effecting hematopoiesis. *WT-DOT1L, Δ10-DOT1L, I867A-DOT1L,* and *RCR-DOT1L* retroviral constructs were transduced *ex vivo* into *Mx-Cre+ Dot1l f/f* B6-CD45.2 mouse donor cells, in addition to a *NUP98-HOXA10*-mCherry construct. Introduction of NUP98-HOXA10 was used to enhance the proliferation of donor HSCs *ex vivo* after retroviral transduction, based on past work showing that NUP98-HOXA10 can dramatically increase HSC expansion without inducing transformation.[51,52] Indeed, cells transplanted in the absence of *NUP98-HOXA10* allowed for frequent host-derived reconstitution after *Dot1l* excision, which prevented efficient structure-function analysis of transduced donor-derived cells (not shown). First, we verified that NUP98-HOXA10 could not rescue the maintenance of bone marrow HSCs after *Dot1l* excision. We used a dual color readout system where cells derived from *Mx1-Cre+ Dot1Lf/f* B6-CD45.2 and *Mx1-Cre- Dot1Lf/f* B6-CD45.2 were transduced with either *Nup98HoxA10*-mCherry or *Nup98HoxA10*-eGFP. These 4 cell populations were then mixed into

two complementary groups with *Cre+* and *Cre-* hematopoietic stem cells expressing

complementary mCherry and eGFP *NUP98-HOXA10* constructs. These two groups were

transplanted into WT B6-CD45.1 recipient mice and used for endpoint analysis after *Dot1l*

excision (Figure 2-11A). LSK and myeloid cells from the *Mx1-Cre+ Dot1Lf/f* B6-CD45.2 mice

did not persist in the presence of Nup98HoxA10 regardless of the mCherry or eGFP reporter

construct (Figure 2-11B-C).
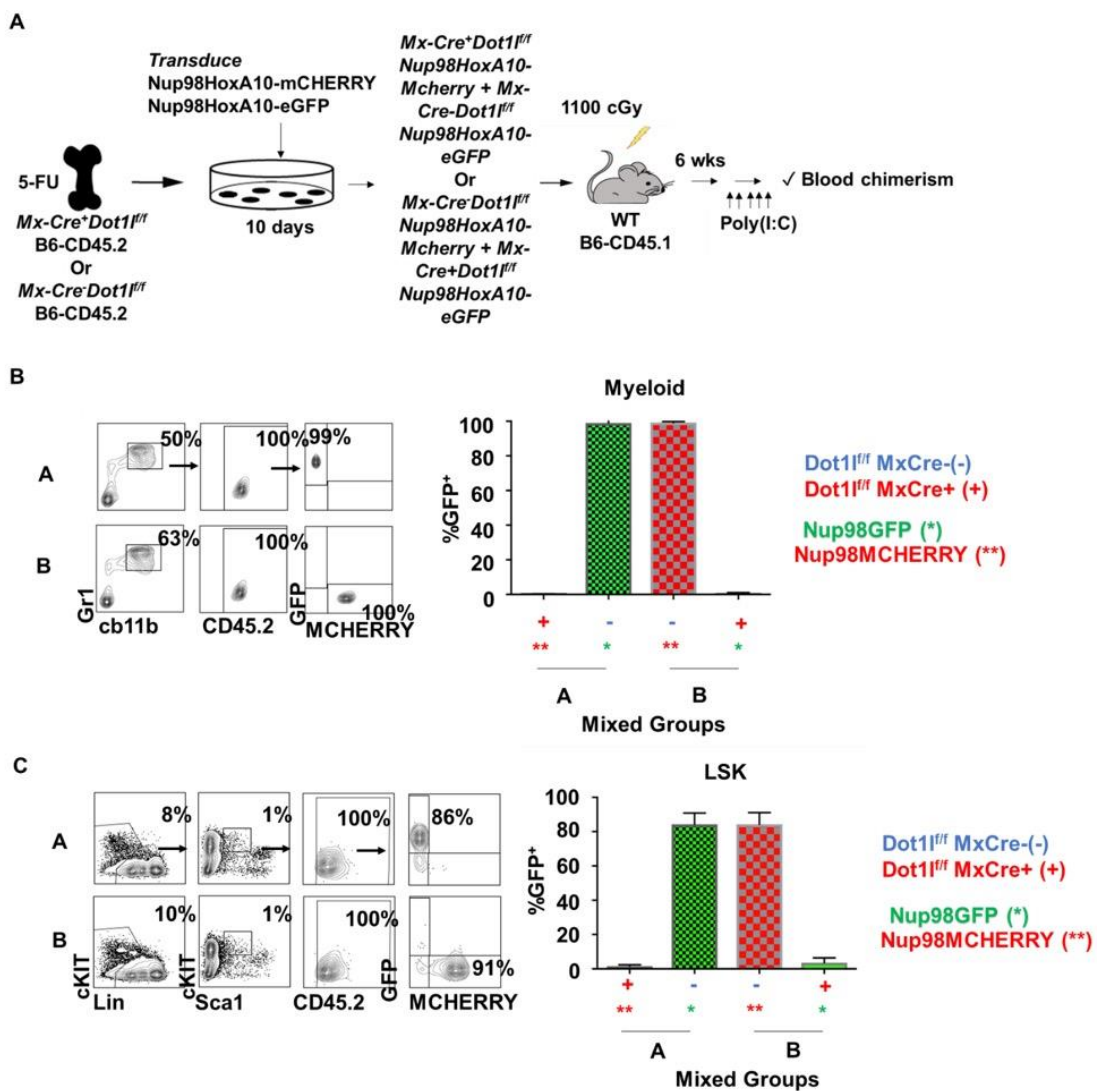
Figure 2-11 Nup98HoxA10 does not rescue DOT1L.

(A) Experimental schematic of Nup98HoxA10 control experiment where bone marrow from
Mx1-Cre+ Dot1f/f or *Mx1-Cre- Dot1f/f* B6-CD45.2 were transduced with *Nup98HoxA10-*

mCherry and *Nup98HoxA10*-eGFP. The cells were mixed where the Cre+ and Cre- cells had different Nup98HoxA10 colors to follow their growth *in vivo*. Cell mixtures were transplanted into WT B6-CD45.1 mice and 5 injections of poly(I:C) was administered 6 weeks post-transplant. (B) (left)Representative flow panels showing the myeloid population is only comprised of *Mx1-Cre- Dot1f/f Nup98HoxA10*; whereas, *Mx1-Cre+ Dot1f/f* B6-CD45.2 *Nup98HoxA10* cells are not able to grow *in vivo*. (right) Quantification of all flow data. (C) (left)Representative flow panels showing the LSK population is only comprised of *Mx1-Cre-Dot1f/f Nup98HoxA10*; whereas, *Mx1-Cre+ Dot1f/f* B6-CD45.2 *Nup98HoxA10* cells are not able to grow *in vivo*. (right) Quantification of all flow data.

After *ex vivo* expansion, CD45.2+ hematopoietic progenitors carrying *NUP98-HoxA10* plus one of the *DOT1L* constructs were transplanted into irradiated B6-CD45.1 recipient mice allowing for a clear delineation of host and recipient-derived cells. After hematopoietic reconstitution, poly(I:C) was administered (Figure 2-12A). Blood from the recipient mice was collected 16-weeks post poly(I:C) injection and analyzed by flow cytometry for CD45.2+ donor-derived CD11b+Gr1+ myeloid cells with both mCherry and eGFP colors (Figure 2-12B). Rates of transduction by the DOT1L constructs differed between the groups as shown by the various percentages of eGFP+mCherry+ at baseline before poly(I:C) injection. However, the presence of WT-DOT1L, Δ10-DOT1L, and I867A-DOT1L in donor cell populations led to an increased representation for eGFP+mCherry+ cells in the blood after loss of endogenous *Dot1l*, indicating that these cells were selected on the basis of exogenous DOT1L expression, and thus that these mutant forms of DOT1L could rescue the function of endogenous *Dot1l*. In contrast, empty vector and RCR-DOT1L did not induce a systematic increase in eGFP+ cells from 2 to 16 weeks post poly(I:C) injection (Figure 2-12C and Figure 2-13A). This trend was also observed in circulating B cells (Figure 2-12D-E and Figure 2-13B). We observed that the LT-HSC cell population was made up entirely of donor–derived WT-DOT1L, Δ10-DOT1L, and I867A-DOT1L, but not RCR-DOT1L and eGFP cells (Figure 2-12F). We then tested these mice for persistent excision of endogenous *Dot1l* to account for the selection of rare escapees. As

observed by PCR analysis the donor cells in the eGFP and RCR-DOT1L mice retained endogenous *Dot1l* which sustained their hematopoiesis (Figure 2-12G). In contrast, short-lived myeloid cells harvested at the end of the experiment still had an excised endogenous *Dot1l* locus when rescued with WT-DOT1L, Δ10-DOT1L, or I867A-DOT1L. Herein, we demonstrate that targeting the AF9-DOT1L PPI shows no profound effects on the maintenance of non-leukemic hematopoiesis in adult mice and exhibits significant consequences on leukemogenesis. Thus, these findings validate the AF9-DOT1L PPI as a therapeutic target that overcomes the on-target side effects of directly targeting DOT1L activity.
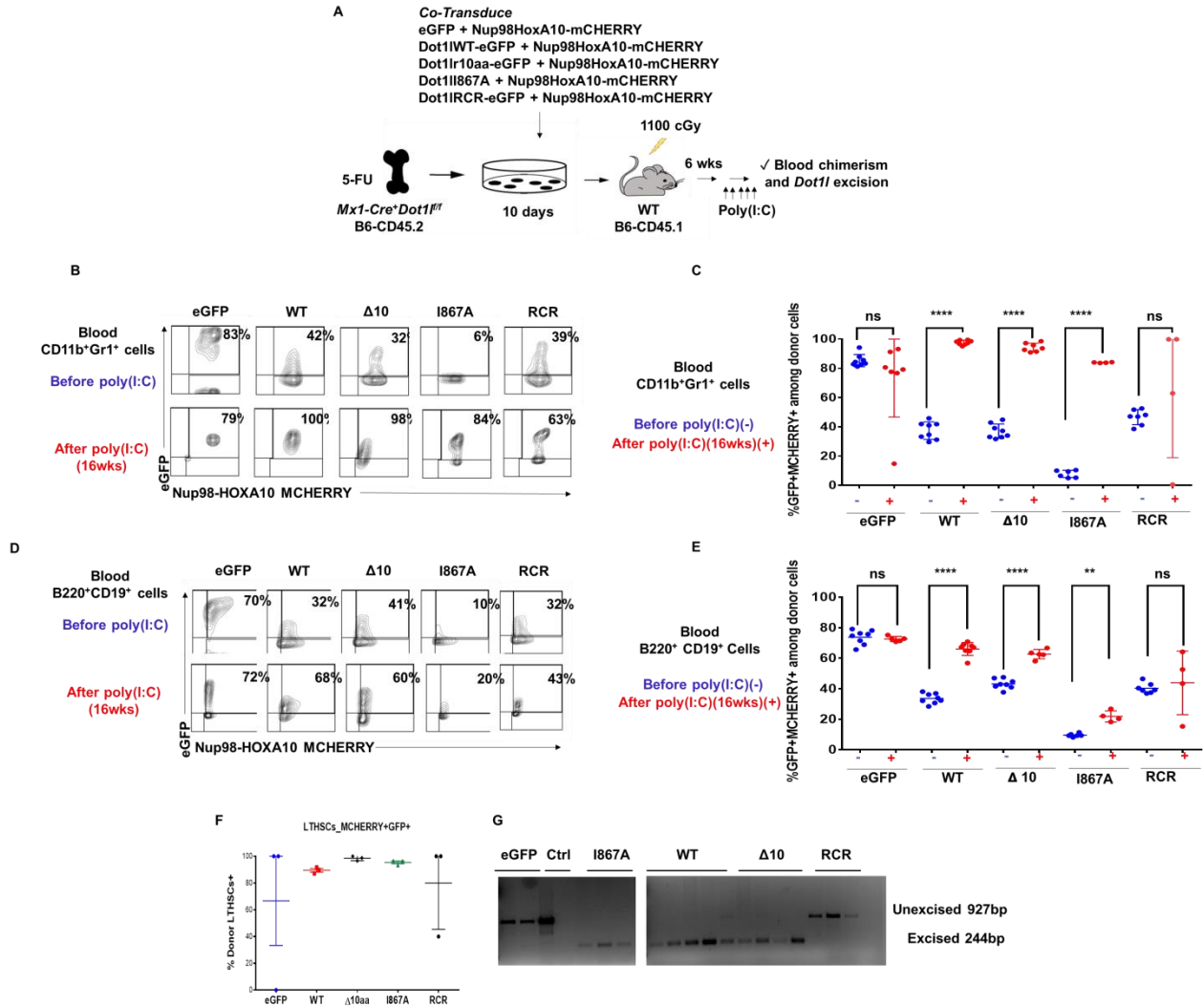
Figure 2-12 DOT1L's enzymatic activity is essential in hematopoiesis, but its AF9-binding domain is dispensable.

(A) Experimental approach. BM harvested from 5-FU-treated *Mx-Cre*[+]*Dot1l*[f/f] B6-CD45.2 donors was co-transduced ex vivo with MSCV-based constructs expressing NUP98-HOXA10-mCherry and eGFP alone vs. eGFP + DOT1L-WT, DOT1L-D10, DOT1L I867A or DOT1L-RCR. After ex vivo expansion, these cells were transplanted into irradiated B6-CD45.1 recipients. After hematopoietic reconstitution, poly(I:C) was administered to inactivate endogenous *Dot1l,* followed by analysis of chimerism and *Dot1l* excision; (B) Representative examples of flow cytometric data. Numbers show the percentage of mCherry^{+}eGFP^{+} in blood myeloid cells; (C) Flow cytometric analysis of blood CD45.2^{+} donor-derived CD11b^{+}Gr1^{+} myeloid cells for mCherry and eGFP expression, before (blue) and 16 wks after (red) poly(I:C) (5 i.p. doses). Data from individual mice are shown. Increased representation of cells expressing DOT1L-WT, DOT1L-D10, and DOT1L-I867A, but not eGFP or DOT1L-RCR was seen after poly(I:C); (D) Flow cytometric analysis of blood CD45.2^{+} donor-derived B220^{+}CD19^{+} myeloid cells for mCherry and eGFP expression, before (blue) and 16 wks after (red) poly(I:C) (5 i.p. doses). Data from individual mice are shown. Increased representation of cells expressing DOT1L-WT, DOT1L-D10, and DOT1L-I867A, but not eGFP or DOT1L-RCR was seen after

poly(I:C); (E) LT-HSCs after poly(I:C) administration at the termination of the study. DOT1L-WT, DOT1L-D10 and DOT1L-I867A recipients have LT-HSCs that are comprised of the donor cells; whereas, eGFP or DOT1L-RCR are not except for the unexcised mice; (F) PCR analysis of *Dot1l* excision in sort-purified blood CD45.2$^+$mCherry$^+$eGFP$^+$ myeloid cells 20 weeks after poly(I:C) administration. DOT1L-WT, DOT1L-D10 and DOT1L-I867A recipients had ongoing myelopoiesis with fully excised *Dot1l*, while eGFP and DOT1L-RCR recipients had selected cells escaping *Dot1l* inactivation. MW, molecular weight marker.
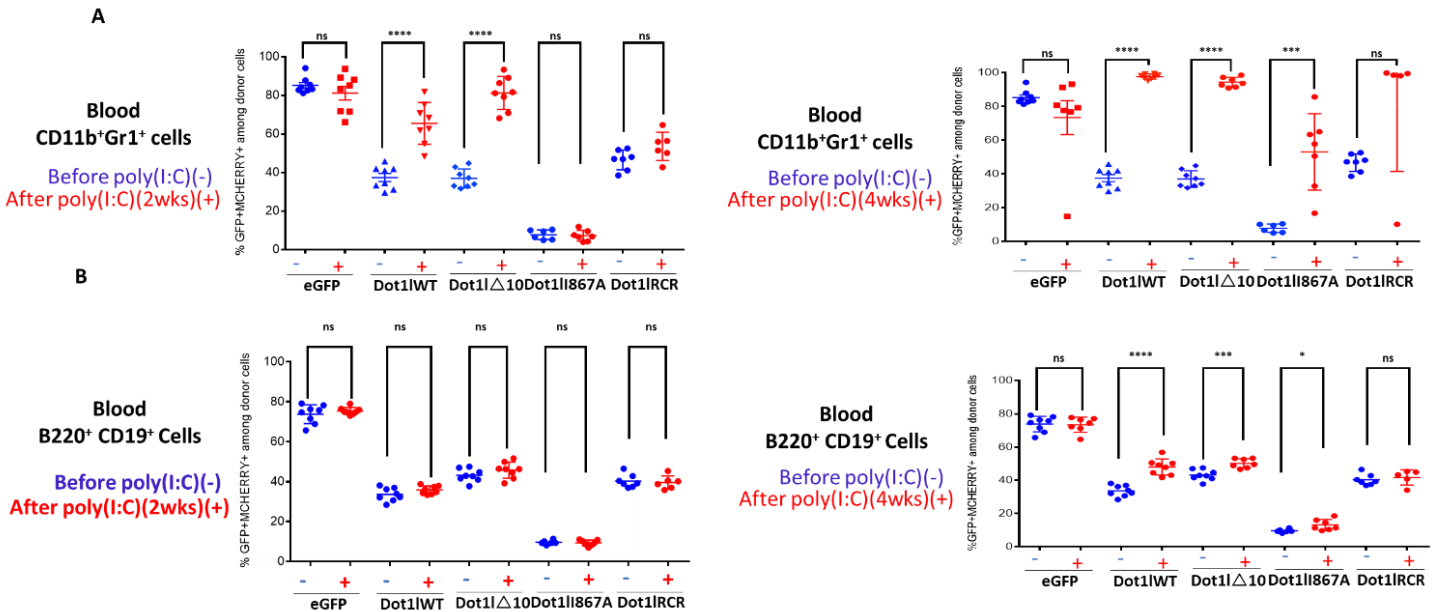
Figure 2-13 The AF9-binding domain of DOT1L is dispensable for adult hematopoiesis.

(A) (top) Quantification of flow data showing the donor *Mx1-Cre+ Dot1f/f Nup98HoxA10* DOT1L WT and DOT1L Δ10 cells proliferate and repopulate the myeloid cells in the host mice 2 weeks post poly(I:C) injection. DOT1L I867A cells maintained constant due to the low starting cell number. *Mx1-Cre+ Dot1f/f Nup98HoxA10* eGFP and DOT1L RCR cells showed no significant changes due to unexcised endogenous *Dot1* escapee cells. (bottom) Quantification of flow data showing the donor *Mx1-Cre+ Dot1f/f Nup98HoxA10* B220$^+$ CD19$^+$ B cells did not have significant changes compared to baseline 2 weeks post poly(I:C) injection. (B) Quantification of flow data showing the donor *Mx1-Cre+ Dot1f/f Nup98HoxA10* DOT1L WT, DOT1L Δ10, and DOT1L I867A cells proliferate and repopulate the myeloid cells in the host mice 4 weeks post poly(I:C) injection. *Mx1-Cre+ Dot1f/f Nup98HoxA10* eGFP and DOT1L RCR cells showed no significant changes due to unexcised endogenous *Dot1* escapee cells. (bottom) Quantification of flow data showing the donor *Mx1-Cre+ Dot1f/f Nup98HoxA10* B220$^+$ CD19$^+$ B cells DOT1L WT, DOT1L Δ10, and DOT1L I867A cells proliferate and repopulate the B cells in the host mice 4 weeks post poly(I:C) injection. (C) (left) Bone marrow (BM) cellularity after starting poly(I:C) administration (5 i.p. injections) at the termination of the study showing all mice in the various test groups had similar BM cellularity noting the eGFP and RCR were comprised on unexcised cells (Figure 2-12F). (right) Thymic cellularity after starting poly(I:C) administration (5 i.p. injections) at the termination of the study showing an increase in thymic cells derived from *Mx1-Cre+ Dot1f/f Nup98HoxA10* DOT1L WT, DOT1L Δ10, and DOT1L I867A cells and not eGFP or DOT1L-RCR cells.

2.4 Conclusions

MLL-AF4, MLL-AF9, MLL-ENL, and MLL-AF10 are the most common MLL-fusions proteins that reside in multiprotein complexes involved in transcriptional activation/elongation.[53,54] One of the mechanisms by which MLL-fusion-target genes are constitutively activated is by the recruitment of DOT1L.[55] DOT1L enzymatic inhibition emerged as an attractive therapeutic target leading to the development of Pinometastat and other SAM competitive inhibitors.[40,56-58] In the clinic, Pinometastat showed some promise with a few patients reaching an objective response; however, H3K79me downregulation was variable.[25,26] These trials further confirmed DOT1L's HMTase activity as critical for leukemogenesis, but there is still concern about the potential on-target toxicities of prolonged global H3K79me inhibition. Pre-clinical studies have demonstrated that there is a strong functional interconnection between complexes formed by MLL -fusion proteins and DOT1L illustrating the central role of the DOT1L recruitment and H3K79 methylation in leukemogenesis.[29,55] We and others have characterized the PPIs between fusion proteins AF9/ENL and DOT1L on a biochemical, structural and functional level as novel drug targets for MLL-fusion luekemia.[9,33,34]

In this study, we further explore the therapeutic value of targeting DOT1L recruitment by MLL-AF9 in AML and elucidate the role of this PPI in non-leukemic hematopoiesis. For this purpose, we established MLL-AF9 transformed leukemia cell lines transduced with several different DOT1L constructs, including wild type and mutants to disrupt the PPIs and enzymatic activity. Consistent with the essential role of DOT1L and H3K79 methylation in the initiation and maintenance of MLL-rearranged leukemia,[15-17] the MLL-AF9 interaction with DOT1L play crucial role for MLL-AF9 transformed leukemia cells, in a similar manner to that seen with inhibition of the DOT1L enzymatic domain (Figure 2-5). Our work demonstrates that by

blocking the PPIs between MLL-AF9 and DOT1L only by a single point mutation in the AF9 binding site of DOT1L, 1867A, we can mimic the phenotype obtained by the enzymatic inhibition of DOT1L leading to impaired leukemic cell growth, inducing differentiation and apoptosis (Figure 2-7). As expected, DOT1L mutant proteins, Δ10-DOT1L and I867A-DOT1L, disrupted the MLL-AF9 and DOT1L interactions, thus blocking DOT1L recruitment to the target *Hoxa9* and *Meis1* gene loci, leading to significant decrease in H3K79me2 in the promoter regions of these genes. Importantly, evaluation the global H3K79 methylation provided insights into the slower dynamic rate of the H3K79me2 loss in these cells, in comparison to the RCR-DOT1L cells. This suggests that disruption of the AF9/ENL-DOT1L might provide a selective targeting of MLL fusion proteins and bring advantages and fewer adverse effects in comparison with the enzymatic inhibition. Overall, these data point to a potential novel therapeutic strategy and benefit for the treatment of patients bearing the MLL-AF9 translocation by blocking the recruitment of DOT1L.

To identify and elucidate the potential therapeutic benefits of this therapeutic strategy we investigated the effect of DOT1L mutants with impaired AF9 binding site on non-leukemic hematopoiesis. There have been several reports indicating adverse effects of DOT1L loss on normal hematopoiesis in mice, after two or more weeks of *Dot1l* excision.[30,31] In our studies, the focus was on assessing the early effects of *Dot1l* loss on hematopoiesis and identify the cell populations that are the most affected. We found that as early as one week after *Dot1l* excision, myeloid progenitor cells and other progenitor populations were most sensitive, while total BM cellularity remained normal. By day 10, BM cellularity significantly decreased with a significant loss of LT-HSCs cells and progenitor cells. These findings are in agreement with previous studies showing profound effects on progenitor cell populations in mice lacking DOT1L at later

time points.[30,31] The rapid effects on adult hematopoiesis upon *Dot1l* inactivation point towards the potential of on target side effects on hematopoiesis when enzymatically inhibiting DOT1L. Interestingly, in our studies using Δ10 and I867A DOT1L mutants, which are not recruited to target genes in leukemic cells, our results demonstrated a potent reconstitution of the non-leukemic bone marrow in these mice. On the contrary, the RCR and empty vector derived cells revealed impaired bone marrow reconstitution with strong selection for progenitors that escaped excision of endogenous *Dot1l*. These data suggest that non-leukemic hematopoiesis can be sustained when the PPI between MLL-AF9 and DOT1L is disrupted, demonstrating that potential therapeutic advantages might be afforded by selective targeting of these PPIs.

We have successfully developed the first class of peptidomimetics that target PPIs between DOT1L and MLL-fusion partners, AF9 and ENL, based on the 10mer DOT1L peptide.[35] In this series of peptidomimetics, compound **28** was the most potent in terms of binding affinity, with a Ki value of 9 nM against AF9 recombinant protein (Chapter 3).[35] Performing a coimmunoprecipitation (co-IP) experiment in HEK 293T cells co-transfected with Flag-DOT1L and Myc-CxxC-AF9, we demonstrated that **28** recognizes and binds to the cellular AF9 protein, and effectively inhibits the DOT1L−AF9 interactions in cells (Figure 2-14A). Together, the findings of this study provide further evidence for targeting the AF9-DOT1L interaction as a promising therapeutic strategy. We further propose that targeting these PPIs with an inhibitor like compound **28** DOT1L recruitment will be blocked leading to downregulation of the MLL-target genes by decreasing the H3K79 methylation, followed with induced cell differentiation and apoptosis. Importantly, the DOT1L enzyme activity will be left intact and will be able to carry out its normal functions in the hematopoietic compartment (Figure 2-14B). This

study provides proof-of-concept for further development of nonpeptidic, cell-permeable, compounds that will inhibit the AF9-DOT1L PPI in MLL-AF9 leukemia.
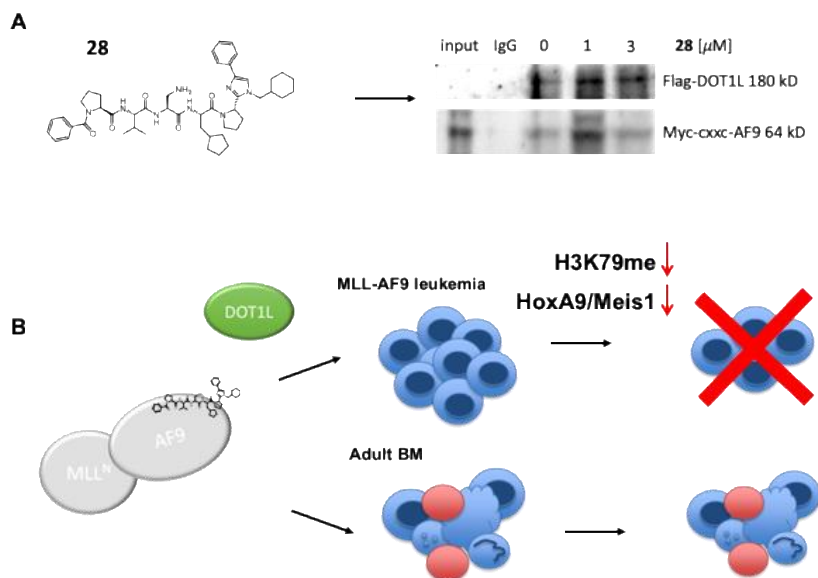
Figure 2-14 Proposed model for targeting the AF9-DOT1L interaction with a small molecule.

(A) Co-immunoprecipitation with Flag-DOT1L and Myc-CxxC-AF9 with various concentrations of peptidomimetic 28, that binds to the AHD domain of AF9, dose-dependently inhibits the AF9-DOT1L interaction (ACS med. chem. Letters, 2018). (B) Based on the experimental data, disrupting the PPI between AF9 and DOT1L with a compound can lead to the downregulation of H3K79me and HoxA9 and Meis1 expression leading to cell differentiation and cell death. In contrast, in non-leukemic bone marrow (BM), the AF9-DOT1L interaction is dispensable wherein hematopoietic stem cells and progenitor cells are sustained.

2.5   Materials and methods

Fluorescence Polarization

Competitive FP binding experiments were performed in 96-well black, round-bottom plates (Corning 3792) with serial dilutions of peptide or compounds, with a fixed concentration of MBP-AF9 (200nM) and N-Flu-DOT1L (10nM) in assay buffer (100mM NaH_2PO_4, 150mM NaCl, 0.1% β-ME, 0.01% Triton X-100). to a final volume of 125ul. The polarization units were

measured after mixing and incubating at room temperature for 3 hours. Negative controls with MBP-AF9 and N-Flu-DOT1L probe only (0% inhibition) and positive controls with N-Flu-DOT1L probe only (100% inhibition) were included in the assay plate. IC50 values were determined by nonlinear regression fitting of the competitive curves using GraphPad Prism 5.0.

Mice

C57BL/6.Ptprca (B6-SJL, CD45.1+) were bred in-house or obtained from Charles River (Frederick, MD). C57BL/6 Dot1lf/f mice were obtained from Dr. Jay Hess and crossed to Mx1-Cre+ mice for in vivo experiments, or to Cre-ERT2 mice for in vitro experiments. Specifically, for the C57BL/6 *Dot1lf/f Mx1- Cre+* mice, breeding was complicated by genetically linked loci on mouse chromosome 10, although Dot1lf/+ Mx1- Cre+ progeny was eventually obtained and then intercrossed.[59] Dot1l excision was achieved using poly(I:C) (Amersham; 50 µg i.p. every 2 days for 3-5 doses) in vivo or 4-hydroxytamoxifen (4-OHT) in vitro (Sigma-Aldrich; 7.5 nM at experimental day 0 and day 2). Genotypes of animals were confirmed by polymerase chain reaction (PCR). All experiments in mice were approved by the University of Michigan's Committee for the Use and Care of Animals.

Cell line generation

Bone marrow from *Dot1lf/f CreER(T2)*[+] mice was harvested 4 days after i.p. injection of 150 mg/kg 5-fluorouracil (Sigma-Aldrich) and lineage-depleted using the EasySep Mouse Hematopoietic progenitor cell isolation kit (Stem Cell Technologies). Retroviruses were produced by transfecting MSCV-neo-Flag-MLL-AF9 construct into Plat E cell line with Fugene 6 (Roche Diagnostics). Fresh viral supernatant was used for transduction of the lineage depleted *Dot1lf/f CrER(T2)*^{+} stem cells using two subsequent rounds of spinoculation. For spinoculation, cells were spun at high speed in the presence of viral supernatant for 90 minutes at room

temperature. Cells underwent neomycin selection for 6 days and weaned off stem cell factor (SCF) 9 days after starting selection. These selected cells were then transduced 14 days following initial antibiotic selection using the same spinoculation method described above with one of the following vectors: MigR1 (empty vector), MigR1-HA-DOT1L (WT-DOT1L), MigR1-HA-DOT1L deletion aa865-874 (Δ10-DOT1L), MigR1-HA-DOT1L I867A (I867A-DOT1L), and MigR1-HA-DOT1L RCR (RCR-DOT1L). Cells were left to recover for 3 days, then sorted for GFP positivity using a MoFlo Astrios FACS sorter. Cells were expanded and resorted to get a majority of GFP+ cells expressing the DOT1L constructs.

Cell growth

Cell numbers was assessed using a hemocytometer. Cells were treated with either 7.5nM 4-OHT or equivalent concentration of solvent (100% ethanol) on day 0 and day 2 to achieve excision of Dot1l, followed by daily counting.

Chromatin Immunoprecipitation

ChIP experiments were performed by treating the Dot1lf/f CreER-(T2) MLL-AF9 cell lines with the reintroduced DOT1L WT/mutant constructs or empty vector control with 7.5nM 4-OHT for 3 days as described cell growth protocol. Briefly, 3×10^7 cells were crosslinked with 1% formaldehyde, lysed with 1% SDS lysis buffer (50 mM Tris HCl pH 8, 10 mM EDTA, 1 Roche mini tablet of protease inhibitors diluted in 1 ml (for 10 ml), 1% SDS) and sonicated on a Biorupter Pico sonication device (Diabenode). Lysates were diluted in ChIP dilution buffer (1% triton, 1.2 mM EDTA, 167 mM NaCl, 16.7 mM Tris HCl pH8) and precleared with appropriate mouse or rabbit IgG beads. Cleared lysates were immunoprecipitated with anti-HA (Abcam; ab1424), anti-Flag (ThermoFisher), anti-H3K79me2 (Abcam; ab3594), anti-H3 (Abcam; 24834) using protein A/G agarose beads (SantaCruz; sc-2003). The IPs were washed with a low salt

(150 mM NaCl, 0.1% SDS, 20 mM Tris–HCl pH8, 2 mM EDTA, 1% Triton X-100), a high salt buffer (500 mM NaCl, 0.1% SDS, 1% Triton X-100, 20 mM Tris–HCl pH8, 2 mM EDTA) and a stringent lithium chloride buffer (0.25 M LiCL, 1% IGEPAL CA-630, 10 Mm Tris–HCl pH8, 1 mM EDTA, 1% sodium deoxycholate). Protein-DNA complexes were eluted in 1% SDS, crosslinked in high salt and treated with RNaseA and Proteinase K. DNA was purified with a Qiagen PCR purification kit. qPCR was performed using the SYBR-green mastermix. Primer sets used were: Meis1_promoter_F- 5'TCAAAGTGACAAAATGCAAGCA3'; Meis1_promoter_R- 5'CCCCCCGCTGTCAGAAG3'; Hoxa9_promoter_F-5'TGACCCCTCAGCAAGACAAAC 3'; Hoxa9_promoter_R- 5'TCCCGCTCCCCAGACTG 3'

Co-Immunoprecipitation

Cells expressing both HA-DOT1L constructs and Flag-MLL-AF9 were collected and lysed using BC-300 lysis buffer: 20 mM Tris-HCl pH 8.0, 300 mM KCl, 1 mM EDTA, 10% glycerol, 0.1% NP-40 and 1x protease inhibitor cocktail (BioMake). The lysate was pre-cleared for 2h in Mouse IgG Agarose (Sigma-Aldrich). The precleared lysates were incubated with different concentrations of the DOT1L peptidomimetic or no compound at 4°C overnight. The next day, the cell lysates were immunoprecipitated with anti-flag M2 magnetic beads (Sigma-Aldrich) at 4°C for 2h. After incubation, the beads were washed extensively, boiled in SDS loading buffer and analyzed by western blotting using anti-flag M2 (Sigma-Aldrich) and anti-HA tag (Abcam) antibody.

Cell Cycle

Cells were treated with either 7.5nM 4-OHT or an equivalent concentration of solvent (100% ethanol) on day 0 and day 2 to achieve excision of Dot1l. On day 3, cells were washed twice with ice-cold PBS and resuspended in 500 μL PBS. While vortexing gently, 4.5 mL ice-cold 70% ethanol was slowly added followed by storage at -20 ℃ overnight. Cell were then washed with PBS and incubated with 100 μg/mL RNase A and 10 μg/mL propidium iodide (Invitrogen). Cells were incubated for 15 minutes at 37 ℃ and then analyzed by FACS.

Histone Methylation

Cells were harvested and processed using a previously reported method.[60] Histones were quantified using Bradford assay and normalized for SDS page electrophoresis. Anti-H3K79me2 and anti-H3 loading controls were used for probing.

Gene Expression

Cells were harvested from the cell proliferation assay on day 3. RNA was isolated, and cDNA was synthesized using Superscript III reverse transcriptase kit (Invitrogen). Quantitative real-time PCR was performed using SyberGreen master mix (Applied Biosystems) and primers for Hoxa9, Meis1, GAPDH, and beta-Actin. Data was analyzed using the 2_DD Ct method. Expression was normalized to GAPDH expression and was performed in triplicate.

Differentiation

Cells were harvested from the cell proliferation assay on day 3 and cytospun onto microscope slides. Cells were then stained with Wright-Giemsa stain (Millipore) and mounted on a slide with a coverslip using Permount (Fisher Chemical) mounting medium. Images were captured using bright field condition with an Olympus IX83 inverted microscope. Cells were stained with anti-c-Kit, anti-CD14 and isotype control antibodies (BD Pharmingen, San Jose, CA & Biolegend,

San Diego, CA) and processed in a LSRII Flow Cytometer (BD Biosciences, San Jose, CA). Data was analyzed using FlowJo X.

Flow cytometry

Single cell suspensions were prepared from bone marrow or blood, followed by red blood cell lysis (ACK buffer, Cambrex, Walkersville, MD). The following antibodies were from BioLegend (San Diego, CA), eBiosciences (San Diego, CA) or BD Biosciences (San Jose, CA): anti-CD3, CD4, CD8, CD11b, CD11c, CD16/32, CD19, CD41, CD48, CD105 CD150, Gr1/Ly-6G, B220, NK1.1, TCRβ, TCRγδ, c-Kit, and Sca-1. We used the following antibody cocktail to exclude Lineage+ cells: anti-CD3, CD8, CD11b, CD11c, B220, CD19, TCRβ, TCRγδ, Gr1, NK1.1 and Ter119. Ter119 was omitted when analyzing erythroid progenitor populations. Ki67 staining was achieved using the BD Ki67 Set (BD Biosciences). Analysis was on FACSFortessa and sorting on FACSAria II/III (BD Biosciences). Dead cells were excluded with 4′6-diamidino-2-phenylindole (Sigma) or with a fixable viability dye (Aqua Zombie, cat. 423102 BioLegend). Files were analyzed in FlowJo (Tree Star, San Carlos, CA).

Retroviral transduction and bone marrow transplantation

Donor Dot1lf/f Mx1-Cre+ CD45.2+ and Dot1lf/f Mx1-Cre- CD45.2+ mice were injected i.p. with 150mg/kg 5-FU to enrich for cycling HSCs. Bone marrow was harvested 4 days after 5-FU treatment and stimulated with SCF, IL-3 and IL-6 overnight, as described[61]. To insure the viable cells were available for analysis, Mx-Cre$^+$Dot1l$^{f/f}$ B6-CD45.2 and Dot1lf/f Mx1-Cr+- CD45.2+ cells were co transduced ex vivo for 10 days with MSCV-based constructs expressing eGFP plus DOT1L-WT, DOT1L- 10, DOT1L-I867A or DOT1L-RCR and NUP98-HOXA10-mCherry so that we could color trace the presence of NUP98-HOXA10 in cells, in the presence or absence or exogenous Dot1L constructs. In selected control experiments, both NUP98-HOXA10-mCherry

and NUP98-HOXA10-eGFP constructs were used. On the day of transplant, 6-8-week-old B6-SJL (CD45.1+) mice were lethally irradiated (5.5 Gy twice 4-6 hours apart, Cesium-137 source). Three hours after the second irradiation dose, mice were transplanted with expanded and retrovirally transduced progenitors. Mice were left to rest for 6 weeks before poly(I:C) injections started. Blood was obtained through retroorbital bleeding and transferred to EDTA-treated tubes. Complete blood counts were determined using the Advia 120 Hematology System (Siemens, Malvern, PA). Flow cytometry was performed as described above, combining eGFP and mCherry fluorescence with staining for selected surface markers.

Western Blot

Whole bone marrow was lysed with 2x Laemmli Sample Buffer (Biorad) plus 2-mercaptoethanol (Sigma, St. Louis, MO). For assessment of H3K79 di-methylation, lysates from 10-15 x10^5 bone marrow cells were probed with Anti-H3K79me2 (Abcam, ab3594, 1:1000 dilution) and Anti-H3 (Abcam, ab1791 1:5000 dilution). CFU-GM20,000 bone marrow cells were plated per mL of Methocult GF M3534 in triplicate for each biological sample (Stem Cell Technologies, Vancouver, BC). Colonies were counted 12 days later.

Statistical analysis

Comparison of two means was performed with 2-tailed unpaired Student's t-test. Welch's correction was utilized when data did not fit a normal distribution.

2.6   Contributions

Sierrah Marie Grigsby established the murine cell lines with contributions from James Ropa and Justin Serio; performed *in vitro* biochemical studies and cell line characterization including all cell proliferation, gene expression, chromatin immunoprecipitation, differentiation, and cell

cycle experiments. Ann Friedman; Jennifer Chase, and Bridget Waas designed conducted the *in vivo* studies.

2.7   References

1.   Hsieh JJ, Cheng EH, Korsmeyer SJ. Taspase1: a threonine aspartase required for cleavage of MLL and proper HOX gene expression. *Cell*. 2003;115(3):293-303.
2.   Martin C, Zhang Y. The diverse functions of histone lysine methylation. *Nat Rev Mol Cell Biol*. 2005;6(11):838-849.
3.   Meyer C, Kowarz E, Hofmann J, et al. New insights to the MLL recombinome of acute leukemias. *Leukemia*. 2009;23(8):1490-1499.
4.   Winters AC, Bernt KM. MLL-Rearranged Leukemias-An Update on Science and Clinical Approaches. *Front Pediatr*. 2017;5:4.
5.   Andrea MM, Peres TB, Luchini LC, Pettinelli A, Jr. Impact of long-term pesticide applications on some soil biological parameters. *J Environ Sci Health B*. 2000;35(3):297-307.
6.   Pui CH, Kane JR, Crist WM. Biology and treatment of infant leukemias. *Leukemia*. 1995;9(5):762-769.
7.   Meyer C, Burmeister T, Groger D, et al. The MLL recombinome of acute leukemias in 2017. *Leukemia*. 2018;32(2):273-284.
8.   Poirel H, Rack K, Delabesse E, et al. Incidence and characterization of MLL gene (11q23) rearrangements in acute myeloid leukemia M1 and M5. *Blood*. 1996;87(6):2496-2505.
9.   Yokoyama A, Lin M, Naresh A, Kitabayashi I, Cleary ML. A Higher-Order Complex Containing AF4 and ENL Family Proteins with P-TEFb Facilitates Oncogenic and Physiologic MLL-Dependent Transcription. *Cancer Cell*. 2010;17(2):198-212.
10.   Mueller D, Garcia-Cuellar MP, Bach C, Buhl S, Maethner E, Slany RK. Misguided transcriptional elongation causes mixed lineage leukemia. *PLoS Biol*. 2009;7(11):e1000249.
11.   Mueller D, Bach C, Zeisig D, et al. A role for the MLL fusion partner ENL in transcriptional elongation and chromatin modification. *Blood*. 2007;110(13):4445-4454.
12.   Mohan M, Herz HM, Takahashi YH, et al. Linking H3K79 trimethylation to Wnt signaling through a novel Dot1-containing complex (DotCom). *Genes Dev*. 2010;24(6):574-589.
13.   Biswas D, Milne TA, Basrur V, et al. Function of leukemogenic mixed lineage leukemia 1 (MLL) fusion proteins through distinct partner protein complexes. *Proc Natl Acad Sci U S A*. 2011;108(38):15751-15756.
14.   Steger DJ, Lefterova MI, Ying L, et al. DOT1L/KMT4 recruitment and H3K79 methylation are ubiquitously coupled with gene transcription in mammalian cells. *Mol Cell Biol*. 2008;28(8):2825-2839.
15.   Bernt Kathrin M, Zhu N, Sinha Amit U, et al. MLL-Rearranged Leukemia Is Dependent on Aberrant H3K79 Methylation by DOT1L. *Cancer Cell*. 2011;20(1):66-78.
16.   Nguyen AT, Taranova O, He J, Zhang Y. DOT1L, the H3K79 methyltransferase, is required for MLL-AF9–mediated leukemogenesis. *Blood*. 2011;117(25):6912-6922.
17.   Farooq Z, Banday S, Pandita TK, Altaf M. The many faces of histone H3K79 methylation. *Mutat Res Rev Mutat Res*. 2016;768:46-52.
18.   Okada Y, Feng Q, Lin Y, et al. hDOT1L links histone methylation to leukemogenesis. *Cell*. 2005;121(2):167-178.

19.   Chang M-J, Wu H, Achille NJ, et al. Histone H3 Lysine 79 Methyltransferase Dot1 Is Required for Immortalization by MLL Oncogenes. *Cancer Research*. 2010;70(24):10234-10242.

20.   Wang X, Chen CW, Armstrong SA. The role of DOT1L in the maintenance of leukemia gene expression. *Curr Opin Genet Dev*. 2016;36:68-72.

21.   Annesley CE, Brown P. Novel agents for the treatment of childhood acute leukemia. *Ther Adv Hematol*. 2015;6(2):61-79.

22.   Basavapathruni A, Olhava EJ, Daigle SR, et al. Nonclinical pharmacokinetics and metabolism of EPZ-5676, a novel DOT1L histone methyltransferase inhibitor. *Biopharm Drug Dispos*. 2014;35(4):237-252.

23.   Daigle SR, Olhava EJ, Therkelsen CA, et al. Potent inhibition of DOT1L as treatment of MLL-fusion leukemia. *Blood*. 2013;122(6):1017-1025.

24.   Stein EM, Tallman MS. Mixed lineage rearranged leukaemia: pathogenesis and targeting DOT1L. *Curr Opin Hematol*. 2015;22(2):92-96.

25.   Stein EMG-M, G.;Rizzieri, D.A.;Tibes, R.; Berdeja, J. G.; Jongen-Lavrencic, M.; Altman, J. K.; Dohner, H.; Thomson, B.; Blakemore, S. J.; Daigle, S.; Fine, G.; Waters, N. J.; Krivstov,A. V.; Koche, R.; Armstrong, S. A.; Ho, P. T.; Lowenberg B.; and Tallman, M. S. A Phase 1 Study of the DOT1L Inhibitor, Pinometostat (EPZ-5676), in Adults with Relapsed or Refractory Leukemia: Safety, Clinical Activity, Exposure and Target Inhibition. *Blood*. 2015;126(23):2547.

26.   Shukla NW, C.; O'Brien, M.M.; Silverman, L.B.; Brown, P.; Cooper, T.M.; Thomson, B.; Blakemore, S.J.; Daigle, S.; Suttle, B.; Waters, N.J.; Krivstov, A.K.; Armstrong, S.A.;Ho, P.T.; Gore, L. Final Report of Phase 1 Study of the DOT1L Inhibitor, Pinometostat (EPZ-5676), in Children with Relapsed or Refractory MLL-r Acute Leukemia. *Blood*. 2016;128(22):2780.

27.   Beloqui A, Polaina J, Vieites JM, et al. Novel hybrid esterase-haloacid dehalogenase enzyme. *Chembiochem*. 2010;11(14):1975-1978.

28.   Carinci F, Pezzetti F, Spina AM, et al. An in vitro model for dissecting distraction osteogenesis. *J Craniofac Surg*. 2005;16(1):71-78; discussion 78-79.

29.   Jones B, Su H, Bhat A, et al. The histone H3K79 methyltransferase Dot1L is essential for mammalian development and heterochromatin structure. *PLoS Genet*. 2008;4(9):e1000190.

30.   Jo SY, Granowicz EM, Maillard I, Thomas D, Hess JL. Requirement for Dot1l in murine postnatal hematopoiesis and leukemogenesis by MLL translocation. *Blood*. 2011;117(18):4759-4768.

31.   Nguyen AT, He J, Taranova O, Zhang Y. Essential role of DOT1L in maintaining normal adult hematopoiesis. *Cell Res*. 2011;21(9):1370-1373.

32.   Feng Y, Yang Y, Ortega MM, et al. Early mammalian erythropoiesis requires the Dot1L methyltransferase. *Blood*. 2010;116(22):4483-4491.

33.   Shen C, Jo SY, Liao C, Hess JL, Nikolovska-Coleska Z. Targeting recruitment of disruptor of telomeric silencing 1-like (DOT1L): characterizing the interactions between DOT1L and mixed lineage leukemia (MLL) fusion proteins. *The Journal of Biological Chemistry*. 2013;288(42):30585-30596.

34.   Kuntimaddi A, Achille NJ, Thorpe J, et al. Degree of recruitment of DOT1L to MLL-AF9 defines level of H3K79 Di- and tri-methylation on target genes and transformation potential. *Cell Rep*. 2015;11(5):808-820.

35.   Du L, Grigsby SM, Yao A, et al. Peptidomimetics for Targeting Protein-Protein Interactions between DOT1L and MLL Oncofusion Proteins AF9 and ENL. *ACS Med Chem Lett*. 2018;9(9):895-900.

36.   Feng Q, Wang H, Ng HH, et al. Methylation of H3-Lysine 79 Is Mediated by a New Family of HMTases without a SET Domain. *Current Biology*. 2002;12(12):1052-1058.

37.   Min J, Feng Q, Li Z, Zhang Y, Xu RM. Structure of the catalytic domain of human DOT1L, a non-SET domain nucleosomal histone methyltransferase. *Cell*. 2003;112(5):711-723.

38.   Jo SY, Granowicz EM, Maillard I, Thomas D, Hess JL. Requirement for Dot1l in murine postnatal hematopoiesis and leukemogenesis by MLL translocation. *Blood*. 2011;117(18):4759-4768.

39.   Daigle SR, Olhava EJ, Therkelsen CA, et al. Selective Killing of Mixed Lineage Leukemia Cells by a Potent Small-Molecule DOT1L Inhibitor. *Cancer Cell*. 2011;20(1):53-65.

40.   Daigle SR, Olhava EJ, Therkelsen CA, et al. Potent inhibition of DOT1L as treatment of MLL-fusion leukemia. *Blood*. 2013;122(6):1017-1025.

41.   Milne TA, Briggs SD, Brock HW, et al. MLL targets SET domain methyltransferase activity to Hox gene promoters. *Mol Cell*. 2002;10(5):1107-1117.

42.   Monroe SC, Jo SY, Sanders DS, et al. MLL-AF9 and MLL-ENL alter the dynamic association of transcriptional regulators with genes critical for leukemia. *Exp Hematol*. 2011;39(1):77-86 e71-75.

43.   Muntean AG, Hess JL. The pathogenesis of mixed-lineage leukemia. *Annu Rev Pathol*. 2012;7:283-301.

44.   Chen CW, Armstrong SA. Targeting DOT1L and HOX gene expression in MLL-rearranged leukemia and beyond. *Exp Hematol*. 2015;43(8):673-684.

45.   McLean CM, Karemaker ID, van Leeuwen F. The emerging roles of DOT1L in leukemia and normal development. *Leukemia*. 2014;28(11):2131-2138.

46.   Nguyen AT, He J, Taranova O, Zhang Y. Essential role of DOT1L in maintaining normal adult hematopoiesis. *Cell Research*. 2011;21(9):1370-1373.

47.   Braun BS, Tuveson DA, Kong N, et al. Somatic activation of oncogenic Kras in hematopoietic cells initiates a rapidly fatal myeloproliferative disorder. *Proc Natl Acad Sci U S A*. 2004;101(2):597-602.

48.   Kuhn R, Schwenk F, Aguet M, Rajewsky K. Inducible gene targeting in mice. *Science*. 1995;269(5229):1427-1429.

49.   Kiel MJ, Yilmaz OH, Iwashita T, Yilmaz OH, Terhorst C, Morrison SJ. SLAM family receptors distinguish hematopoietic stem and progenitor cells and reveal endothelial niches for stem cells. *Cell*. 2005;121(7):1109-1121.

50.   Pronk CJ, Rossi DJ, Mansson R, et al. Elucidation of the phenotypic, functional, and molecular topography of a myeloerythroid progenitor cell hierarchy. *Cell Stem Cell*. 2007;1(4):428-442.

51.   Ohta H, Sekulovic S, Bakovic S, et al. Near-maximal expansions of hematopoietic stem cells in culture using NUP98-HOX fusions. *Exp Hematol*. 2007;35(5):817-830.

52.   Abraham A, Kim YS, Zhao H, Humphries K, Persons DA. Increased Engraftment of Human Short Term Repopulating Hematopoietic Cells in NOD/SCID/IL2rgammanull Mice by Lentiviral Expression of NUP98-HOXA10HD. *PLoS One*. 2016;11(1):e0147059.

53.   Zeisig DT, Bittner CB, Zeisig BB, Garcia-Cuellar MP, Hess JL, Slany RK. The eleven-nineteen-leukemia protein ENL connects nuclear MLL fusion partners with chromatin. *Oncogene*. 2005;24(35):5525-5532.

54.   Bitoun E, Oliver PL, Davies KE. The mixed-lineage leukemia fusion partner AF4 stimulates RNA polymerase II transcriptional elongation and mediates coordinated chromatin remodeling. *Hum Mol Genet*. 2007;16(1):92-106.

55.   Ayton PM, Cleary ML. Molecular mechanisms of leukemogenesis mediated by MLL fusion proteins. *Oncogene*. 2001;20(40):5695-5707.

56.   Anglin JL, Deng L, Yao Y, et al. Synthesis and structure-activity relationship investigation of adenosine-containing inhibitors of histone methyltransferase DOT1L. *J Med Chem*. 2012;55(18):8066-8074.

57.   Deng L, Zhang L, Yao Y, et al. Synthesis, Activity and Metabolic Stability of Non-Ribose Containing Inhibitors of Histone Methyltransferase DOT1L. *Medchemcomm*. 2013;4(5):822-826.

58.   Mobitz H, Machauer R, Holzer P, et al. Discovery of Potent, Selective, and Structurally Novel Dot1L Inhibitors by a Fragment Linking Approach. *ACS Med Chem Lett*. 2017;8(3):338-343.

59.   Paul E, Cronan R, Weston PJ, et al. Disruption of Supv3L1 damages the skin and causes sarcopenia, loss of fat, and death. *Mamm Genome*. 2009;20(2):92-108.

60.   Gibbons GS, Owens SR, Fearon ER, Nikolovska-Coleska Z. Regulation of Wnt signaling target gene expression by the histone methyltransferase DOT1L. *ACS Chem Biol*. 2015;10(1):109-114.

61.   Maillard I, Weng AP, Carpenter AC, et al. Mastermind critically regulates Notch-mediated lymphoid cell fate decisions. *Blood*. 2004;104(6):1696-1702.

CHAPTER 3

Peptidomimetics Targeting Protein-Protein Interactions Between DOT1L and MLL Oncofusion Proteins AF9 and ENL

3.1   Abstract

MLL-AF9 and MLL-ENL have frequently identified MLL fusion proteins in human leukemia which mediates leukemogenesis by recruiting a methyltransferase DOT1L to the gene loci of MLL1 target genes, such as HOXA9 and MEIS1. The protein-protein interactions between DOT1L and MLL-fusion proteins, AF9 and ENL, play an essential role in the regulation of the H3K79 methyltransferase activity of DOT1L at the target genes; therefore, blocking these interactions using small molecules may represent a novel therapeutic approach for targeting this subset of leukemia. Based on the 7 mer peptide (peptide **2**), derived from DOT1L, a class of peptidomimetics was designed. By modifying the side chains of the middle three residues in peptide **2**, compound **21** was designed and achieved Ki values of 20 and 90 nM to AF9 and ENL, respectively, 8 times more potent than the original 7 mer peptide **2**. The binding affinity of **21** was confirmed by a biotinylated analog **22** which shows comparable affinity to both AF9 and ENL in two different assays, the fluorescence polarization, and the biolayer interferometry (BLI) binding assays. Using transiently co-transfected HEK 293t cells with Myc-tagged CxxC-AF9, it was demonstrated that biotinylated analog **22** recognizes and binds to the cellular Myc-CxxC-AF9 protein in a dose-dependent manner. Modifications of the N- and C-termini of the lead compound **21** resulted in the identification of peptidomimetic **28** which shows 2-fold more

potent binding affinity to AF9 and similar binding to ENL than **21** but has much decreased

peptidic characteristics. We also demonstrate peptidomimetic **29** is cellularly active and selective

for MLL-AF9 transduces murine cells over a non-DOT1L dependent E2A-HLF cell line. Our

study, for the first time, provides a foundation for the design of potent nonpeptidic compounds to

inhibit DOT1L activity by targeting its recruitment and the interactions between DOT1L and

MLL-fusion proteins, AF9 and ENL.

3.2   Introduction

Translocation of the mixed lineage leukemia gene (*MLL1*) is one of the most common chromosome rearrangements found in leukemia patients.[1] To date more than 80 genes have been reported to fuse with *MLL1*.[2] Among MLL fusion proteins, MLL-AF4, MLL-AF9, MLL-AF10, and MLL-ENL account for more than 80% of MLL leukemias.[3] AF9 and ENL are closely related members of YEATS domain protein family and have been identified as part of several reported complexes known as Super Elongation Complex (SEC), AEP (AF4, ENL, P-TEFb) and DotCom Complex.[4-6] They share high homology in their C-terminal hydrophobic domain known as ANC1 Homology Domain (AHD) that is responsible for the recruitment of several multiprotein complexes.[4-6] Through these protein-protein protein interactions (PPIs) AF9 and ENL recruits both gene repressive complexes through CXB8 and BCoR as well as gene activating complexes through AF4 and DOT1L.[7-10] Both AF4 and DOT1L share a conserved AF9/ENL binding domain that interacts with the same AHD domain of AF9 and ENL in a mutually exclusive manner.[5,11-13] One of the molecular mechanisms of leukemogenesis is mediated by the recruitment of the histone methyltransferase DOT1L, Disruptor of Telomeric silencing 1-like, by MLL-AF9/ENL, to MLL1 target genes, such as *HOXA9* and *MEIS1*. The recruitment of DOT1L results in hypermethylation of H3K79 at the *HOXA9* and *MEIS1* loci and sustained expression of these genes, which is pivotal for leukemogenesis induced by these MLL oncogenic fusion proteins.[14-16] DOT1L has been validated as a therapeutic target for the treatment of MLL-rearranged leukemias. As a result, a small molecule, SAM competitive, DOT1L inhibitor, EPZ-5676, has entered phase I clinical trials.[17] However, several groups, using conditional DOT1L-knockout mouse models, have demonstrated that DOT1L plays an important role in maintaining

normal adult hematopoiesis[18,19], which raise the possibility of side effects by direct targeting of the catalytic domain. Therefore, investigating and developing alternative strategies for inhibiting DOT1L activity is essential and necessary.

3.2.1 Approaches to identify inhibitors of protein-protein interactions (PPIs)

Discovering potent inhibitors of protein-protein interactions is not as straightforward as targeting enzymatic function. Enzymes have a well-defined binding pocket specific to their co-factors and substrates where a small molecule can bind with high potency and inhibit its function in a reversible or irreversible manner.[20] Unlike substrate binding sites in an enzyme, PPIs do not have a defined binding pocket. Usually they cover a large surface of a protein with several essential contacts known as hot spots.[21] The traditional method of identifying small-molecule inhibitors is the High Throughput screening method (HTS).[22] Although it can be challenging, there are several successful examples of identifying small-molecules that target PPIs.[23-25]

In recent years, fragment-based drug discovery (FBDD) has been widely used strategy to the discovery of small-molecule inhibitors that can bind in different protein's hot spots. Usually, the hit fragments bind with low potency, mM to high uM, which need to be further optimized by applying different strategies, such as growing the identified hit fragment or linking together if two fragments bind to the adjacent pockets in the target protein.[26] The successfulness of this strategy depends on the structural knowledge of the fragment(s) binding to the protein target. ABT737, an inhibitor of the PPIs between anti-apoptotic proteins Bcl-2, Bcl-xL and Bcl-w and proapoptotic proteins, Bim, Bak, and Bax, is the first successful example for discovery and development of potent small-molecule by using FBDD approach.[23]

Another well-established strategy to discover inhibitors of PPIs is developing peptidomimetics.[27] This approach has been applied to many PPIs including XIAP and caspase-9 and developed potent Smac mimetics, currently in clinical trials, MDM2 inhibitors blocking the interactions between MDM2 and p53 and MLL1 inhibitors, blocking the formation of MLL1 complex by disrupting the interactions between MLL1 and WDR5.[28-32] These peptide-based small molecules are mimicking the natural peptide of the protein that interacts with the target, with improved drug-like properties, including solubility metabolic stability and etc.

3.2.2 Utilizing known AF9-binding domains of DOT1L as a starting point to peptide design

Our group characterized for the first time the protein-protein interactions between DOT1L and MLL fusion oncogenic proteins, AF9 and ENL, on a biochemical, biophysical and functional level.[11] The AF9/ENL binding site in DOT1L was mapped and identified to a 10 amino-acid region, aa 865-874 (peptide **1**, Table 3-2). Peptide 1 binds to AF9/ENL and blocks the interaction between DOT1L and AF9/ENL in the cell lysate.[11] Importantly, functional studies show that the mapped 10-amino acid interacting site is essential for immortalization by MLL-AF9, indicating that DOT1L interaction and recruitment with MLL-AF9 are required for hematopoietic transformation.[11] In an independent study using ^{15}N-^{1}H HSQC NMR, Kuntimaddi et al. confirmed the interaction site through the 10 mer peptide 1, labeled as site 2, and identified two additional DOT1L motifs: site 1 (aa 628-653), and site 3 (aa 878-900) which can bind to the same region in AF9 (aa 499-568) as site 2.[33] The sequence between site 2 and site 3 is highly conserved and represent high-affinity binding motifs (Table 3-1).

Table 3-1 Binding affinity of 10 mer peptides derived from binding sites 2 and 3

Binding Site	Sequence	AF9 K_D [nM]	ENL K_D [nM]
2	K(FAM)-βAla-βAla-LPISIPLSTV (865-874)	45±17	551±144
3	K(FITC)-βAla-βAla- LPVSIPLASV (879-888)	19±5	198±22

We synthesized two corresponding fluorescent-labeled 10 mer peptides based on the sequence extracted from site 2 and site 3, respectively. Using a fluorescent polarization (FP) based assay, their binding affinities to AF9 and ENL were determined. Both peptides potently bound to AF9 and ENL, with the peptide derived from site 3 showing about 2 times more potent binding in comparison with the peptide derived from site 2 (Table 3-1). We and others have shown that DOT1L and AF4 bind with similar binding affinity and compete for the same AHD domain in AF9 and ENL protein.[11,33] Consistently, NMR studies indicate that the AF4 protein,[5] as well as DOT1L binding motifs at sites 2 and 3, have similar binding modes to AF9.[33] The NMR solution structure of the DOT1L-AF9 complex showed that DOT1L residues 879 to 884 from site 3 form a β strand (Figure 3-1). The protein-protein interface is mainly hydrophobic, and the side chains of L879, V881, I883, L885, and V888 have critical hydrophobic interactions with AF9 (Figure 3-1). Furthermore, the amino and carbonyl groups of Val881 and Ile883 form two pairs of hydrogen bonds with Phe545 and Phe543 in AF9, respectively. These studies provide a concrete basis for using DOT1L conserved binding motif (site 2 and site 3) as a

promising lead structure towards the design of potent peptidomimetics and nonpeptidic compounds that target the interactions between MLL-AF9/ENL and DOT1L.
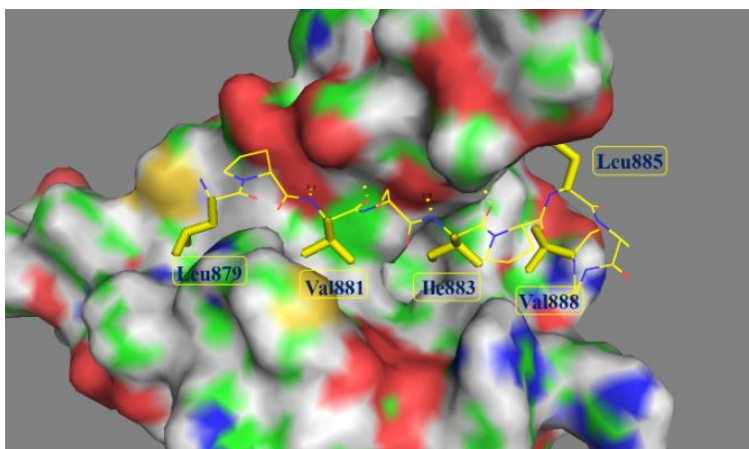
Figure 3-1 NMR solution structure of the DOT1L-AF9 complex (PDB ID: 2MV7).

3.2.3   Goal for Study

Herein, we provide the rational design for developing peptidomimetics based on the AF9 and ENL binding site of DOT1L in order to generate chemical tools targeting this PPI. Based on the previously mentioned examples of PPI inhibitor design based on peptidomimetics, we aim to shorten and optimize DOT1L peptide binding. We first truncate the peptide to reduce the number of peptide bonds that are susceptible to cleavage while retaining binding to AF9 and ENL. We use unnatural amino acid changes to the core of the peptide to minimize protease recognition and improve peptide stability and to regain potency. Since the PPI is a large hydrophobic groove, adding hydrophobic moieties to either terminus of the peptide, we further modify the *C-* and *N-*termini to further improve peptide, potency, stability, and cellular activity. Utilizing this strategy, we developed a potent and selective peptidomimetic that disrupts the AF9-DOT1L PPI,

downregulate MLL-target gene expression and induce cell differentiation. These data lay the groundwork for the further development of DOT1L peptidomimetics as future therapeutics for MLL-AF9/MLL-ENL leukemia.
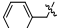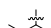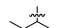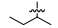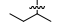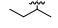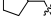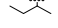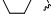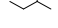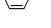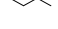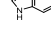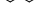
3.3 Results

3.3.1 Optimization of WT DOT1L peptide

Table 3-2 Optimization of the middle three residues
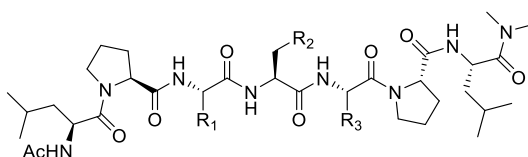
Peptides	R_1	R_2	R_3	AF9 IC_{50}, μM (K_i, μM)	ENL IC_{50}, μM (K_i, μM)
1	10 mer site 2 (865-874) Ac-LPISIPLSTV-NH$_2$			0.14±0.03 0.02±0.005	0.63±0.19 0.15±0.05
2	7 mer site 2 (865-871) Ac-LPISIPL-NH$_2$			1.04±0.10 0.16±0.03	10.3±0.55 3.37±0.19
3	7 mer site 3 (879-885) Ac-LPVSIPL-NH$_2$			1.02±0.13 0.16±0.02	4.79±0.89 1.43±0.32
4	⟋⟍	OH	⟋⟍	1.78±0.13 0.30±0.02	6.83±0.51 2.15±0.18
5	⟋⟍	OH	⟋⟍	1.10±0.29 0.17±0.10	3.60±0.50 1.01±0.18
6	⟍⟋	OH	⟋⟍	6.40±0.23 1.16±0.04	43.9±2.481 5.2±0.87
7	▷	OH	⟋⟍	4.29±0.71 0.78±0.15	14.6±2.73 4.89±0.96
8	◻	OH	⟋⟍	7.23±0.38 1.31±0.07	23.6±2.53 8.04±0.89

#					
9		OH		30.52±1.75 / 5.62±0.3	177±10.2 / 62.0±3.39
10		OH		1.49±0.50 / 0.25±0.09	4.54±0.81 / 1.34±0.29
11		OH		3.49±0.41 / 0.62±0.08	10.5±2.63 / 3.44±0.93
12		OH		4.66±0.13 / 0.83±0.02	18.6±1.67 / 6.29±0.59
13		OH		0.85±0.12 / 0.13±0.02	2.17±0.710.5 / 1±0.25
14		OH		1.14±0.02 / 0.18±0.01	6.06±1.54 / 1.88±0.54
15		OH		1.66±0.47 / 0.28±0.09	22.7±4.67 / 7.73±1.65
16		OH		2.37±0.82 / 0.41±0.15	7.42±0.39 / 2.35±0.14
17		OH		4.11±0.43 / 0.73±0.08	42.2±3.031 / 4.6±0.07
18		OH		14.19±0.38 / 2.6±0.07	57.8±4.37 / 20.1±1.54
19		H_2N∼∼		24.28±2.03 / 4.25±0.1	172±15.8 / 60.2±5.57
20		NH$_2$		1.20±0.33 / 0.19±0.06	4.25±1.15 / 1.24±0.41
21		NH$_2$		0.12±0.02 / 0.02±0.001	0.39±0.10 / 0.09±0.02

In our previous study,[11] we performed alanine-scanning mutagenesis of DOT1L peptide **1** (Table 3-2). Four critical hydrophobic residues, L865, I867, I869, and L871, failed to tolerate alanine substitution with a significant decrease in binding affinity to both AF9 and ENL proteins. Interestingly, mutation of the last three residues in the DOT1L 10 mer peptide was well tolerated

and showed only a 2-6-fold decrease in the binding affinity in comparison with the wild type peptide.[34] As expected, 7 mer peptide **2** showed reasonable binding affinity to AF9 with a K_i value of 0.16 μM, 8-fold less than 10 mer peptide **1** (Table 3-2). Importantly, the 7 mer peptide derived from site 3, peptide **3**, showed identical binding affinity as **2** (Table 3-2), consistent with the binding affinities of the 10 mer peptides obtained from these two binding sites (Table 3-1). Therefore, in our follow up chemical modifications, we selected 7 mer peptide **2** as a promising lead structure for further optimization. Based on the structural information and essential key binding elements in DOT1L, we separated peptide **2** into three parts: the *N*-terminal two residues, the middle three residues and the *C*-terminal two residues (Figure 3-2). We demonstrated that the I867 and I869 are critical hydrophobic residues that are buried within the DOT1L-AF9 interface.[11] Therefore, the peptide scaffold of the middle three residues was preserved to maintain the hydrogen bonds with the protein and focused on the modification of the I867 and I869 side chains. In the *N*-terminal and *C*-terminal dipeptide moieties, the side chains of L865 and L871 respectively, have hydrophobic interactions with AF9. Thus, these two parts were replaced with non-peptidic scaffolds and hydrophobic groups to mimic the side chains of these leucine residues.
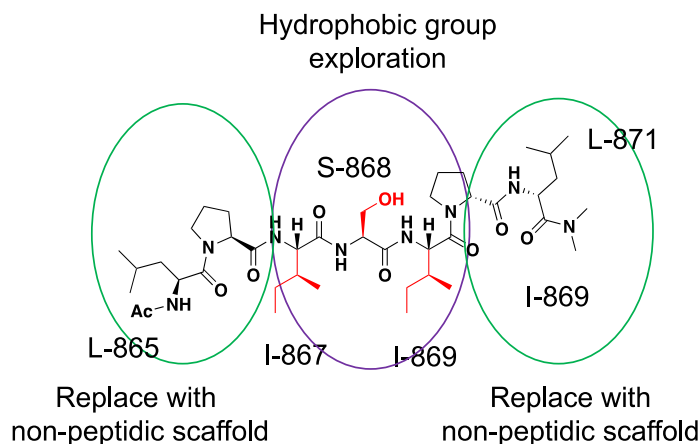
Figure 3-2. Modification strategy for 7 mer DOT1L peptide 2.

To improve the synthetic efficiency, we used a convergent method for the synthesis of the designed compounds by linking different fragments. Therefore, homogeneous reactions instead of solid phase synthesis were used. For the convenience of synthesis, we designed compound **4** by replacing the primary amide in **2** with a dimethylated tertiary amide. In our FP competitive binding assay, **4** binds to AF9 with a K_i value of 0.30 μM and is only slightly less potent than **2** and **3**, indicating that this modification is not detrimental to the binding. To probe the hydrophobic interactions of I867, we designed compounds **5-9** where the isoleucine was replaced with a series of natural or unnatural amino acids. The binding results showed that this pocket is very sensitive to the modifications, and only when the isoleucine residue is replaced with valine, the binding affinity can be slightly improved (**5**, K_i 0.17 μM). Introducing other amino acids at this position, such as leucine, cyclopropyl alaninel, and cyclobutyl alanine, resulting in reduced binding affinity by 3-5-fold (compounds **6-8**). Replacing isoleucine with larger phenylalanine in **9**, significantly decreased the binding by about 20-fold (K_i 5.62 μM), indicating that this pocket can accommodate a small hydrophobic group.

We then explored the hydrophobic interactions of I869. The NMR structure indicated that this pocket could accommodate a larger hydrophobic group and therefore we tried a series of amino acids with a larger hydrophobic side chain. Replacement of the isoleucine residue with a cyclopentyl glycine does not influence the binding affinity (**10**, K_i 0.25 μM). However, enlarging the five-membered ring to a six-membered ring decreases the binding affinity by two-fold (**11** vs **10**). This might suggest that the pocket is not deep enough to accommodate a larger cyclohexyl group. Replacement of the isoleucine with leucine (**12**, K_i 0.83 μM) decreases the binding by 3 fold but using an unnatural cyclopentyl alanine at this position can slightly improve the binding affinity. The resulted compound **13** shows a K_i of 0.13 μM in our competitive FP-based binding assay and is 2 times more potent than **4**. Replacing the cyclopentyl ring in **13** with a cyclohexyl in **14** (K_i 0.18 μM) or a phenyl ring in **15** (K_i 0.28 μM) only slightly decreases the binding affinity. Replacing the cyclopentyl ring in **13** with a larger hydrophobic group, such as an indole (**16**) or a naphthyl group (**17**, **18**), led to decrease binding in comparison with **13**. **16** with a K_i 0.41 μM is about three-fold less potent than **13**, while β-naphthyl group containing compound **17**, is five-fold less potent (K_i 0.73 μM). The α-naphthyl ring-containing compound **18** shows a K_i value of 2.6 μM, being 15 times less potent than **13** and the least potent peptide in this series. Overall, among all the amino acids we have tried at this position, cyclopentyl alanine is the most optimal substitution for R_3 (compound **13**).

The AF9-DOT1L NMR complex structure showed that the side chain of a serine residue, S882, is exposed to the solvent and has no interaction with the protein.[33] Therefore, this residue was used to modify the physicochemical properties and solubility of the peptides, since the other residues are largely hydrophobic. Replacing serine with lysine, dramatically decreases the

86

binding affinity by 15-fold (**19** vs **4**), indicating that a larger group at this site is detrimental to the binding. Replacement of the hydroxyl group in the serine residue of **4** with an amino group led to the compound **20** with slightly improved K_i value of 0.19 μM. Combining the SAR information obtained from studying the middle three residues we designed compound **21**. Interestingly, this compound binds to AF9 with a K_i of 0.02 μM, being 10 times more potent than **4** and as potent as the 10 mer peptide **1**. All of these compounds have been tested for their binding to the highly homologous ENL protein (Table 3-2). The results indicated that these compounds bind to ENL with 5-10 times less potent binding affinities in comparison to AF9, consistent with the binding profile of 10 mer DOT1L peptide **1**.

3.3.2 Further characterization of peptide 21 using biophysical and cell-based assays

To further confirm the binding affinity of the most potent compound **21**, and to determine whether **21** recognizes and binds cellular oncofusion proteins, a biotin-labeled analog **22** was synthesized. As was expected, biochemical assays show that **22** has similar low nanomolar binding affinities as **21** to AF9 and ENL recombinant proteins. In FP-based binding assay, **22** shows K_i values of 10 nM and 63 nM to AF9 and ENL, respectively (Figure 3-3A). Using biolayer interferometry assay (BLI), it was determined that this compound binds to AF9 and ENL with K_D values of 15 nM and 57 nM, respectively (Figure 3-3B), consistent with the K_i values obtained by the competitive FP-based assay. The recombinant proteins used for the binding studies are tagged with maltose binding protein (MBP) to preserve the stability and solubility of the intrinsically disordered AHD domain of AF9 and ENL proteins. The specific interactions of the compound **22** with fusion proteins was confirmed by testing it for its binding to the MBP tag protein only and didn't show any binding (Figure 3-3C). To assess whether

87

peptide **22** can bind to the cellular AF9 oncofusion protein, we have transfected HEK 293t cells with Myc-tagged CxxC-AF9 protein. In streptavidin-biotin pull-down experiments, compound **22** efficiently pulls down cellular Myc-CxxC-AF9 protein in a dose-dependent manner using HEK 293t cell lysates (Figure 3-3D).

Moreover, in a competitive pull-down assay, compound **21** dose-dependently inhibits the binding of biotinylated compound **22** to the cellular Myc-CxxC-AF9 protein, with approximately 60% inhibition at 100 nM (Figure 3-3E). To test if the most potent compound **21** can disrupt the MLL-AF9-DOT1L interaction in cells, we performed a co-immunoprecipitation (co-IP) experiment in HEK 293t cells co-transfected with Flag-DOT1L and Myc-CxxC-AF9 (Figure 3-3F). In the absence of **21**, DOT1L was able to pull down AF9 effectively in the cell lysate. Incubation of the cell lysates with various doses of **21** disrupted the DOT1L-AF9 complex in a dose-dependent manner. Together these experiments demonstrate that both, compounds **21** and biotinylated **22**, recognize and bind to the cellular AF9 protein. Furthermore, **21** effectively competes with compound **22** providing evidence that they bind at the same AF9 binding site and disrupts the DOT1L-AF9 interaction and **21** effectively inhibits the DOT1L-AF9 interactions.
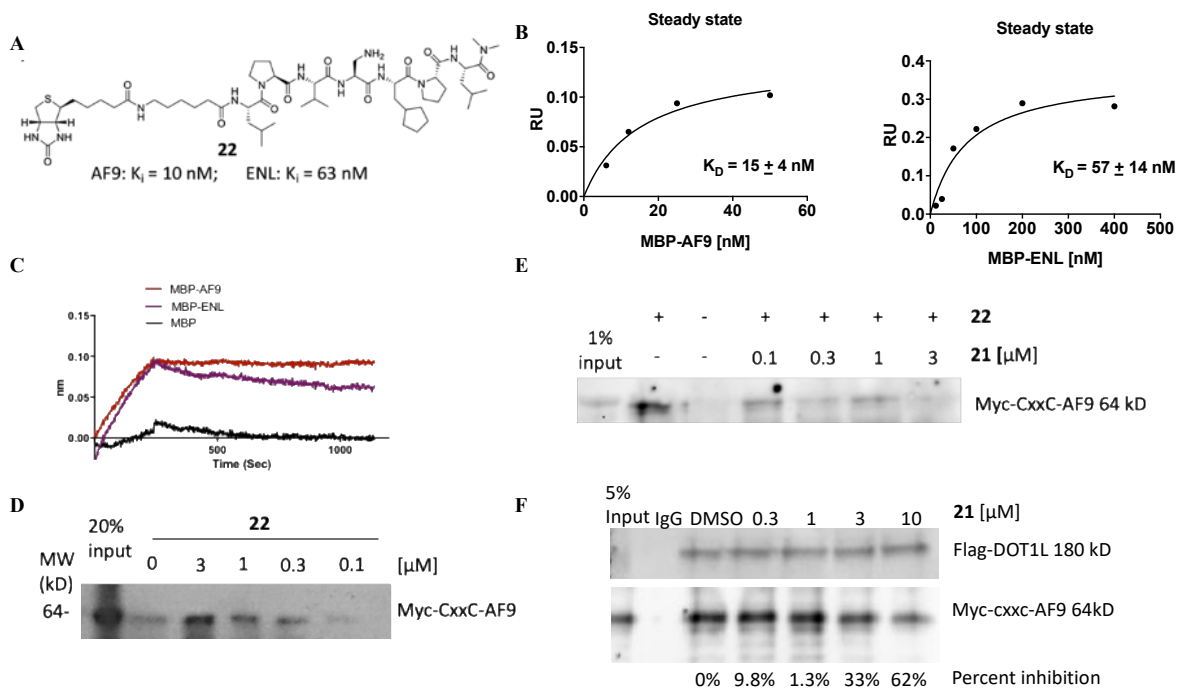
Figure 3-3 Biotinylated compound 22

(A) Chemical structure and Ki values obtained by FP-based binding assay; (B) Binding affinity determined by BLI against two oncofusion proteins, AF9 and ENL; (C) Compound **22** specifically binds to MBP-AF9 and MBP-ENL and not to MBP tag protein. (D)Pull down assay using HEK-239 cells transiently transfected with Myc-CxxC-AF9. (E) Compound **21** in a competitive manner inhibits binding of biotinylated **22** to cellular Myc-CxxC-AF9. (F) Co-IP experiment in HEK-239 cells co-transfected with Flag-DOT1L and Myc-CxxC-AF9.

3.3.3 Modification of C-terminal and N-terminal di-peptidic motifs

Table 3-3 Modification of the C-terminal and N-terminal dipeptidic motifs
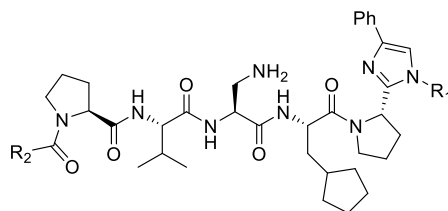
Peptides	R_1	R_2	MBP-AF9 IC_{50}, nM (K_i, nM)	MBP-ENL IC_{50}, nM (K_i, nM)
23	Me	(structure, NHAc)	372 ± 141 57 ± 22	$1{,}773 \pm 194$ 417 ± 46
24	Et	(structure, NHAc)	341 ± 75 50 ± 15	$1{,}570 \pm 438$ 369 ± 103
25	i-Pr	(structure, NHAc)	369 ± 113 57 ± 17	$1{,}220 \pm 130$ 287 ± 31
26	(cyclohexyl)	(structure, NHAc)	82 ± 17 13 ± 3	427 ± 74 101 ± 18
27	(cyclohexyl)	(structure)	149 ± 37 23 ± 6	237 ± 30 56 ± 7
28	(cyclohexyl)	Ph	57 ± 17 9 ± 3	504 ± 39 119 ± 9

Towards the development of DOT1L peptidomimetics, we performed preliminary studies for the modifications of both the *C*- and *N*-termini (Table 3-3). In the following design, the middle three residues were kept as in the most potent compound **21**. Both the *C*- and *N*-termini

dipeptide motifs contain a proline residue and a leucine residue. Among all-natural amino acids, proline is unique in that it can strongly influence the conformation of the peptide; therefore, in our initial studies, the pyrrolidine ring was kept on both termini. In peptide modifications, replacing the amide bond with a hetero-aromatic ring is a frequently used method to mimic the planar structure of the amide and to improve the metabolic stability. Thus, for the *C*-terminal modifications, we designed compounds **23-26** by replacing the amide bond between proline and leucine with an imidazole ring and by introducing substitute groups to mimic the side chain of leucine involved in interaction with AF9. In these compounds, a phenyl ring was introduced to the C_4 position of the imidazole, and various hydrophobic groups were introduced to the N_1, respectively. These compounds have been tested in the FP competitive binding assay, and the results indicated that compounds with a small hydrophobic group on N_1 (**23-25**) had decreased binding affinity compared with **21**. However, compound **26** which has a cyclohexyl group on N_1 shows a K_i value of 13 nM to AF9 and is slightly more potent than **21**. These results suggest that a larger hydrophobic group at N_1 could bind to a bigger hydrophobic pocket and improve the binding affinity.

The acetylamido group at the *N*-terminus is exposed to the solvent and doesn't interact with the protein. Therefore, we designed compound **27** by removing this group. Compound **27** has a K_i value of 23 nM for AF9 protein and is about 2 times weaker than **26**, indicating that the acetylamido group could play a role in controlling the orientation of the hydrophobic side chain of the leucine residue. We then designed compound **28** by replacing the 2-methyl-butyl group in **27** with a phenyl ring. This compound binds to AF9 with a Ki value of 9 nM, about 3 times more potent than **27** and 2 times more potent than **21**, indicating that non-peptidic modifications of the

91

two terminal residues not only can reduce the peptidic characteristic of the compounds but can also improve the binding affinity.

These compounds have also been evaluated for their binding affinities to ENL. Similar to the 7 mer analogs, the *C*-terminal modified compounds **23**-**26** bind to ENL 5-10-fold less potent than to AF9. However, the *N*-terminal modified compounds **27** and **28** show a different trend. **27** binds to ENL with a K_i value of 56 nM and is only 2-3 times less potent to AF9, but **28** binds to AF9 13-fold more potently than to ENL, suggesting that *N*-terminal modifications could alter the selectivity in binding to the two fusion proteins. As a continuation of this work, after developing and characterizing this small series of peptides, we aimed to develop further non-peptidic small molecules that bind to the AHD domain to displace DOT1L in cells.

3.3.4   Development and characterization of cellularly active peptidomimetics

To improve the stability and cellular permeability of the peptidomimetics, the *C*- and *N*-termini of **28** were further modified leading to peptidomimetic **29**. **29**, retained the potency of **28** with a K_i of 10 nM to AF9 and an overall improvement of 16-fold over the initial peptide **2** (Figure 3-4A). To test its cellular activity and to demonstrate target specific phenotype, murine established leukemia cell lines harboring either the MLL-AF9 fusion or E2A-HLF fusion proteins were used. E2A-HLF cells are known to not depend on DOT1L's presence or function for leukemogenesis and act as a negative control for the initial studies since compounds which are disrupting the PPIs between fusion proteins and DOT1L should not show activity. As was expected, peptidomimetic **29** selectively killed MLL-AF9 cells in a dose-dependent manner up to 10 μM, while no effect was observed against E2A-HLF cells (Figure 3-4B-C). Importantly, this

translated to a dose-dependent decrease in MLL-target genes *HoxA9* and *Meis1* and induced cell

differentiation (Figure 3-4D-E).
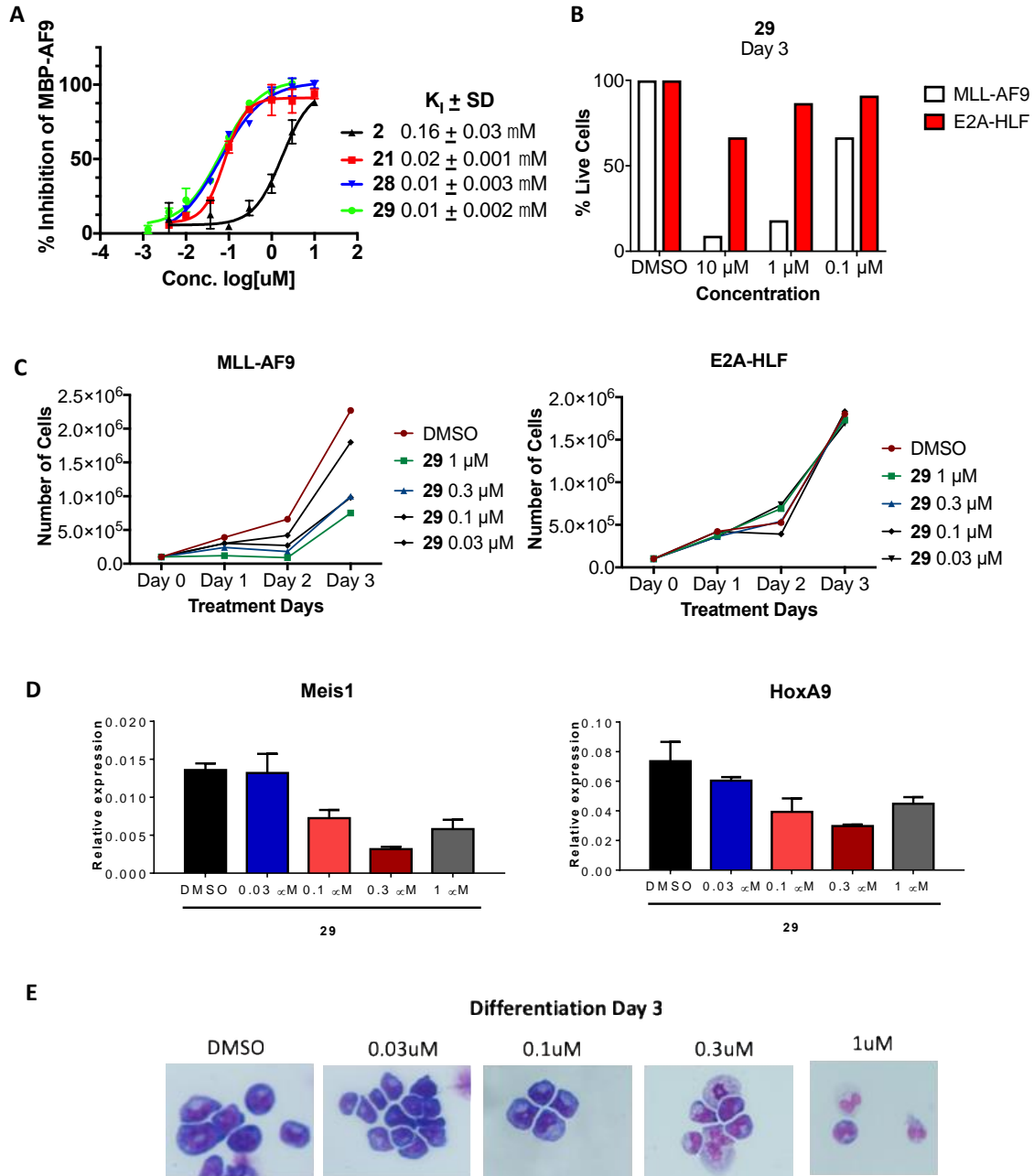
Figure 3-4 Further chemical modifications to improve the cell permeability and stability of DOT1L peptidomimetics.

(A) FP based assay showing a 10-fold improvement between peptide **21** and WT peptide **2** and a 17-fold improvement in peptidomimetic **28** and **29** and WT 7 mer peptide **2**. (B) Selectivity

profile of **29** showing significant killing of murine cell lines transformed with MLL-AF9 in comparison to E2A-HLF after 3 days of treatment. Up to 10 µM there is minimal toxicity in E2A-HLF. (C) Cells were treated at day 0 and day 2 with peptidomimetic **29** and monitored for cell growth gene expression and differentiation. The compound inhibited cell growth in MLL-AF9 murine cell line and not in E2A-HLF even at 100 nM. (D) At day 3, cells were harvested and tested for the gene expression of MLL-target genes *HoxA9* and *Meis1*. (E) Wright-Giemsa stain of cells after treatment with **29** at various doses inducing cell differentiation at 10 *µ*M and 300 nM (Olympus IX83 Inverted Microscope; Original magnification x400).

3.4   Conclusions

Based on the 7 mer DOT1L peptide, a series of peptidomimetics was designed and synthesized to improve the binding affinity to AF9 and decrease the peptidic characteristics. By optimizing the middle three residues, we identified peptide **21** which has a significantly improved binding affinity compared to the original peptide **2**. Based on **21**, we have performed preliminary modifications to both the *C-* and *N*-termini of **21**. For *C*-terminal dipeptide motif, we found that the amide bond in the dipeptide can be replaced with an imidazole ring and hydrophobic groups can be introduced to the imidazole ring to mimic the hydrophobic interaction of the DOT1L leucine residue L871. For the *N*-terminal dipeptide motif, replacement of the leucine residue L865 with a suitable hydrophobic group can improve the binding affinity.

Furthermore, modifications to the *C-* and *N*-terminal hydrophobic groups led to peptidomimetic **29** that has improved stability and selective cellular activity against MLL-AF9 transformed cells that depend on DOT1L activity, but not affecting the growth of E2A-HLF cell line. Furthermore, **29** demonstrates on target activity by downregulating known MLL-target genes and inducing cell differentiation. Overall these results are providing a prove of principle for targeting the DOT1L recruitment and blocking its interaction with AF9 and demonstrate the

utility of peptidomimetics as potential chemical tools and therapeutics for MLL-rearrangement leukemia.

3.5 Materials and methods

Fluorescence Polarization (FP) binding measurements

MBP-AF9 (487-568) was cloned into pMBP-LIC vector and MBP-ENL (489-559) into pMSCG9-LIC vector. Both proteins were expressed in Escherichia coli strain BL21 (DE3) (Invitrogen). The proteins were induced with 200 μM IPTG at 20°C and cells were harvested after 20 h and resuspended in cold lysis buffer (50 mM Tris HCl, pH 7.5, 150mM NaCl, 0.01% β-mercatoethanol). The proteins were purified by affinity chromatography employing Ni-agarose (Qiagen), followed by size exclusion chromatography in 50 mM Tris HCl, pH 7.5, 150 mM NaCl, 3 mM DTT. Purified recombinant proteins were stored at -80 ℃ for further experiments.

N-terminal fluorescein labeled DOT1L (N-Flu-DOT1L) 10-mer peptide (N-Flu-βAla-βAla-LPISIPLSTV) with K_D values of 45 nM and 544 nM for MBP-AF9 and MBP-ENL respectively, was used as a fluorescent probe in the competitive FP binding assays. The FP assays were carried out with serial dilutions of tested peptides and fixed concentration of N-Flu-DOT1L (10 nM) and MBP-AF9 (200 nM) or MBP-ENL (1 μM) in assay buffer (100mM NaH_2PO_4, 150mM NaCl, 0.1% β-ME, 0.01% Triton X-100). The polarization values were measured after 3-hour incubation at an excitation wavelength of 485 nm and an emission wavelength of 530 nm using the plate reader Synergy H1 Hybrid, BioTek. IC_{50} values were determined by nonlinear regression fitting of the competitive curves using GraphPad Prism 6.0. The K_i values were calculated as described previously (Anal Biochem 2004, 332 (2), 261-73).

Bio-layer interferometry (BLI) binding studies

BLI experiments were performed using an OctetRED96 instrument from PALL/ForteBio. All assays were run at 30 ℃ using HEPES buffer (10 mM HEPES pH 7.4, 150 mM NaCl, 0.005% tween-20) with continuous 1000 rpm shaking. Compound **22** was immobilized on Super Streptavidin (SSA) biosensors by dipping sensors in 2 μg/mL solution to reach saturation response level of 2-3 nm. Biotinylated blocked Streptavidin sensors were used as control sensors prepared by the protocol provided from the manufacturer. Compound **22** loaded sensors were dipped in a serial dilution of MBP-AF9 (aa 487-568) in concentration range from 40 to 5 nM, MBP-ENL (aa 489-559) from 10 to 200 nM and MBP (aa 27-392) at single concentration of 1000 nM, and allowed to associate for 6 minutes and dissociate for 12 minutes. Buffer only reference was included in all assays. Collected raw kinetic data were processed in the Data Analysis software provided by ForteBio using double referencing for binding analysis in which both buffers only sensors and control sensors were subtracted. Resulting binding kinetics were fitted to a 1:1 binding model from which steady state K_D values were calculated.

Pull-down assay

HEK293t cells were transfected for 48 hours with Myc-tagged CxxC-AF9 protein using Fugene 6 (Promega). Cells were lysed in BC-300 lysis buffer (20 mM Tris-HCl, pH 8.0, 300 mM KCl, 1 mM EDTA, 10% glycerol, 0.1% Nonidet P-40, and protease inhibitor mixture; Biomake). The supernatant was pre-cleared for 2h in streptavidin agarose beads (Millipore). The pre-cleared lysates were incubated with several concentrations of biotin-labeled **22** at 4 ℃ overnight. For the competitive pull-down assay, lysate was incubated with a fixed concentration of **22** (1 μM) with various concentrations of **21** at 4 ℃ overnight. The next day, the cell lysate was incubated with

streptavidin agarose beads at 4 ℃ for 2 hours. After extensive washing the beads with the BC-300 lysis buffer, the pull-down samples were applied to SDS-PAGE electrophoresis and pulldown Myc-CxxC-AF9 protein was probed with goat monoclonal anti-Myc antibody (Abcam). Band quantification was analyzed using ImageJ software.

Co-Immunoprecipitation assay

HEK293t cells were co-transfected for 48 hours with Myc-CxxC-AF9 and Flag-DOT1L using Fugene6 (Promega). Cells were lysed in BC-300 lysis buffer and precleared in mouse IgG-agarose (Sigma-Aldrich) for 2 hours. The precleared lysates were incubated with different concentrations of **21** at 4 ℃ overnight. The next day, the cell lysates were immunoprecipitated with anti-FLAG M2 magnetic beads (Sigma-Aldrich) at 4 ℃ for 2 h. After incubation, the beads were washed extensively, boiled in SDS loading buffer, and analyzed by Western blotting using mouse monoclonal anti-FLAG M2 (Sigma-Aldrich) and goat monoclonal anti-Myc (Abcam) antibody. Band quantification was analyzed using ImageJ software.

Cell Proliferation Assay

Cell numbers was assessed using a hemocytometer. Cells were treated with various doses of **29** or equivalent percentage of solvent (DMSO) on day 0 and day 2, followed by daily counting.

Gene Expression

Cells were harvested from the cell proliferation assay on day 3. RNA was isolated, and cDNA was synthesized using Superscript III reverse transcriptase kit (Invitrogen). Quantitative real-time PCR was performed using SyberGreen master mix (Applied Biosystems) and primers for Hoxa9, Meis1, GAPDH, and beta-Actin. Data was analyzed using the 2_DD Ct method. Expression was normalized to GAPDH expression and was performed in triplicate.

Cells were harvested from the cell proliferation assay on day 3 and cytospun onto microscope slides. Cells were then stained with Wright-Giemsa stain (Millipore) and mounted on a slide with a coverslip using Permount (Fisher Chemical) mounting medium. Images were captured using bright field condition with an Olympus IX83 inverted microscope.

3.6   Contributions

Sierrah Marie Grigsby performed presented biochemical and biological characterization of the peptidomimetics synthesized by Lei Du, Aihong Yao, and Garrett Johnson.

3.7   References

1.   Muntean AG, Hess JL. The pathogenesis of mixed-lineage leukemia. *Annu Rev Pathol*. 2012;7:283-301.
2.   Yokoyama A. Transcriptional activation by MLL fusion proteins in leukemogenesis. *Exp Hematol*. 2017;46:21-30.
3.   Krivtsov AV, Armstrong SA. MLL translocations, histone modifications and leukaemia stem-cell development. *Nature Reviews Cancer*. 2007;7(11):823-833.
4.   Lin C, Smith ER, Takahashi H, et al. AFF4, a Component of the ELL/P-TEFb Elongation Complex and a Shared Subunit of MLL Chimeras, Can Link Transcription Elongation to Leukemia. *Molecular Cell*. 2010;37(3):429-437.
5.   Yokoyama A, Lin M, Naresh A, Kitabayashi I, Cleary ML. A Higher-Order Complex Containing AF4 and ENL Family Proteins with P-TEFb Facilitates Oncogenic and Physiologic MLL-Dependent Transcription. *Cancer Cell*. 2010;17(2):198-212.
6.   Mohan M, Lin C, Guest E, Shilatifard A. Licensed to elongate: a molecular mechanism for MLL-based leukaemogenesis. *Nature Reviews Cancer*. 2010;10(10):721-728.
7.   Bardos JI, Saurin AJ, Tissot C, Duprez E, Freemont PS. HPC3 is a new human polycomb orthologue that interacts and associates with RING1 and Bmi1 and has transcriptional repression properties. *J Biol Chem*. 2000;275(37):28785-28792.
8.   Huynh KD, Fischle W, Verdin E, Bardwell VJ. BCoR, a novel corepressor involved in BCL-6 repression. *Genes Dev*. 2000;14(14):1810-1823.
9.   Luo Z, Lin C, Guest E, et al. The super elongation complex family of RNA polymerase II elongation factors: gene target specificity and transcriptional output. *Mol Cell Biol*. 2012;32(13):2608-2617.
10.   Steger DJ, Lefterova MI, Ying L, et al. DOT1L/KMT4 recruitment and H3K79 methylation are ubiquitously coupled with gene transcription in mammalian cells. *Mol Cell Biol*. 2008;28(8):2825-2839.

11.   Shen C, Jo SY, Liao C, Hess JL, Nikolovska-Coleska Z. Targeting recruitment of disruptor of telomeric silencing 1-like (DOT1L): characterizing the interactions between DOT1L and mixed lineage leukemia (MLL) fusion proteins. *The Journal of Biological Chemistry*. 2013;288(42):30585-30596.

12.   Leach BI, Kuntimaddi A, Schmidt CR, Cierpicki T, Johnson SA, Bushweller JH. Leukemia fusion target AF9 is an intrinsically disordered transcriptional regulator that recruits multiple partners via coupled folding and binding. *Structure*. 2013;21(1):176-183.

13.   Biswas D, Milne TA, Basrur V, et al. Function of leukemogenic mixed lineage leukemia 1 (MLL) fusion proteins through distinct partner protein complexes. *Proc Natl Acad Sci U S A*. 2011;108(38):15751-15756.

14.   Krivtsov AV, Feng Z, Lemieux ME, et al. H3K79 methylation profiles define murine and human MLL-AF4 leukemias. *Cancer cell*. 2008;14(5):355-368.

15.   Bernt KM, Zhu N, Sinha AU, et al. MLL-rearranged Leukemia is Dependent on Aberrant H3K79 Methylation by DOT1L. *Cancer Cell*. 2011;20(1):66-78.

16.   Nguyen AT, Taranova O, He J, Zhang Y. DOT1L, the H3K79 methyltransferase, is required for MLL-AF9–mediated leukemogenesis. *Blood*. 2011;117(25):6912-6922.

17.   Daigle SR, Olhava EJ, Therkelsen CA, et al. Selective Killing of Mixed Lineage Leukemia Cells by a Potent Small-Molecule DOT1L Inhibitor. *Cancer Cell*. 2011;20(1):53-65.

18.   Nguyen AT, Zhang Y. The diverse functions of Dot1 and H3K79 methylation. *Genes & Development*. 2011;25(13):1345-1358.

19.   Jo SY, Granowicz EM, Maillard I, Thomas D, Hess JL. Requirement for Dot1l in murine postnatal hematopoiesis and leukemogenesis by MLL translocation. *Blood*. 2011;117(18):4759-4768.

20.   Copeland RA, Harpel MR, Tummino PJ. Targeting enzyme inhibitors in drug discovery. *Expert Opin Ther Targets*. 2007;11(7):967-978.

21.   Fry DC. Targeting protein-protein interactions for drug discovery. *Methods Mol Biol*. 2015;1278:93-106.

22.   Macarron R, Banks MN, Bojanic D, et al. Impact of high-throughput screening in biomedical research. *Nat Rev Drug Discov*. 2011;10(3):188-195.

23.   Chauhan D, Velankar M, Brahmandam M, et al. A novel Bcl-2/Bcl-X(L)/Bcl-w inhibitor ABT-737 as therapy in multiple myeloma. *Oncogene*. 2007;26(16):2374-2380.

24.   Mady ASA, Liao C, Bajwa N, et al. Discovery of Mcl-1 inhibitors from integrated high throughput and virtual screening. *Sci Rep*. 2018;8(1):10210.

25.   Ran X, Gestwicki JE. Inhibitors of protein-protein interactions (PPIs): an analysis of scaffold choices and buried surface area. *Curr Opin Chem Biol*. 2018;44:75-86.

26.   Kumar A, Voet A, Zhang KY. Fragment based drug design: from experimental to computational approaches. *Curr Med Chem*. 2012;19(30):5128-5147.

27.   Vagner J, Qu H, Hruby VJ. Peptidomimetics, a synthetic tool of drug discovery. *Curr Opin Chem Biol*. 2008;12(3):292-296.

28.   Yu S, Qin D, Shangary S, et al. Potent and orally active small-molecule inhibitors of the MDM2-p53 interaction. *J Med Chem*. 2009;52(24):7970-7973.

29.   Zhao Y, Aguilar A, Bernard D, Wang S. Small-molecule inhibitors of the MDM2-p53 protein-protein interaction (MDM2 Inhibitors) in clinical trials for cancer treatment. *J Med Chem*. 2015;58(3):1038-1052.

30.   Carter BZ, Mak DH, Morris SJ, et al. XIAP antisense oligonucleotide (AEG35156) achieves target knockdown and induces apoptosis preferentially in CD34+38- cells in a phase 1/2 study of patients with relapsed/refractory AML. *Apoptosis*. 2011;16(1):67-74.

31.   Hurwitz H, Pitot H, Strickler J, et al. 76 Preliminary Report of a First-in-human, Open-label, Multicenter, Phase I Study of AT-406 (Debio 1143), an Oral Small Molecule Multi-IAP Inhibitor, in Solid Tumors and Lymphomas. *European Journal of Cancer*. 2012;48:25.

32.   Cao F, Townsend EC, Karatas H, et al. Targeting MLL1 H3K4 methyltransferase activity in mixed-lineage leukemia. *Mol Cell*. 2014;53(2):247-261.

33.   Kuntimaddi A, Achille NJ, Thorpe J, et al. Degree of recruitment of DOT1L to MLL-AF9 defines level of H3K79 Di- and tri-methylation on target genes and transformation potential. *Cell Rep*. 2015;11(5):808-820.

34.   Shen C, Jo SY, Liao C, Hess JL, Nikolovska-Coleska Z. Targeting recruitment of disruptor of telomeric silencing 1-like (DOT1L): characterizing the interactions between DOT1L and mixed lineage leukemia (MLL) fusion proteins. *J Biol Chem*. 2013;288(42):30585-30596.

CHAPTER 4

Interactions of the ENL YEATS Domain Protein

4.1   Abstract

The human YEATS domain family proteins ENL and AF9 are homologous proteins containing an N-terminal YEATS domain and a C-terminal ANC1 Homology Domain (AHD). Both proteins recruit, DOT1L, a histone methyltransferase that activates genes, through its AHD domain. AF9 and ENL are commonly mutated in MLL-rearrangement leukemia, but despite being paralogs, MLL-AF9 and MLL-ENL leukemia in patients vary in aggression and disease latency. MLL-ENL is more aggressive leukemia with a 20% less 5-year survival rate than MLL-AF9. The difference in these fusion proteins is the retention of the YEATS domain in the MLL-ENL fusion that is lost in MLL-AF9. The YEATS domain is a highly-conserved H3K acyl reader motif present in a diverse family of chromatin-associated proteins. It was also reported that ENL YEATS domain resides in a complex with Paf1 of the PAFc complex. Based on these findings we hypothesized that both, recruitment of PAFc and lysine acyl reader function could potentially contribute to the aggressive behavior of MLL-ENL leukemia. In this chapter, the goal was to study MLL-ENL fusion protein and the effect of disrupting interactions with DOT1L on leukemic cell growth and biochemical and biophysical characterization of YEATS-ENL interactions. We demonstrate that established MLL-ENL cell lines containing the YEATS domain were significantly less sensitive to DOT1L loss than MLL-AF9. To determine if the YEATS domain and Paf1 interact directly or indirectly, we quantified the PPI using the biophysical method, BLI, and we confirmed the direct and potent interaction (KD =15 nM).

Furthermore, we mapped the interaction to an 80 aa region of Paf1 from 170-250 aa. Based on the reported studies and our exciting results, we developed a differential scanning fluorimetry (DSF) based binding assay for initiating a campaign for fragment-based screening and identifying compounds that bind to YEATS domain and either the reader function or Paf1 PPI. The development of these tools will allow us to further probe the YEATS interactions with Paf1 and H3 and their role in MLL-ENL driven leukemia.

4.2   Introduction

There are 4 classifications of acute myeloid leukemia (AML) 1) AML with recurring genetic aberrations 2) AML with multilineage dysplasia 3) AML, therapy-related and 4) AML not otherwise characterized.[1] All of which vary in severity and disease latency. AML with 11q23;MLL abnormalities have the poorest prognosis in comparison to intermediate, normal cytogenetics patients, AML with t(8;21)(a22;q22); AML1/ETO, AML with abnormal bone marrow eosinophils inv(16)(p13q22) or t(16;16)(p13;q22); CBFB/MYH11, and acute promyelocytic leukemia (AML with t(15;17)(q22;q12); PML-RARA.[1] In two independent studies comparing non-MLL vs MLL AML patient survival, patients with MLL aberrations have a 50% survival of less than 1 year in comparison to more than 2-year survival for patients with non-MLL genetic cytogenetics (Figure 4-1A).[1,2] Among the various MLL-fusion leukemias, there is also a stratification amongst the fusions and disease progression.[1] Clinically and in mouse models, out of the most common fusions, there are 3 clusters, severe, moderate and favorable, based on median survival.[1,3] MLL-ENL along with MLL-AF6 and MLL-AF10 are the most aggressive oncofusion proteins, followed by MLL-AF9 in the moderate category, with MLL-AF1p as the least aggressive exhibiting a good prognosis (Figure 4-1B-C).[1,3] AF9, ENL, ELL, AF10, and AF6 account for more than 70% of all MLL-rearrangement leukemia seen in patients.[4] These fusions have a 63%, 45%, 60%, 44%, and 22% 5-year survival rate respectively.[3] The differences in overall survival are striking among the fusions especially when comparing MLL-AF9 and MLL-ENL where patients have a decrease in survival by roughly 20% when diagnosed with an ENL fusion versus an AF9 fusion.
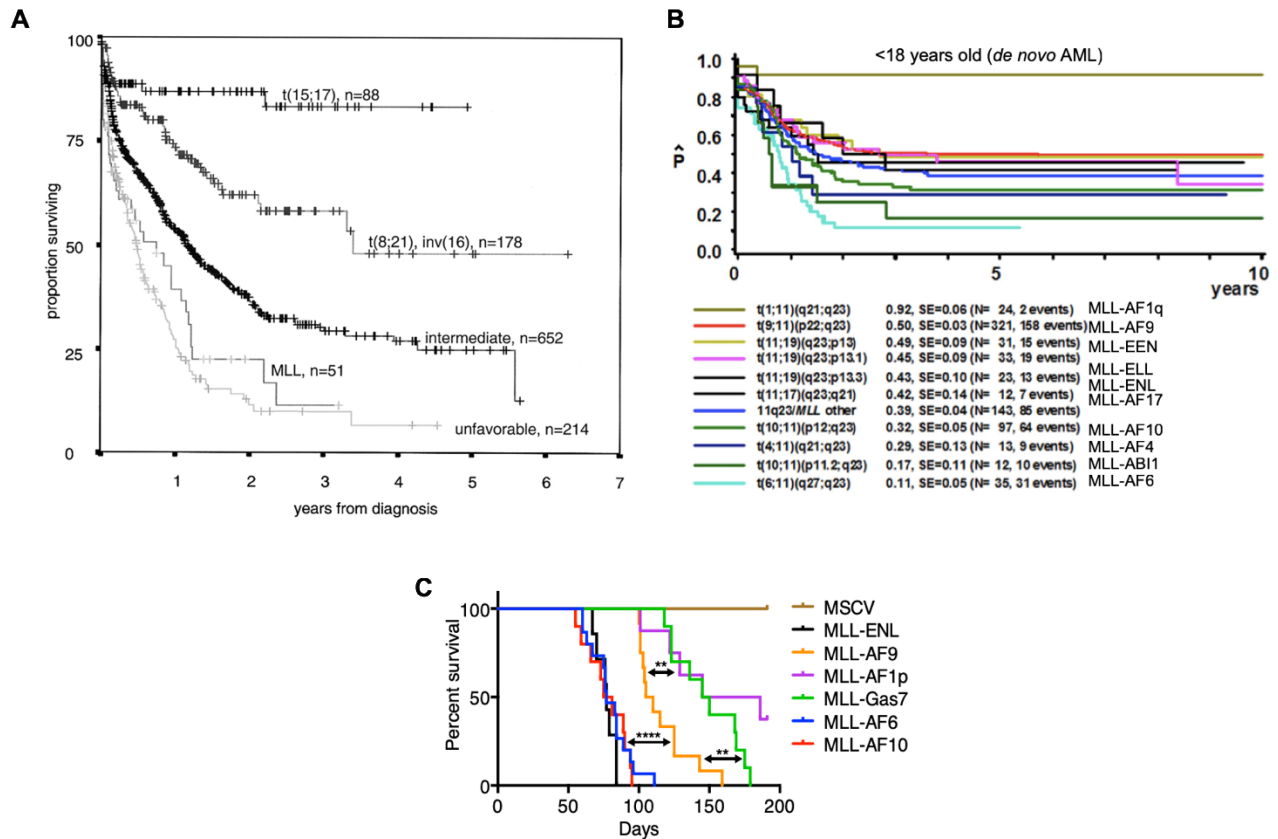
Figure 4-1 Overall survival of patients and mice with MLL1 rearrangement leukemia.

(A) Overall survival of 1183 patients with AML according to cytogenetics.[1] Patients harboring a MLL rearrangement have the poorest prognosis with 50% survival post diagnosis at less than 1 year. (B) Survival of patients with 11q23/MLL-rearrangements of pediatric AML patients with various MLL-fusions.[5] This patient data shows that amongst the various translocations there is a wide range of disease latencies, with MLL-AF6 being the most aggressive and MLL-AF1q as the least aggressive. (C) Survival curves of mice transplanted with various cell lines with differing MLL-rearrangements.[3] In this mouse model, there is a clear stratification amongst the MLL-fusions. With MLL-AF6, MLL-AF10 and MLL-ENL as the most aggressive, MLL-AF9 as moderate, and MLL-AF1p as least aggressive.

Interestingly, AF9 and ENL are homologous proteins containing an **N**-terminal YEATS domain and *C*-terminal AHD domain (Figure 4-2A-B). However, their MLL-fusion proteins yield a very different patient survival rate. As mentioned previously, the AHD domain has been well characterized in its role of recruiting both gene activating and repressive complexes (Chapter 1 and 2). Studies have indicated that there is a difference in the translocation point at

chromosomes for AF9 and ENL where MLL-AF9 has a truncated AF9 segment only containing the AHD domain while MLL-ENL retains the majority of the protein including the YEATS domain (Figure 4-2C).[6,7]
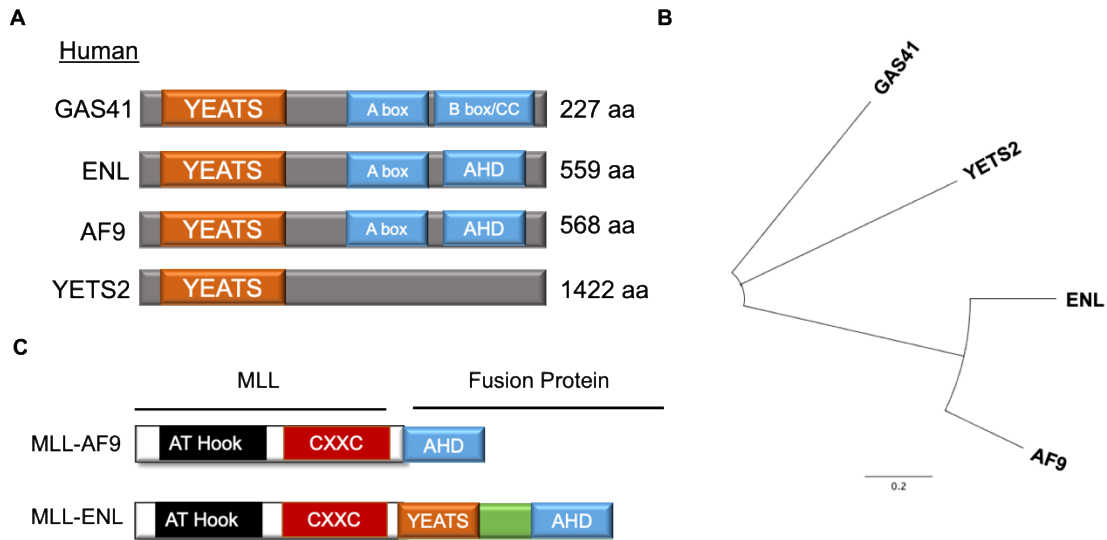
Figure 4-2 YEATS domain family of protiens.

(A)Protein schematic of the 4 human YEATS domain containing protein. (B) Phylogenetic tree of the YEATS proteins showing AF9 and ENL are the most similar in structure; whereas, GAS41 and YETS2 are more distant relatives. (C) Protein schematic of the most common MLL-AF9 and MLL-ENL proteins found in patients.[6,7]

4.1.1 YEATS domain as an acetylation reader

The YEATS domain is an epigenetic reader for histone acetylation and similar modifications.[8,9] This family of proteins was classified as a distinct family separate from classic BRD and PHD domain acetylation readers. The complex structure between AF9 YEATS domain with a H3K9ac peptide, showed that the protein recognized acetylated lysine by adopting an immunoglobulin type fold and uses a serine-lines aromatic cage to specifically read these residue modifications.[8] Mutagenesis studies further showed when mutating phenylalanine 59 (F59) or tyrosine 78 (Y78) to alanine significantly impacted the YEATS domains ability to recognize acetyl-lysine and other acyl-lysine residues.[8] The ENL YEATS domain was later crystallized

with an H3K27ac peptide confirming the same recognition sandwiching and dependence of the serine and aromatic cage with critical interactions with F59 and Y78.[10] Functionally, the YEATS domain is required for AF9 and ENL recruitment to chromatin. In the absence of YEATS-H3ac binding, transcriptional control at H3ac enriched loci is lost.[8,11] Moreover, targeted deletion of YEATS suppresses transcriptional initiation and elongate at active genes.[12] This demonstrates the importance of the YEATS domain for targeting AHD associated complexes like SEC and DOT1L to chromatin that have been shown to be important for acute myeloid leukemia.[8,10,12]

4.1.2   Paf1 and YEATS interaction

Recent studies have linked PAFc to the YEATS domain by identifying a novel association of PAFc subunit Paf1 to the YEATS domain. Paf1 is a part of the RNA Polymerase II-Association Factor complex (PAFc) along with its other subunits, CDC73, CTR9, LEO1, RTF1, and SKI8.[13,14] PAFc is known for its participation in histone modification and transcriptional regulation ranging from initiation to termination. PAFc primarily functions through PPIs with histone modifiers, elongation factors, and RNA 3'-end processing factors.[15-17] PAFc is important in regulating many cellular processes ranging from cell cycle and development to tumor progression.[18] Abnormal expression of PAFc has been correlated with many cancer types.[19] Studies show the YEATS domain can target SEC and PAFc to chromatin in the absence of sequence-specific recruitment factors to initiate transcription elongation through Pol II.[20] This study and others have implicated the YEATS domain as a potentially important factor for MLL-fusion leukemia.[10,12,20,21] However, the direct interaction between the YEATS domain and Paf1 have not been quantified and confirmed nor has the increase in MLL-ENL disease severity been contributed to either the WT function of YEATS as an acetyl-lysine reader or the novel PAFc recruitment.

4.1.3 Goals for the study

In this study, we aimed first to compare the role of DOT1L recruitment by MLL-ENL fusion protein in the same system described in Chapter 2 in order to compare and weigh its contribution to leukemogenesis in a model system. We found that while DOT1L recruitment is critical for MLL-AF9 leukemic cell growth (Chapter 2), in cells harboring the MLL-ENL rearrangement containing the YEATS domain, cell proliferation is not significantly affected. We next, explored the other 2-interactions that the YEATS domain could be mediating through MLL-ENL to drive the aberrant MLL-target gene activation. Outside of the acetylation reading function of YEATS, we aimed to characterize the PPI with Paf1 to determine if Paf1 directly interacts and recruits PAFc to MLL-target genes in addition to the already known interaction between the *N*-terminus of MLL and PAFc.[22] In these preliminary studies, we confirmed that the YEATS domain interacts directly with Paf1 with a low nanomolar binding affinity of 15 nM and identified the interaction to the Leo1 binding site from 170-250 aa on Paf1. Furthermore, we developed a Differential Scanning Fluorimetry (DSF) fragment-based screening assay to identify molecules that could bind to the YEATS domain with the hopes to develop small molecules specific for inhibiting acetylation binding or Paf1 binding. The small molecules developed can be used as chemical tools to understand further the biology attributed to these interactions in leukemia and other contexts.

4.2   Results

4.2.1 DOT1L is not solely responsible for leukemic cell growth in MLL-ENL transformed cells

Due to the similarity in the wild type AF9 and ENL proteins, they were regarded as having similar functions on leukemia.[23] To address whether MLL-AF9 and MLL-ENL leukemic

cells have the same functional dependence on DOT1L's enzymatic activity, *Dot1lf/f CreER(T2)*[+] cell lines carrying retroviral vectors expressing the Δ10 deletion mutant, I867A, and a catalytically inactive mutant lacking H3K79 methyltransferase activity (RCR mutant) were generated (Figure 4-3A). These cells underwent the same treatment schedule as the MLL-AF9 cells in Chapter 2, 7.5 nM tamoxifen every other day. We show that even when endogenous protein is completely removed, there is only a delay in cell proliferation; however, the cells continue to divide. The slowed growth is shown in both enzymatically inactivated DOT1L cells and the blocked recruitment cells. This data highlights that the effect on growth we are seeing is due to DOT1L's recruitment which is what we see in MLL-AF9 cells; however, the effect on growth is significantly less in MLL-ENL than MLL-AF9 (Figure 4-3B). We also see a profound decrease in H3K79me2, which we know is due to the lack of DOT1L recruitment or enzymatic activity suggesting that targeting DOT1L alone when the YEATS domain is present in the fusion protein is not sufficient to inhibit leukemic cell growth (Figure 4-3C).
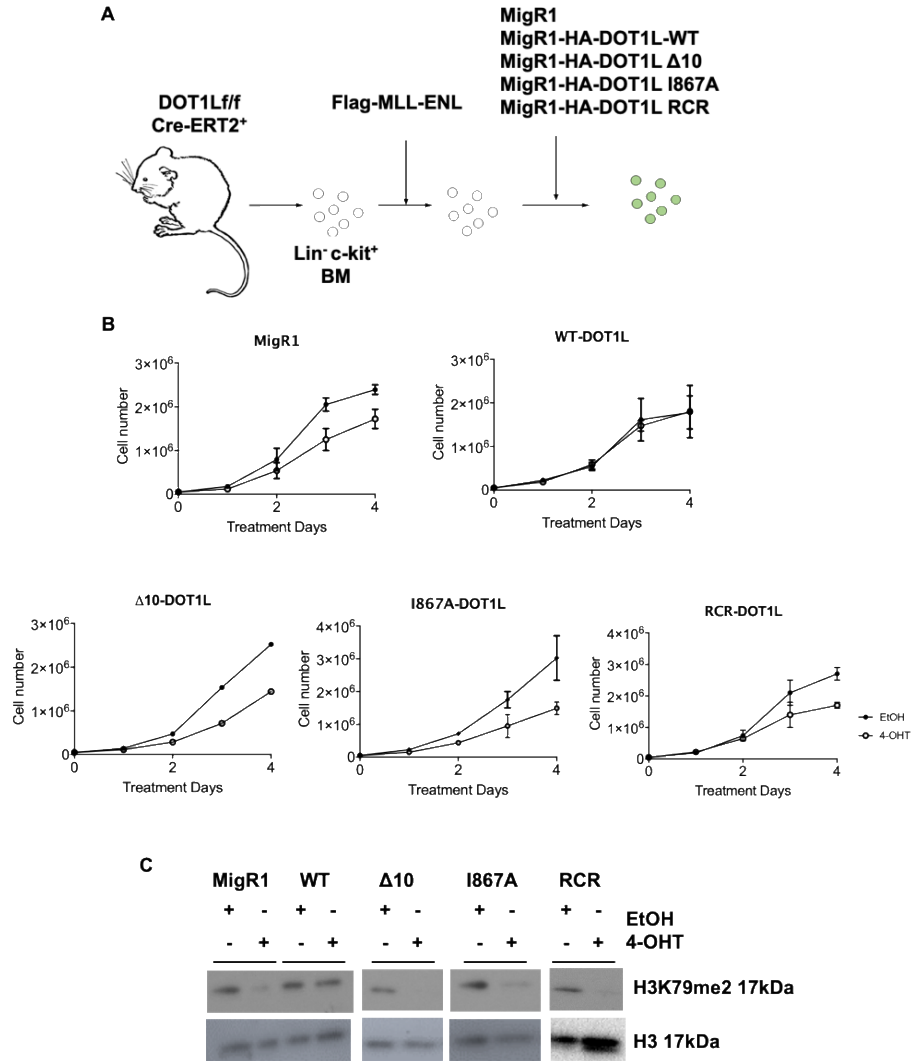
Figure 4-3 MLL-ENL rearaangement leukemic cells are not solely dependent on DOT1L.

(A) Schematic of the process of generating *f/f DOT1L* ENL cell lines with different DOT1L constructs reintroduced. Cells were harvested from the bone marrow of *f/f DOT1L CreERT2* mice. The bone marrow was lineage depleted and transduced with MLL-ENL. MLL-ENL were selected by neomycin treatment then subjected to a secondary transduction with either MigR1 as an empty vector control of one of four DOT1L constructs including, DOT1l-WT, DOT1L-Δ10, DOT1L-I867A (Δ10 and I867A mutants block ENL-DOT1L interaction), and DOT1L-RCR (enzymatically inactive DOT1L protein). These cells were then GFP sorted and used for DOT1L excision studies. (B) Cells were treated at day 0 and day 2 with 7.5nM tamoxifen (4-OHT) and monitored for cell proliferation. Mutating the ENL-DOT1L interaction site (Δ10 and I867A) reduces cellular proliferation at a similar level to complete deletion (MigR1) or enzymatic inhibition (RCR) of DOT1L in MLL-ENL cells. (n≥2) (C) H3K79me2 for Day 3 of the proliferation assay showing overall decrease in H3K79me2 in the PPI and enzymatic DOT1L mutant cell lines.
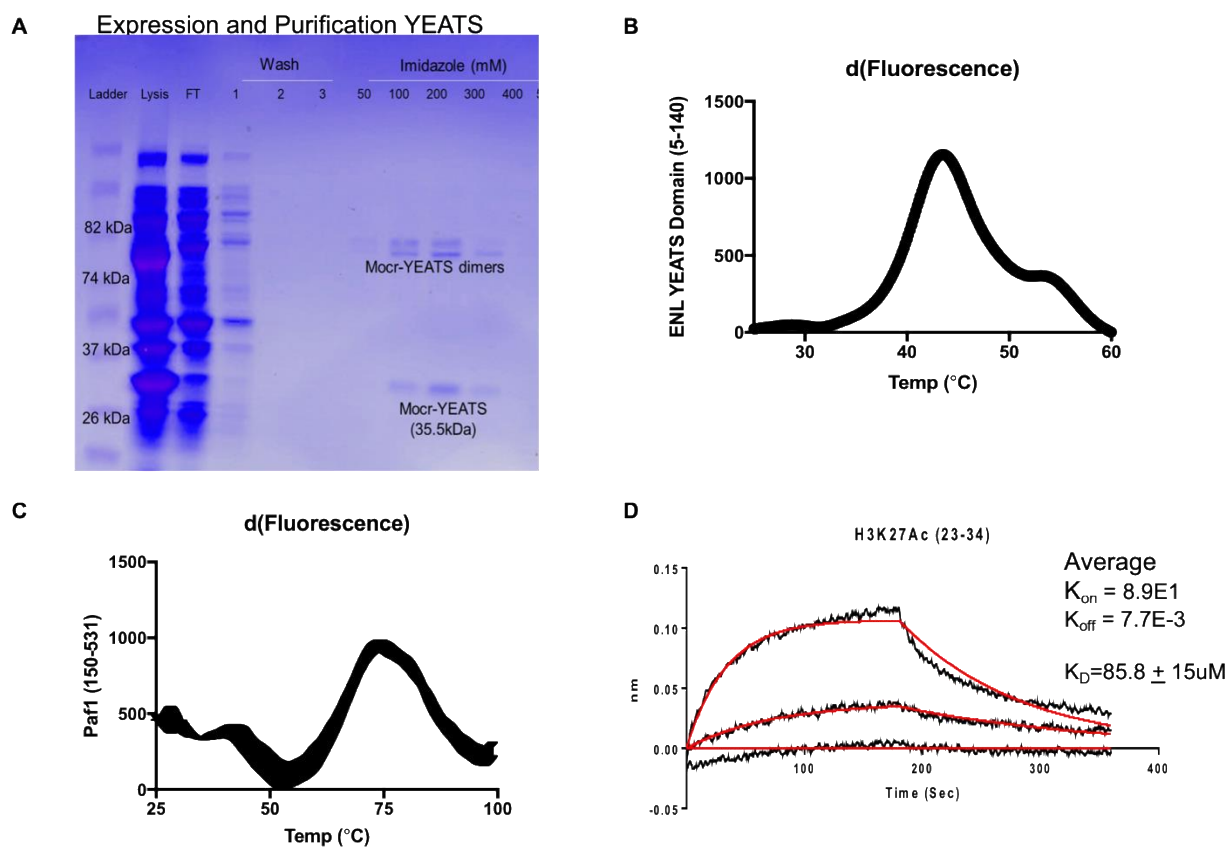
Figure 4-4 Expression, purification, and characterization of recombinant Mocr-ENL YEATS domain.

(A) Coomassie stained SDS page gel of the protein expression and purification steps to obtain pure Mocr-ENL YEATS protein used for biophysical studies. (B) Differential Scanning Fluorimetry (DSF) showing the obtained melting curve for the Mocr-YEATS (5-140) proteins. With an observed T_m between 40 and 50°C. (C) DSF of recombinantly expressed Paf1 (150-531) with an observed T_m between 70 and 80°C. (D) Association and Dissociation curves and constants of a H3K27ac (23-34) peptide binding to the immobilized Mocr-YEATS proteins giving an overall K_D of 86 ± 15 μM.

4.2.2   ENL YEATS domain directly interacts with Paf1

Previous studies showed a relationship between Paf1 and the *N*-terminal YEATS domain of ENL.[20,21] However, there was a lack of quantitative characterization of the binding affinities between these proteins or an in-depth mapping study. Since Paf1 is associated with a generally

gene activating complex PAFc, we wanted to understand this interaction further. For this purpose, ENL YEATS protein was expressed in a Mocr-tagged vector using the purification method published by Li et al. (Figure 4-4A).[8] We confirmed that the recombinant YEATS protein and Paf1 were well folded using differential scanning fluorimetry (DSF), obtaining a melting temperature of about 42°C and 74°C, respectively, in the tested conditions (Figure 4-4B-C). In order to determine the binding affinity with PAF1. ENL YEATS domain was labeled with biotin and immobilized on biolayer interferometry (BLI) sensors. We first, confirmed the binding of ENL YEATS to its natural ligand, H3K27ac, and obtained a K_D of $86 \pm 15\mu M$. Subsequently, different Paf1 constructs were tested for ENL YEATS binding. The smallest construct of Paf1 (aa 170-250) showed similar binding as the full protein with K_D of 15 nM demonstrating the YEATS-Paf1 is a direct and potent interaction (Figure 4-5).

111
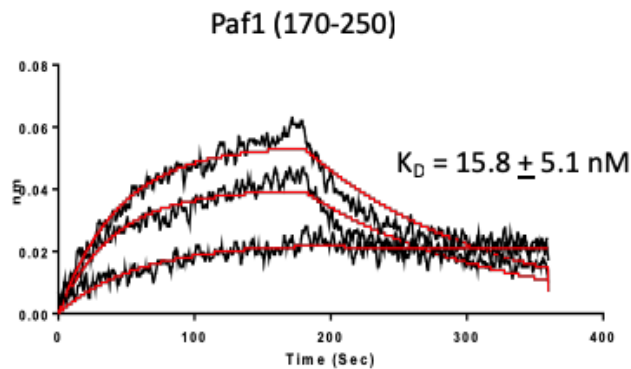
Figure 4-5 Paf1 potently and directly interacts with the ENL YEATS domain.

Representative bind curves for Paf1 170-250 aa binding to the immobilized Mocr-YEATS proteins giving an overall K_D of 16 ± 5 nM. Consistent with the binding affinities of the larger constructs of Paf1 proteins.

4.2.3 Development of a fragment-based screen for the ENL YEATS domain

To further probe the importance of the YEATS domain interactions with Paf1 and acetylated histones in leukemogenesis, we developed a fragment-based screening method to identify compounds that bind to the YEATS domain. We chose to employ this strategy on the YEATS domain for several reasons:(1) Unlike the Paf1-YEATS interaction, the YEATS-H3ac interaction is weak making it difficult to develop an assay with the sensitivity to identify potent inhibitors of acetylated histone binding. (2) Using a fragment-based approach, we can identify fragments that bind various regions of the protein which gives us the flexibility of designing small molecules to target either interaction depending on where the fragments bind to the protein. (3) Moreover, we are confident in our ability to obtain structural information about the fragment binding surfaces due to the wealth of biophysical characterization that is already available (Figure 4-6A).

The expression and purification of the ENL YEATS domain was optimized to improve the protein yield. We cloned the Mocr-YEATS (5-140) into a SUMO vector to increase the yield and simplify the purification so that we would have sufficient proteins for screening and crystallography. With the new SUMO tagged protein, we performed a Ni-NTA purification, SUMO protease cleavage, Heparin column, and anion exchange to increase the yield from 0.2 mg, obtained from the Mocr-YEATS purification method, to 1-2 mg from a 1 L expression (Figure 4-6B). The heparin column was used to separate the SUMO tag and YEATS domain from all other contaminants (Figure 4-6C). Subsequently, the SUMO tag and YEATS solution

was run on an Anion-exchange to separate the tag from the YEATS protein that comes off the column in the flow through fraction (Figure 4-6D). This method allows us to purify the YEATS domain with greater than 95% purity which is needed for screening and crystallography (Figure 4-6E).
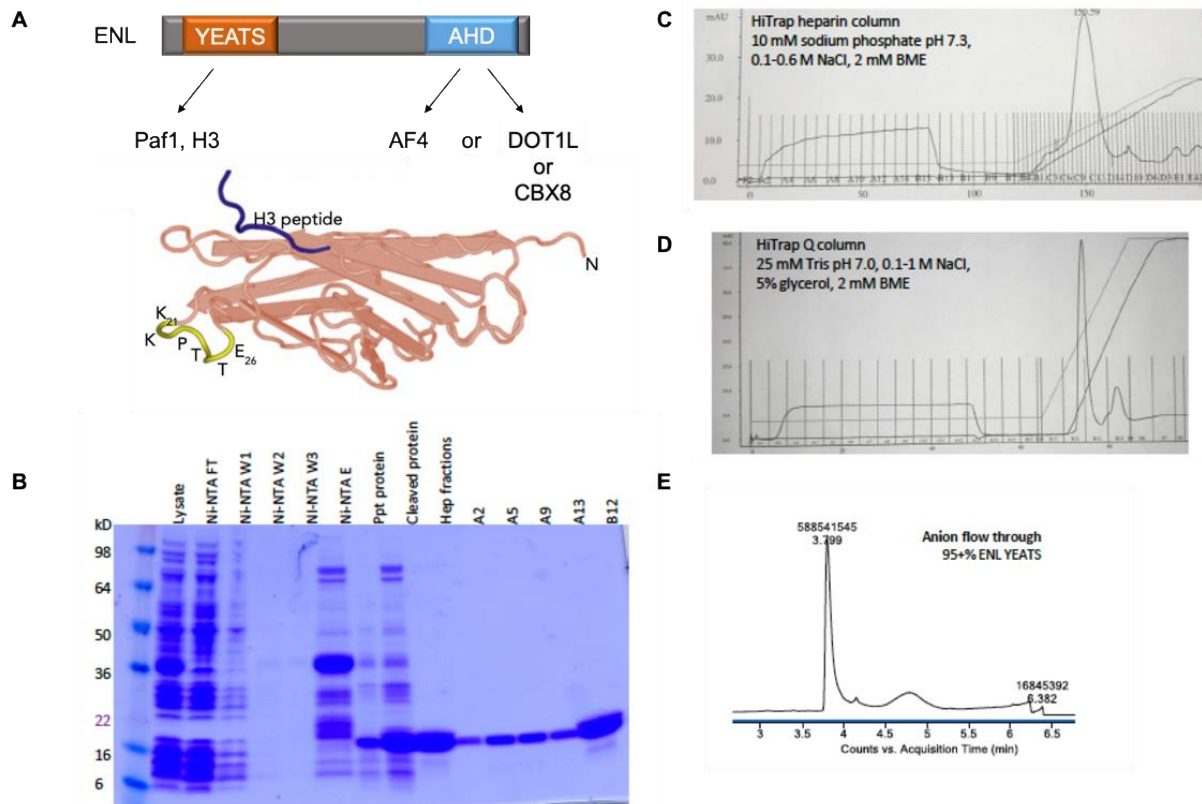
Figure 4-6 Expression and purification of recombinant ENL YEATS domain for fragment based screening assay development.

(A) Protein domain schematic and co-crystal structure (PDB: 4TMP) of ENL and H3 peptide noting the *N*-terminal interactions between the YEATS domain with Paf1 and H3 and the *C*-terminal interaction between the AHD domain with AF4, DOT1L or CBX8.[21] (B) Coomassie stained SDS page gel of the protein expression and purification steps to obtain pure ENL YEATS protein used for the fragment based screening assay. (C) HiTrap heparin column chromatogram showing a single, large peak containing a mixture of ENL YEATS domain and the cleaved SUMO tag. (D) HiTrap Q (anion exchange) column chromatogram of the ENL YEATS domain coming off in the flow through fractions A2-A9. (E) The pooled flow through was collected and run on a mass spectrometer to confirm the protein purity at greater than 95%.

After solidifying our protein preparation procedure, we tested the stability of the YEATS domain in various buffer conditions to identify a buffer that the protein alone would have the most stable T_m and in the presence of our positive control (H3K27 ac peptide) showed a dose-dependent increase in T_m relative to the concentration tested. Out of all of the conditions screened, Tris, HEPES, PIPES, and sodium phosphate buffers at 25 mM with various pH and salt concentrations behaved the best in the assay. The 25 mM sodium phosphate pH 7.5, 250 mM sodium chloride buffer provided the best stabilization of the protein by itself with a T_m of 60°C with more than half a degree increase in T_m around the measured K_D from BLI (Figure 4-7A). We also replotted the data from the DSF experiment to generate a saturation curve plotting the change in T_m (ΔT_m) over the concentration confirming the K_D of the ENL YEATS domain to H3K27ac at ~ 80 μM (Figure 4-7B). With these optimized conditions, the assay is ready for a 384-well format screen of fragment libraries.

A

- 25 mM Tris pH 7.0, 500 mM NaCl
- 25 mM HEPES pH 6.5, 250 mM NaCl, 5 mM MgCl2
- 25 mM PIPES pH 7.4, 250 mM NaCl
- 25 mM PIPES pH 7.4, 500 mM NaCl
- **25 mM sodium phosphate pH 7.5, 250 mM NaCl**

B

25 mM sodium phosphate pH 7.5, 250 mM NaCl		
[H3K27ac]	T_m (°C)	ΔT_m (°C)
0	60.70 ± 0.09	0.00 ± 0.09
10	60.74 ± 0.04	0.03 ± 0.04
30	61.09 ± 0.06	0.38 ± 0.06
100	61.47 ± 0.22	0.77 ± 0.22
200	61.47 ± 0.10	0.77 ± 0.10
400	61.79 ± 0.11	1.08 ± 0.11

$R^2 = 0.963$
$\Delta T_{m, max} = 1.24 ± 0.16$ °C
$Kd = 80 ± 30$ μM
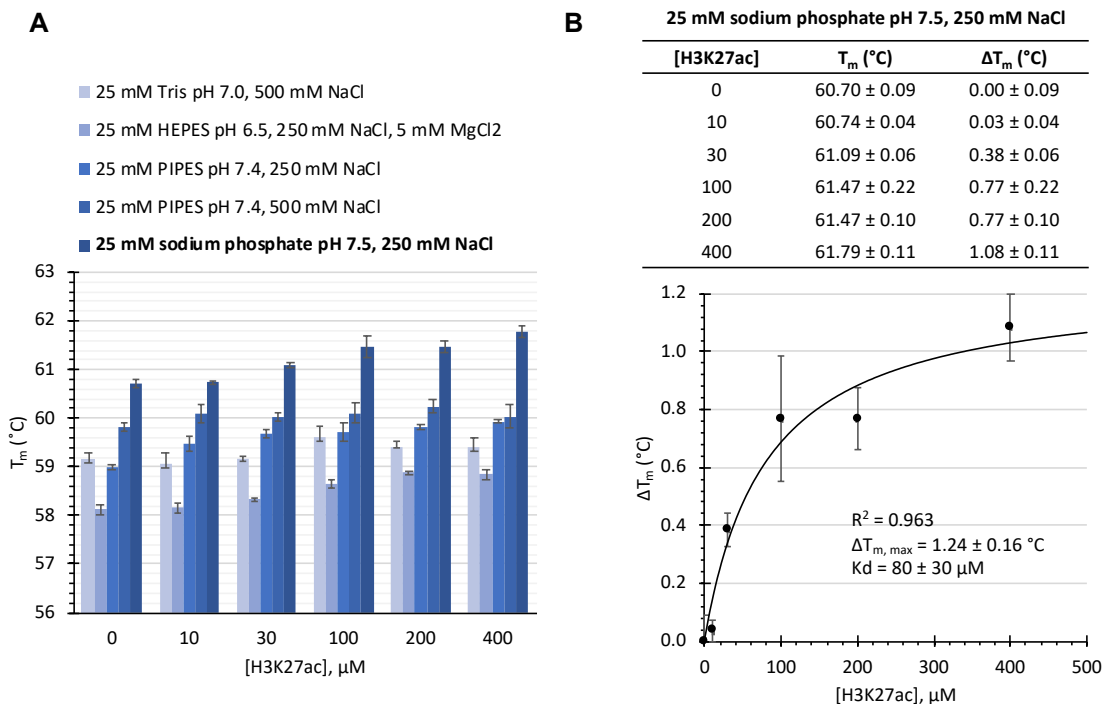
Figure 4-7 Development and validation of a DSF assay for high throughput fragment screening.

(A) Buffer stability screen of various buffer conditions to visualize the stability of the YEATS domain protein noted by a change in melting temperature (T_m). More favorable buffers were 25mM Tris, HEPES, PIPES, or sodium phosphate at pHs ranging from 6.5 to 7.4 in salt concentrations from 250 to 500 mM. The most stabilizing buffer was 25mM sodium phosphate pH 7.4 with 250 mM sodium chloride. This buffer gave a T_m of 60°C and a dose-dependent increase in T_m in the presence of its known interactor, H3K27ac peptide. (B) The change in T_m (ΔT_m) values were transformed into a saturation binging curve plotting ΔT_m over concentration to H3K27ac peptide giving a K_D of 80 ± 30 μM.

4.3   Conclusions

Starting from clinical observation and subsequent reports of the emerging role of the YEATS domain in leukemia we hypothesized that either the Paf1-YEATS or YEATS-H3 interactions are potential mechanisms for the added aggressiveness of MLL-ENL leukemia over MLL-AF9. In this chapter, we focused on developing tools for further elucidating the roles of each interaction in leukemogenesis. For the first time, we confirm the direct, potent interaction between the YEATS domain and Paf1 proteins. Furthermore, we mapped the interaction to residues 170-250 aa of Paf1. In order to have sufficient protein for both assay optimization and hit validation, we optimized the expression and purification methods for the YEATS domain. With this pure protein, we developed a DSF-based assay to screen fragment libraries and identify hits that bind to the YEATS domain. Overall, the studies with the MLL-ENL leukemic cells highlight the need of understanding the impact of the YEATS domain on leukemogenesis, and with the chemical tools that we develop for both interactions, we will be able to elucidate which interaction should be targeted as a future therapeutic.

4.4 Materials and Methods

Mice

C57BL/6.Ptprca (B6-SJL, CD45.1+) were bred in-house or obtained from Charles River (Frederick, MD). C57BL/6 *Dot1lf/f mice* were obtained from Dr. Jay Hess and crossed to Cre-ERT2 mice for in vitro experiments. Dot1l excision was achieved 4-hydroxytamoxifen (4-OHT) in vitro (Sigma-Aldrich; 7.5 nM at experimental day 0 and day 2). All experiments in mice were approved by the University of Michigan's Committee for the Use and Care of Animals.

Cell line generation

Bone marrow from *Dot1lf/f CreER(T2)*[+] mice was harvested 4 days after i.p. injection of 150 mg/kg 5-fluorouracil (Sigma-Aldrich) and lineage-depleted using the EasySep Mouse Hematopoietic progenitor cell isolation kit (Stem Cell Technologies). Retroviruses were produced by transfecting MSCV-neo-Flag-MLL-ENL construct into Plat E cell line with Fugene 6 (Roche Diagnostics). Fresh viral supernatant was used for transduction of the lineage depleted *Dot1lf/f CrER(T2)*^{+} stem cells using two subsequent rounds of spinoculation. For spinoculation, cells were spun at high speed in the presence of viral supernatant for 90 minutes at room temperature. Cells underwent neomycin selection for 6 days and weaned off stem cell factor (SCF) 9 days after starting selection. These selected cells were then transduced 14 days following initial antibiotic selection using the same spinoculation method described above with one of the following vectors: MigR1 (empty vector), MigR1-HA-DOT1L (WT-DOT1L), MigR1-HA-DOT1L deletion aa865-874 (Δ10-DOT1L), MigR1-HA-DOT1L I867A (I867A-DOT1L), and MigR1-HA-DOT1L RCR (RCR-DOT1L). Cells were left to recover for 3 days,

then sorted for GFP positivity using a MoFlo Astrios FACS sorter. Cells were expanded and resorted to get a majority of GFP+ cells expressing the DOT1L constructs.

Cell growth

Cell numbers was assessed using a hemocytometer. Cells were treated with either 7.5nM 4-OHT or equivalent concentration of solvent (100% ethanol) on day 0 and day 2 to achieve excision of Dot1l, followed by daily counting.

Protein Expression and Purification

The ENL YEATS domain was cloned into a pMocr-LIC vector (amino acids 5-140) and a pHisSUMO vector (amino acids 1-148). Paf1 was cloned into a pMocr-LIC vector (amino acids 150-200, 170-250, and 250-300) All recombinant proteins were expressed in Escherichia coli strain Rosetta 2 (Z-compitent cells) (Invitrogen). The proteins were induced with 400 μM and 200 μM isopropyl -D-1-thiogalactopyranoside (IPTG) for ENL YEATS and Paf1; respectively, at 20 ℃ overnight. Cells with Mocr-ENL YEATS and Paf1 were lysed in pMocr lysis buffer (25 mM Tris HCl pH 7.5, 500 mM NaCl, 2 mM BME, 10% Glycerol, 20 mM Imidazole, and 1× protease inhibitor). Cells with pHisSUMO-ENL YEATS were lysed in pSUMO lysis buffer (1x PBS, pH 7.4; Gibco, 350 mM NaCl, 10% glycerol, 10 mM Iminazole, 2 mM BME, 1 mM PMSF, 0.5% CHAPS. 30 μg/mL lysozyme). Lysates were purified by affinity chromatography employing nickel-agarose (Qiagen). SUMO-ENL YEATS was further cleaved overnight with SUMO protease at 4 ℃ in dialysis buffer (1x PBS, pH 7.3, 5% glycerol, 2 mM BME). The cleaved mixture was further purified using a HiTrap Heparin HP column with the following buffers: Binding buffer (10 mM phosphate, pH 7.3 2 mM BME) and Elution buffer (10 mM phosphate, pH 7.3, 1 M sodium chloride, 2 mM BME). His-SUMO ENL YEATS eluted in the 200-400 mM NaCl range. The protein underwent a buffer exchange to the Anion exchange

binding buffer (25 mM Tris-HCl, 100 mM NaCl, 5% glycerol, 2 mM BME, pH 7). The protein was further purified by a HiTrap Q HP column. The cleaved SUMO-ENL YEATS comes off of the column in the flow through and the SUMO tag is eluted off the column in elution buffer (25 mM Tris-HCl, 1 M NaCl, 5% glycerol, 2 mM BME, pH 7) around 300 mM NaCl. The final pure protein was then analyzed by mass spectroscopy on the Q-TOF (Agilent).

Paf1 proteins (amino acids 150-531, 150-450, 150-400, and 150-300) were provided by the Muntean lab.

BLI

Recombinant ENL YEATS domain (Mocr-ENL YEATS aa 5-140; MW = 36kDa) protein was biotinylated using the Thermo EZ-link Sulpho-NHS-LC-biotin biotinylation kit (cat. 21435) protein and biotin were mixed in a 1:1 molar ratio in PBS on ice for 2 hours. Reaction mixture was dialyzed in PBS buffer to remove excess biotin.

BLI experiments were performed using an OctetRED96 instrument from PALL/ForteBio. ENL YEATS-Ac-peptide assays were run at 30 °C using Tris buffer (25 mM Tris pH 7.4, 500 mM NaCl, 2 mM BME) with continuous 1000rpm shaking. Biotinylated ENL YEATS was immobilized on Super Streptavidin (SSA) biosensors (ForteBio) by dipping sensors in 20 µg/mL protein solutions. Biotin labeled Streptavidin protein blocked SSA sensors were prepared were prepared as inactive reference controls. H3K27Ac peptide (aa 23-34; MW = 1156.3; Anaspec) allowed to associate and dissociate for 2 minutes.

ENL YEATS-Paf1 assays were run at 30 °C using HBS-P buffer (10 mM HEPES pH 7.4, 150 mM NaCl, 0.005% tween-20) with continuous 1000rpm shaking. Biotinylated Mocr-ENL YEATS was immobilized on Super Streptavidin (SSA) biosensors (ForteBio) by dipping sensors in 20 µg/mL protein solutions. Biotin labeled Streptavidin protein blocked SSA sensors were

prepared were prepared as inactive reference controls. Recombinant Paf1 proteins were allowed to associate and dissociate for 1 minute 30 seconds.

Raw kinetic data collected were processed in the Data Analysis software provide by ForteBio using double referencing in which both buffer only sensors and inactive protein sensors were subtracted. Resulting data were analyzed based on the 1:1 binding model from which k_{on} and k_{off} values were obtained and then K_D values were calculated.

DSF

DSF was performed in a 10uL reaction mixture using 10 μM of recombinant ENL YEATS domain (ENL YEATS aa 5-140; MW = 18kDa) protein in Tris buffer (25 mM sodium phosphate pH 7.5, 250 mM NaCl), various concentrations of H3K27Ac peptide (aa 23-34; MW = 1156.3; Anaspec) at 5% DMSO, and 2x SYPRO orange dye (ThermoFisher Scientific). Raw data was analyzed using Protein Thermal Shift software (Applied Biosystems) to determine Tm of the protein in DMSO and Protein with peptide.

4.5   Contributions

Sierrah Marie Grigsby developed of the MLL-ENL transduced cell lines performed cell culture experiments, biophysical characterization of the proteins and determined the binding affinity of PPIs; Sierrah Marie Grigsby and Lara Zetzsche contributed to cloning, expressing and purifying recombinant ENL YEATS and Paf1 proteins and optimizing the DSF screening assay.

4.6   References

1.   Schoch C, Schnittger S, Klaus M, Kern W, Hiddemann W, Haferlach T. AML with 11q23/MLL abnormalities as defined by the WHO classification: incidence, partner chromosomes, FAB subtype, age distribution, and prognostic impact in an unselected series of 1897 cytogenetically analyzed AML cases. *Blood*. 2003;102(7):2395-2402.
2.   Muñoz L, Nomdedéu JF, Villamor N, et al. Acute myeloid leukemia with MLL rearrangements: clinicobiological features, prognostic impact and value of flow cytometry in the detection of residual leukemic cells. *Leukemia*. 2003;17(1):76-82.

3.	Chen L, Sun Y, Wang J, Jiang H, Muntean AG. Differential regulation of the c-Myc/Lin28 axis discriminates subclasses of rearranged MLL leukemia. *Oncotarget*. 2016;7(18):25208-25223.

4.	Mohan M, Lin C, Guest E, Shilatifard A. Licensed to elongate: a molecular mechanism for MLL-based leukaemogenesis. *Nature Reviews Cancer*. 2010;10(10):721-728.

5.	Balgobind BV, Raimondi SC, Harbott J, et al. Novel prognostic subgroups in childhood 11q23/MLL-rearranged acute myeloid leukemia: results of an international retrospective study. *Blood*. 2009;114(12):2489-2496.

6.	Fu JF, Liang DC, Shih LY. Analysis of acute leukemias with MLL/ENL fusion transcripts: identification of two novel breakpoints in ENL. *Am J Clin Pathol*. 2007;127(1):24-30.

7.	Alonso CN, Longo PLR, Gallego MS, Medina A, Felice MS. A novel AF9 breakpoint in MLL-AF9-positive acute monoblastic leukemia. *Pediatric Blood & Cancer*. 2008;50(4):869-871.

8.	Li Y, Wen H, Xi Y, et al. AF9 YEATS domain links histone acetylation to DOT1L-mediated H3K79 methylation. *Cell*. 2014;159(3):558-571.

9.	Li Y, Sabari BR, Panchenko T, et al. Molecular Coupling of Histone Crotonylation and Active Transcription by AF9 YEATS Domain. *Mol Cell*. 2016;62(2):181-193.

10.	Wan L, Wen H, Li Y, et al. ENL links histone acetylation to oncogenic gene expression in acute myeloid leukaemia. *Nature*. 2017;543(7644):265-269.

11.	He N, Chan CK, Sobhian B, et al. Human Polymerase-Associated Factor complex (PAFc) connects the Super Elongation Complex (SEC) to RNA polymerase II on chromatin. *Proceedings of the National Academy of Sciences of the United States of America*. 2011;108(36):E636-645.

12.	Erb MA, Scott TG, Li BE, et al. Transcription control by the ENL YEATS domain in acute leukaemia. *Nature*. 2017;543(7644):270-274.

13.	Jaehning JA. The Paf1 complex: platform or player in RNA polymerase II transcription? *Biochim Biophys Acta*. 2010;1799(5-6):379-388.

14.	Tomson BN, Arndt KM. The many roles of the conserved eukaryotic Paf1 complex in regulating transcription, histone modifications, and disease states. *Biochim Biophys Acta*. 2013;1829(1):116-126.

15.	Nordick K, Hoffman MG, Betz JL, Jaehning JA. Direct interactions between the Paf1 complex and a cleavage and polyadenylation factor are revealed by dissociation of Paf1 from RNA polymerase II. *Eukaryot Cell*. 2008;7(7):1158-1167.

16.	Kim J, Guermah M, Roeder RG. The human PAF1 complex acts in chromatin transcription elongation both independently and cooperatively with SII/TFIIS. *Cell*. 2010;140(4):491-503.

17.	Kim J, Guermah M, McGinty RK, et al. RAD6-Mediated transcription-coupled H2B ubiquitylation directly stimulates H3K4 methylation in human cells. *Cell*. 2009;137(3):459-471.

18.	Moniaux N, Nemos C, Schmied BM, et al. The human homologue of the RNA polymerase II-associated factor 1 (hPaf1), localized on the 19q13 amplicon, is associated with tumorigenesis. *Oncogene*. 2006;25(23):3247-3257.

19.	Chaudhary K, Deb S, Moniaux N, Ponnusamy MP, Batra SK. Human RNA polymerase II-associated factor complex: dysregulation in cancer. *Oncogene*. 2007;26(54):7499-7507.

20. He N, Chan CK, Sobhian B, et al. Human Polymerase-Associated Factor complex (PAFc) connects the Super Elongation Complex (SEC) to RNA polymerase II on chromatin. *Proc Natl Acad Sci U S A*. 2011;108(36):E636-645.

21. Hetzner K, Garcia-Cuellar MP, Buttner C, Slany RK. The interaction of ENL with PAF1 mitigates polycomb silencing and facilitates murine leukemogenesis. *Blood*. 2018;131(6):662-673.

22. Muntean AG, Tan J, Sitwala K, et al. The PAF Complex Synergizes with MLL Fusion Proteins at HOX Loci to Promote Leukemogenesis. *Cancer Cell*. 2010;17(6):609-621.

23. Barretto NN, Karahalios DS, You D, Hemenway CS. An AF9/ENL-targted peptide with therapeutic potential in mixed lineage leukemias. *J Exp Ther Oncol*. 2014;10(4):293-300.

CHAPTER 5

Summary and Future Directions

5.1   Summary

Epigenetic regulators and protein-protein interactions (PPIs) are emerging as attractive therapeutic targets for a variety of cancers.[1,2] This in part is due to the ineffectiveness and harshness of conventional cytotoxic chemotherapy agents that have been the staple of frontline therapy. To date, there is only 1 FDA approved drug that targets protein-protein interactions; Venetoclax. Venetoclax, a Bcl-2 selective inhibitor, was developed to trigger apoptosis in cancer cells that overexpress Bcl-2 for their survival to evade apoptosis.[3] At this time, there are several PPI inhibitors in clinical trials for various indications with different targets and mechanism of action.[4-7]   In the context of MLL-rearrangement leukemia, DOT1L, the only H3K79 methyltransferase, was identified and validated as a therapeutic target for several MLL driven leukemias including the most common MLL-AF9 and MLL-ENL.[8-10] These fusion proteins recruit DOT1L to MLL target genes leading to their aberrant activation and leukemic transformation.[11,12] With the initial proof-of-concept studies initiated with EPZ004777 and further developed clinical candidate EPZ5676, DOT1L was validated as a therapeutic target for *MLL1* translocated leukemia.[13-15] However, based on pre-clinical studies showing long-term toxicity in non-leukemic blood cell development[16,17] and the known importance in other tissues like cardiomyocytes[18,19], global enzymatic inhibition may be deleterious to patients. In this dissertation, we aimed to identify and validate novel therapeutic approaches to inhibit DOT1L

specifically in the context of MLL-fusion transformed cells while allowing the enzyme to function normally in its other cellular contexts.

5.1.1 AF9 binding domain is critical for leukemogenesis and dispensable in non-leukemic cell growth

Due to the importance of DOT1L in MLL-rearrangement leukemia and the emerging evidence of the importance of DOT1L activity in non-leukemic cell proliferation[16,17], in chapter 2, we designed a genetic study to validate the therapeutic advantage in targeting the PPI in comparison to enzymatic inactivation. We confirmed that indeed DOT1L recruitment to MLL-target genes by MLL-AF9 is critical for leukemic transformation. More strikingly, a single amino acid mutation in the AF9-binding domain is sufficient to inhibit cell proliferation, downregulate H3H79me2 at MLL-target gene, downregulate *HoxA9/Meis1* expression, induce cell death and cell differentiation similarly as enzymatically inhibiting DOT1L.

We next characterized the early events of DOT1L enzymatic inactivation in non-leukemic blood cells as a complement to previous studies that have shown hematopoietic stem cell depletion at later time points more than 4 weeks post inactivation.[16,17] The study identified that initially, hematopoietic stem cells are not severely affected at 1-week post DOT1L inactivation; however, some progenitor cell populations impacted shown by a decrease in number and loss of self-renewal capabilities in the case for GMPs. Furthermore, as early as 10 days after DOT1L inactivation, total bone marrow cellularity decreases with a significant depletion of long-term hematopoietic stem cells, indicating that the previously reported events at 16 weeks,[16] occur more rapidly after DOT1L is excised.

Finally, we tested the effects of blocking DOT1L recruitment on hematopoiesis *in vivo* in comparison to enzymatic inactivation. We demonstrated that both PPI mutant cell lines were able

123

to reconstitute the bone marrow similarly to cells expressing wild type DOT1L indicating that the AF9-binding domain is not critical for hematopoiesis. We also noted that the mice that did survive in the empty vector and enzymatically inactivated groups did not have full excision of their endogenous DOT1L and were reconstituted with a rare population of escapee cells. These results together make a case for targeting the AF9-DOT1L interaction as a potential therapeutic approach in MLL-AF9 driven leukemia with potentially fewer side effects.

5.1.2 The development of DOT1L peptidomimetics

In Chapter 3, we used the knowledge gained from our previous DOT1L interaction mapping studies[10] to design inhibitors of the AF9/ENL and DOT1L interaction and reported NMR studies[11,20] A class of peptidomimetics was designed based on the 7 mer peptide (peptide **2**), derived from DOT1L. The middle three residue side chains were modified from peptide **2** to develop compound **21** with K_i values of 20 and 90 nM to AF9 and ENL; respectively, showing a 8-fold improvement in binding affinity. The direct binding of **21** was confirmed by its biotinylated counterpart **22** using BioLayer Interferometry (BLI) against both AF9 and ENL proteins. **22** recognizes and binds to the cellular AF9 protein in a dose-dependent manner. Peptide **21** was further modified on the *C*- and *N*- terminus resulting in the identification of peptidomimetic **28** which shows 2-fold improvement in potency binding affinity to AF9 with a significant reduction in its peptidic characteristics.

In order to improve the stability and cell permeability of the peptidomimetics, the *C*- and *N*- terminus were further modified. Peptidomimetic **29** showed promising selectivity profile in murine-derived leukemia cell lines. These peptidomimetics bind potently to the AF9 AHD domain with a K_i of 10 nM and displace full-length DOT1L. **29** specifically inhibits leukemogenesis in MLL-AF9 cells in comparison to the DOT1L independent fusion E2A-HLF,

decreasing *HoxA9/Meis1* expression and inducing cell differentiation. These initial peptidomimetics are the beginning of several cellularly active analogs that we hope to further develop as chemical tools and eventually novel therapeutics for MLL-AF9/ENL driven leukemia in combination with other chemotherapy agents.

5.1.3   ENL YEATS domain and MLL leukemia

AF9 and ENL are homologous proteins with an *N*-terminal YEATS domain and *C*-terminal AHD domain. Both MLL-fusion products retain the AHD domain; however, the YEATS domain is lost in MLL-AF9 fusion proteins. Clinical and model system studies have shown that MLL-ENL is more aggressive and predominantly contains both YEATS and AHD.[21-25] In Chapter 4, we aimed to start studies to identify the dependency of MLL-ENL leukemia on DOT1L recruitment and validate potential interactors with the YEATS domain to determine their contribution on leukemia as well. To do this, we utilized the same *Dot1l f/f Cre+* mouse cells and transformed with MLL-ENL that contained both YEATS and AHD and DOT1L constructs. These studied showed a modest decrease in cell proliferation, but the cells were not as dependent on DOT1L as the MLL-AF9 cells that lack DOT1L's interaction or function. This indicates that DOT1L contributes to leukemogenesis in these cells, but another mechanism in addition to DOT1L recruitment is important.

Canonically, the YEATS domain is an acetylation reader as well as other modification like crotonylation.[26-29] However, a previous study highlighted the association of Paf1 of the polymerase associated factor complex (PAFc) as a novel interactor with ENL YEATS domain.[30,31] Since YEATS-acetyl lysine has been well characterized; we focused on mapping the binding site on Paf1 that interacts with ENL YEATS using direct binding assay BLI to confirm if the interaction was direct or through a complex. We determined an 80-residue sequence between

170 aa to 250 aa was sufficient to sustain low nanomolar binding between the YEATS domain and Paf1.

Studies have reported the importance of YEATS chromatin binding for transcription initiation, and elongation of RNA polymerase II.[27] This transcriptional regulation was reported to be through the YEATS domain's ability to bind Paf1 and target PAFc and SEC to chromatin as well as directly recruit DOT1L to chromatin in the absence of other scaffolding machinery.[32] Furthermore, the YEATS domain has been identified as a transcriptional controller in acute leukemia.[27] These studies are implicating the YEATS domain as a potential therapeutic target; however, the exact mechanism or interaction that is controlling leukemogenesis in not know. To understand which YEATS domain interactions are critical for leukemia, we developed a differential scanning fluorimetry (DSF)-based screening method to identify molecules that can be used to probe these interactions in normal and disease states.

5.2 Impact and significance of the dissertation studies

The research presented in the dissertation reports the biological characterization of important protein-protein interactions between MLL-AF9/MLL-ENL and DOT1L in MLL-fusion leukemia as well as the characterization of novel PPIs. We also show the development of peptidomimetics for the AF9/ENL and DOT1L interaction and the development of an assay to identify fragments that bind to the ENL YEATS domain towards the development of chemical tools. The most important scientific contributions are:

- The use of a genetic approach *in vitro* in leukemic cells to clarify the importance of the AF9-binding domain from 865 aa to 874 aa on DOT1L for leukemogenesis. Demonstrating that a single point mutation in the AF9 binding site is sufficient to inhibit leukemic cell proliferation. Clarifying the early onset of hematopoietic defects that occur with global H3K79 known down in the bone marrow and the ability for targeting the AF9-DOT1L interaction to sustain hematopoiesis.

- Applying structural and mutagenesis data to aid in the establishment of Structure-Activity Relationship (SAR) studies to design and develop potent, cell active, and selective peptidomimetics to be used as chemical tools to probe AF9/ENL and DOT1L interactions in various cellular contexts further.
- Illustrating the role of the YEATS domain even in the absence of DOT1L activity or recruitment as an important target for therapeutic intervention in combination with DOT1L PPI inhibition. Establishing a DSF fragment-based screening assay to identify fragments that can bind at various locations on the YEATS domain protein as a way to a build molecule that could inhibit either the acetylated histone interface or the Paf1 binding surface.

5.3 Future directions

5.3.1 Characterization of the redistribution of protein-protein interactions when the AF9 DOT1L interaction is blocked.

As mentioned previously, there are multiple ways to target critical proteins involved in diseases. In this study, we validated the importance of the AF9-binding domain of DOT1L that is critical for leukemogenesis and dispensable in hematopoiesis. To follow up on these findings, studies should be done to look at the redistribution of proteins when the interaction site on DOT1L is blocked. These studies would ascertain the extent of the normal DOT1L interactome in homeostatic conditions and elucidate the changes to the DOT1L interactome associated with disrupting the AF9-DOT1L PPI. A label-free spectral counting approach could be used to detect the differential binding to the following baits: Flag-WT DOT1L, Flag-Δ10aa DOT1L and Flag-I867A DOT1L. Based on known DOT1L interactions, we expect to see AF9, ENL, AF10, β-catenin, among several other PPIs present in the samples from the Flag-DOT1L cells. In the Flag-Δ10aa DOT1L and I867A DOT1L cells should yield similar PPI disruptions including AF9 and ENL; however, the degree of disruption and other changes to the DOT1L are to be determined from these studies. We expect to see more changes to the interactome when deleting

127

10aa in comparison to a single mutation that is specific to the AF9/ENL-DOT1L interaction. Another approach would be to mutate the AHD domain of AF9 and follow the redistribution of known AF9 binding partners CXB8 and BCoR, that are apart of known gene repressive complexes,[33,34] as well as AF4 and DOT1L containing complexes[11,35] to look at the global changes on their localization to gene targets. This will give us insights into how targeting the AHD domain effects known AF9 interaction partners, the interactome, and transcription.

In addition to looking at the redistribution of AF9 or DOT1L in the interactome, it will be important to look at the global changes in gene expression when DOT1L is no longer bound to AF9. A previous study looked at a select few gene loci where H3K79me2/3 were altered after disrupting the interaction between AF9 and DOT1L[11]; however, more in-depth studies are needed to fully determine the potential consequences of targeting this PPI on the transcriptome. This could offer insights on what other pathways might be affected. These studies will help the field further understand the biological roles of these interactions and proactively look for long term implications of inhibiting this interaction and how it affects the interactome and transcriptome.

5.3.3 Characterization of on target activity and selectivity of cellularly active peptidomimetics

The aforementioned, studies aimed to develop peptidomimetics to uses as a framework for the development of molecules with the purpose of inhibiting DOT1L recruitment to MLL-target genes by MLL-fusion proteins. With promising *in vitro* data showing, in a model system, that the peptidomimetics can inhibit full-length DOT1L recruitment and selectively kill MLL-AF9 cells, the next steps will be to further validate their activity in established human cancer cell lines. Due to the genetic diversity of human cancers, it is important to see if the activity will be

maintained in a more complex system. Established human cell lines, like MOLM-13 (MLL-AF9), KOPN-1 (MLL-ENL), and K562 (BCR-ABL1; negative control) will be used to determine the efficacy in human cell lines. The expectation is for the peptidomimetic to show efficacy in the MOLM-13 cell lines, potentially some efficacy, but maybe less in KOPN-1 depending on the isoform of the MLL-ENL fusion that it harbors, and no effect on K562. After developing a peptidomimetic that selectively targets in human-derived cell lines with MLL-AF9 or MLL-ENL translocations, expanding the studies to patient samples would be another way of demonstrating efficacy in human leukemia.

We would also like to determine the pharmacokinetic (PK) and pharmacodynamic (PD) profiles of our most stable peptidomimetics. These studies will be instrumental in determining the dosing schedule and if we can achieve a suitable therapeutic range in the blood to have an effect. After checking these parameters, the next step would be to initiate *in vivo* studies to see if we can effectively treat systemic disease and monitor hematopoiesis. If the minimum dose necessary is tolerable by the animals, we would expect to clear of the leukemic cells and sustained non-leukemic hematopoiesis. In the event the peptidomimetics do not pass PK and PD screening, then more medicinal chemistry efforts will be needed to optimize the pharmacochemical properties of the molecules. The further development and rigorous validation of these molecules will be a significant step towards the development of potent chemical tools to understand the biology behind these interactions and the development of a specific, tolerable therapeutics for MLL-AF9 and MLL-ENL leukemia.

5.3.4 Determine the function consequences of disrupting ENL YEATS domain interactions on leukemogenesis

When evaluating the dependence of MLL-ENL leukemia on DOT1L recruitment, we demonstrated there is not a sole functional dependence on DOT1L's enzymatic activity. We hypothesize that this could be due to the retention of the YEATS domain in MLL-ENL fusion proteins that are lost in MLL-AF9 fusions. There are a few ways that this can be confirmed. The first is to utilize the same system with the *Dot1l f/f Cre+* mice, transform them with MLL-ENL that lacks the YEATS domain and determine if we can see an ablation of leukemogenic *in vitro* when DOT1L is excised. If the cell proliferation decreases to the same degree as we see with the MLL-AF9 fusion protein, then we can conclude that both the YEATS domain and ENL AHD interactions are critical for leukemic cell growth.

Alternatively, based on our studies (Chapter 4) and other published work, we know that the YEATS domain can make two key interactions that might be influential in leukemogenesis, either the acyl-lysine interaction or the novel interaction with the PAFc through Paf1.[30,31,36] To determine which interaction is contributing to the increase in disease severity in MLL-ENL leukemia, genetic studies inhibiting either acetylation binding[36] or Paf1 interaction (Chapter 4 and Hetzner et al.) will be implemented. These studies can be carried out *in vitro* as described previously and *in vivo* to elucidate the importance of these interactions and their ability to either sustain or inhibit leukemogenesis.

In addition to genetically disrupting these interactions at both ENL YEATS and/or AHD domains, developing chemical tools targeting either the acetylated histones or Paf1 binding to compliment the DOT1L peptidomimetics (Chapter 3) would allow for additional validation of these two targets. Utilizing the DSF screening assay described in Chapter 4, we plan to screen

fragment libraries in order to identify fragments that bind to the ENL YEATS domain. These small fragments will bind non-discriminately to the protein, and with validation and crystallography efforts, the various binding modes can be solved. Depending on the binding sites of the fragments they can be linked through medicinal chemistry efforts to make full molecules that can be validated for either the Paf1 interaction or acetylated histones interaction. These studies will be instrumental in identifying useful combinations of therapies for MLL-ENL leukemia.

5.4   References

1.   Gelato KA, Shaikhibrahim Z, Ocker M, Haendler B. Targeting epigenetic regulators for cancer therapy: modulation of bromodomain proteins, methyltransferases, demethylases, and microRNAs. *Expert Opin Ther Targets*. 2016;20(7):783-799.
2.   Fry DC. Targeting protein-protein interactions for drug discovery. *Methods Mol Biol*. 2015;1278:93-106.
3.   Anderson MA, Deng J, Seymour JF, et al. The BCL2 selective inhibitor venetoclax induces rapid onset apoptosis of CLL cells in patients via a TP53-independent mechanism. *Blood*. 2016;127(25):3215-3224.
4.   Yu S, Qin D, Shangary S, et al. Potent and orally active small-molecule inhibitors of the MDM2-p53 interaction. *J Med Chem*. 2009;52(24):7970-7973.
5.   Zhao Y, Aguilar A, Bernard D, Wang S. Small-molecule inhibitors of the MDM2-p53 protein-protein interaction (MDM2 Inhibitors) in clinical trials for cancer treatment. *J Med Chem*. 2015;58(3):1038-1052.
6.   Carter BZ, Mak DH, Morris SJ, et al. XIAP antisense oligonucleotide (AEG35156) achieves target knockdown and induces apoptosis preferentially in CD34+38- cells in a phase 1/2 study of patients with relapsed/refractory AML. *Apoptosis*. 2011;16(1):67-74.
7.   Hurwitz H, Pitot H, Strickler J, et al. 76 Preliminary Report of a First-in-human, Open-label, Multicenter, Phase I Study of AT-406 (Debio 1143), an Oral Small Molecule Multi-IAP Inhibitor, in Solid Tumors and Lymphomas. *European Journal of Cancer*. 2012;48:25.
8.   Bernt KM, Zhu N, Sinha AU, et al. MLL-rearranged leukemia is dependent on aberrant H3K79 methylation by DOT1L. *Cancer Cell*. 2011;20(1):66-78.
9.   Nguyen AT, Taranova O, He J, Zhang Y. DOT1L, the H3K79 methyltransferase, is required for MLL-AF9–mediated leukemogenesis. *Blood*. 2011;117(25):6912-6922.
10.   Shen C, Jo SY, Liao C, Hess JL, Nikolovska-Coleska Z. Targeting recruitment of disruptor of telomeric silencing 1-like (DOT1L): characterizing the interactions between DOT1L and mixed lineage leukemia (MLL) fusion proteins. *The Journal of Biological Chemistry*. 2013;288(42):30585-30596.
11.   Kuntimaddi A, Achille NJ, Thorpe J, et al. Degree of recruitment of DOT1L to MLL-AF9 defines level of H3K79 Di- and tri-methylation on target genes and transformation potential. *Cell Rep*. 2015;11(5):808-820.

12.   Okuda H, Stanojevic B, Kanai A, et al. Cooperative gene activation by AF4 and DOT1L drives MLL-rearranged leukemia. *J Clin Invest*. 2017;127(5):1918-1931.

13.   Stein EMG-M, G.;Rizzieri, D.A.;Tibes, R.; Berdeja, J. G.; Jongen-Lavrencic, M.; Altman, J. K.; Dohner, H.; Thomson, B.; Blakemore, S. J.; Daigle, S.; Fine, G.; Waters, N. J.; Krivstov,A. V.; Koche, R.; Armstrong, S. A.; Ho, P. T.; Lowenberg B.; and Tallman, M. S. A Phase 1 Study of the DOT1L Inhibitor, Pinometostat (EPZ-5676), in Adults with Relapsed or Refractory Leukemia: Safety, Clinical Activity, Exposure and Target Inhibition. *Blood*. 2015;126(23):2547.

14.   Shukla NW, C.; O'Brien, M.M.; Silverman, L.B.; Brown, P.; Cooper, T.M.; Thomson, B.; Blakemore, S.J.; Daigle, S.; Suttle, B.; Waters, N.J.; Krivstov, A.K.; Armstrong, S.A.;Ho, P.T.; Gore, L. Final Report of Phase 1 Study of the DOT1L Inhibitor, Pinometostat (EPZ-5676), in Children with Relapsed or Refractory MLL-r Acute Leukemia. *Blood*. 2016;128(22):2780.

15.   Daigle SR, Olhava EJ, Therkelsen CA, et al. Selective Killing of Mixed Lineage Leukemia Cells by a Potent Small-Molecule DOT1L Inhibitor. *Cancer Cell*. 2011;20(1):53-65.

16.   Jo SY, Granowicz EM, Maillard I, Thomas D, Hess JL. Requirement for Dot1l in murine postnatal hematopoiesis and leukemogenesis by MLL translocation. *Blood*. 2011;117(18):4759-4768.

17.   Nguyen AT, He J, Taranova O, Zhang Y. Essential role of DOT1L in maintaining normal adult hematopoiesis. *Cell Res*. 2011;21(9):1370-1373.

18.   Nguyen AT, Xiao B, Neppl RL, et al. DOT1L regulates dystrophin expression and is critical for cardiac function. *Genes Dev*. 2011;25(3):263-274.

19.   Cattaneo P, Kunderfranco P, Greco C, et al. DOT1L-mediated H3K79me2 modification critically regulates gene expression during cardiomyocyte differentiation. *Cell Death Differ*. 2016;23(4):555-564.

20.   Leach BI, Kuntimaddi A, Schmidt CR, Cierpicki T, Johnson SA, Bushweller JH. Leukemia fusion target AF9 is an intrinsically disordered transcriptional regulator that recruits multiple partners via coupled folding and binding. *Structure*. 2013;21(1):176-183.

21.   Alonso CN, Longo PLR, Gallego MS, Medina A, Felice MS. A novel AF9 breakpoint in MLL-AF9-positive acute monoblastic leukemia. *Pediatric Blood & Cancer*. 2008;50(4):869-871.

22.   Fu JF, Liang DC, Shih LY. Analysis of acute leukemias with MLL/ENL fusion transcripts: identification of two novel breakpoints in ENL. *Am J Clin Pathol*. 2007;127(1):24-30.

23.   Schoch C, Schnittger S, Klaus M, Kern W, Hiddemann W, Haferlach T. AML with 11q23/MLL abnormalities as defined by the WHO classification: incidence, partner chromosomes, FAB subtype, age distribution, and prognostic impact in an unselected series of 1897 cytogenetically analyzed AML cases. *Blood*. 2003;102(7):2395-2402.

24.   Balgobind BV, Raimondi SC, Harbott J, et al. Novel prognostic subgroups in childhood 11q23/MLL-rearranged acute myeloid leukemia: results of an international retrospective study. *Blood*. 2009;114(12):2489-2496.

25.   Chen L, Sun Y, Wang J, Jiang H, Muntean AG. Differential regulation of the c-Myc/Lin28 axis discriminates subclasses of rearranged MLL leukemia. *Oncotarget*. 2016;7(18):25208-25223.

26.   Li Y, Wen H, Xi Y, et al. AF9 YEATS domain links histone acetylation to DOT1L-mediated H3K79 methylation. *Cell*. 2014;159(3):558-571.

27.   Erb MA, Scott TG, Li BE, et al. Transcription control by the ENL YEATS domain in acute leukaemia. *Nature*. 2017;543(7644):270-274.

28.   Li Y, Zhao D, Chen Z, Li H. YEATS domain: Linking histone crotonylation to gene regulation. *Transcription*. 2017;8(1):9-14.

29.   Zhao D, Li Y, Xiong X, Chen Z, Li H. YEATS Domain-A Histone Acylation Reader in Health and Disease. *J Mol Biol*. 2017;429(13):1994-2002.

30.   Hetzner K, Garcia-Cuellar MP, Buttner C, Slany RK. The interaction of ENL with PAF1 mitigates polycomb silencing and facilitates murine leukemogenesis. *Blood*. 2018;131(6):662-673.

31.   He N, Chan CK, Sobhian B, et al. Human Polymerase-Associated Factor complex (PAFc) connects the Super Elongation Complex (SEC) to RNA polymerase II on chromatin. *Proc Natl Acad Sci U S A*. 2011;108(36):E636-645.

32.   He N, Chan CK, Sobhian B, et al. Human Polymerase-Associated Factor complex (PAFc) connects the Super Elongation Complex (SEC) to RNA polymerase II on chromatin. *Proceedings of the National Academy of Sciences of the United States of America*. 2011;108(36):E636-645.

33.   Malik B, Hemenway CS. CBX8, a component of the Polycomb PRC1 complex, modulates DOT1L-mediated gene expression through AF9/MLLT3. *FEBS Lett*. 2013;587(18):3038-3044.

34.   Srinivasan RS, de Erkenez AC, Hemenway CS. The mixed lineage leukemia fusion partner AF9 binds specific isoforms of the BCL-6 corepressor. *Oncogene*. 2003;22(22):3395-3406.

35.   Yokoyama A, Lin M, Naresh A, Kitabayashi I, Cleary ML. A Higher-Order Complex Containing AF4 and ENL Family Proteins with P-TEFb Facilitates Oncogenic and Physiologic MLL-Dependent Transcription. *Cancer Cell*. 2010;17(2):198-212.

36.   Wan L, Wen H, Li Y, et al. ENL links histone acetylation to oncogenic gene expression in acute myeloid leukaemia. *Nature*. 2017;543(7644):265-269.